

2008

A Modern Sediment Budget for the Continental Shelf off the Waipaoa River, New Zealand

andrea J. Miller

College of William and Mary - Virginia Institute of Marine Science

Follow this and additional works at: <https://scholarworks.wm.edu/etd>



Part of the [Geology Commons](#), and the [Oceanography Commons](#)

Recommended Citation

Miller, andrea J., "A Modern Sediment Budget for the Continental Shelf off the Waipaoa River, New Zealand" (2008). *Dissertations, Theses, and Masters Projects*. Paper 1539617880.

<https://dx.doi.org/doi:10.25773/v5-vdh1-c406>

This Thesis is brought to you for free and open access by the Theses, Dissertations, & Master Projects at W&M ScholarWorks. It has been accepted for inclusion in Dissertations, Theses, and Masters Projects by an authorized administrator of W&M ScholarWorks. For more information, please contact scholarworks@wm.edu.

**A Modern Sediment Budget for the Continental Shelf off the Waipaoa
River, New Zealand**

A Thesis

Presented to

The Faculty of the School of Marine Science

The College of William and Mary in Virginia

In Partial Fulfillment

Of the Requirements for the Degree of

Master of Science

By

Andrea J. Miller

2008

ProQuest Number: 10631973

All rights reserved

INFORMATION TO ALL USERS

The quality of this reproduction is dependent upon the quality of the copy submitted.

In the unlikely event that the author did not send a complete manuscript and there are missing pages, these will be noted. Also, if material had to be removed, a note will indicate the deletion.



ProQuest 10631973

Published by ProQuest LLC (2017). Copyright of the Dissertation is held by the Author.

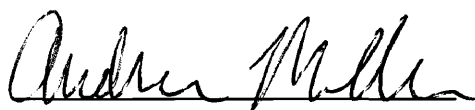
All rights reserved.

This work is protected against unauthorized copying under Title 17, United States Code
Microform Edition © ProQuest LLC.

ProQuest LLC.
789 East Eisenhower Parkway
P.O. Box 1346
Ann Arbor, MI 48106 - 1346

APPROVAL SHEET

This thesis is submitted in partial fulfillment of
the requirements for the degree of
Master of Science

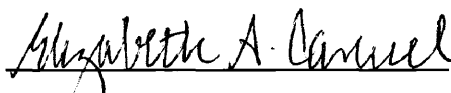


Andrea J. Miller

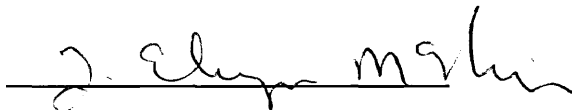
Approved, by the Committee, April 2007



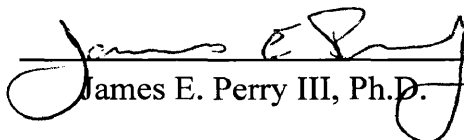
Steven A. Kuehl, Ph.D.
Committee Chairman/Advisor



Elizabeth A. Canuel, Ph.D.



Jesse E. McNinch, Ph.D.



James E. Perry III, Ph.D.

TABLE OF CONTENTS

	Page
ACKNOWLEDGMENTS	V
LIST OF FIGURES	VI
ABSTRACT	VII
INTRODUCTION	2
BACKGROUND	5
Tectonic and Climate Settings of the Waipaoa Catchment.....	5
Continental Shelf.....	6
Radioisotope Geochronology.....	8
MATERIALS AND METHODS	11
Field Techniques and Sampling.....	11
Laboratory Techniques.....	12
RESULTS	14
Radiochemical Data.....	14
Grain Size.....	15
Carbon Analysis.....	16
DISCUSSION	17
Sediment Geochronology.....	17
Accumulation Rate Trends.....	21
Fine-grained Sediment Budget.....	22
Long vs. Short-term Accumulation.....	27
Carbon Analysis.....	30
CONCLUSIONS	34
APPENDICES	47
Appendix A: Kasten and Box Core Locations	47
Appendix B: ²¹⁰Pb Analyses	52

B1: Definition of Terms and Equations.....	52
Used to Determine Excess ²¹⁰ Pb Activity	
B2: ²¹⁰ Pb Depths and Activities.....	54
B3: Accumulation Rate Calculations.....	79
B4: Penetration Depths of Excess ²¹⁰ Pb Activity.....	81
APPENDIX C: ^{239,240}Pu Activities.....	83
APPENDIX D: Kasten Core Grain Size Computations.....	85
APPENDIX E: Carbon Analysis.....	86
E1: Box Core Total Organic Carbon and Nitrogen Data.....	86
E2: Carbon Burial Rate Calculations.....	89
E3: Box Core Carbon Data: δ ¹³ C, Carbon, Nitrogen.....	90
APPENDIX F: X-Radiographs.....	CD
LITERATURE CITED.....	92

ACKNOWLEDGEMENTS

I am very grateful to all of you who have helped in the successful completion of my master's project. First of all, I would like to thank my advisor, Dr. Steve Kuehl, for providing me with amazing opportunities and experiences, and for always having an open door (not to mention a full jar of chocolates). His patience, encouragement, and intellectual guidance have been instrumental in this project as well as in my development as a scientist. I would also like to thank my committee members: Drs. Liz Canuel, Jesse McNinch, and Jim Perry. This project could not have developed without their input, guidance, and support.

Thanks also to everyone working on the Waipaoa Margins S2S project who collected unbelievable numbers of samples for this project and who have provided valuable insight into this work. I also greatly appreciate the help I have received from the members of my lab: Lila Rose, Cielomar Rodriguez, Linda Meneghini, Tara Kniskern, Hiedi Wadman, and Lisa Addington. They continuously provided input and support, and spent enormous amounts of time in the lab helping with the ^{210}Pb analysis. I also want to thank the VIMS faculty and the Physical Sciences staff for their great work.

My experience here has left me with many valuable friends and colleagues. A special thanks goes out to Lindsey Kraatz, Cielomar Rodriguez, Lila Rose, Chris Prosser, Candi Spier, Staci Rice, Payal Dharia and many others for being great friends and making my time here so enjoyable.

Finally, I thank my wonderful family who have loved and supported me through all my endeavors, and have encouraged me to never give up and to put my all into everything I do. I can not thank them enough for everything they have done for me.

LIST OF FIGURES

Figure	Page
1. Map of Waipaoa Shelf.....	36
2. Box and Kasten Core Location Map.....	37
3. Characteristic ^{210}Pb Activity Profiles.....	38
A) Steady-State Profile.....	38
B) Low, Uniform Activity Profile.....	38
C) Non Steady-State Profile.....	38
4. Characteristic ^{210}Pb Activity Profiles Location Map.....	39
5. Across-Shelf Transects of Excess and Total ^{210}Pb Activity Profiles.....	40
6. $^{239,240}\text{Pu}$ and ^{210}Pb Activity Profiles.....	41
7. ^{210}Pb Activity and Percent Clay for KC86 and KC35.....	42
8. N/C vs. $\delta^{13}\text{C}$ for Shelf Regions.....	43
9. Percent Clay and Decay Corrected ^{210}Pb Excess Activity with..... Correlation for KC35	44
10. Spatial Distribution of ^{210}Pb Accumulation Rates.....	45
11. Spatial Distribution of ^{210}Pb Penetration Depths.....	46

ABSTRACT

Rapid uplift and deformation of active continental margins, such as that associated with the Waipaoa River, New Zealand, have the potential to create high sediment yields and accommodation on the shelf which may result in a high resolution stratigraphic record. This study identifies modern sedimentation patterns off the Waipaoa using radioisotopic and sedimentological analyses. ^{210}Pb and $^{239,240}\text{Pu}$ geochronologies reveal two mid-shelf depocenters, landward of the actively deforming Ariel and Lachlan anticlines, which exhibit accumulation rates ranging from 0.75 to 1.5 cm y^{-1} . An outer shelf depocenter, located near the shelf break, was also identified and exhibited accumulation rates as high as 1.0 cm y^{-1} suggesting the bypassing of Waipaoa sediments seaward of the anticlines and possibly off-shelf. The locations of these three depocenters correspond with the location of high accumulation throughout the Holocene indicating that regional tectonics may greatly influence sedimentation patterns. A 100 year sediment budget for the Waipaoa shelf estimates $3.6 \pm 0.9 \times 10^6$ tons y^{-1} of fine-grained sediment remains on the shelf. This amounts to only 24% of the 15 Mt of sediment discharged from the river per year. The carbon burial for the entire shelf was estimated to be $2.62 \pm 1.30 \times 10^4$ tons C y^{-1} , approximately 20% of the POC input from the river. Taken together these observations indicate massive export of sedimentary material from the Waipaoa shelf study area.

**A Modern Sediment Budget for the Continental Shelf off the Waipaoa
River, New Zealand**

INTRODUCTION

Tectonically active continental margins are often characterized by small mountainous rivers carrying large sediment loads to narrow shelves (Milliman and Syvitski, 1992). In some cases, the tectonic activity on these shelves can result in deformation and the formation of mid-shelf synclinal basins, which can control sedimentation on both short and long timescales. For example, these tectonically formed synclinal basins are the primary sediment repositories on the shelf for the Waipaoa and Waiapu Rivers in New Zealand, and the Eel River in California (Foster and Carter, 1997; Lewis et al., 2004; Sommerfield and Nittrouer, 1999). Additionally, the large sediment input of these rivers has the potential to create a high resolution stratigraphic record which could enable both natural and anthropogenic perturbations to the system to be investigated. Alternatively, with the limited accommodation space on narrow shelves, much of the sediment and organic carbon inputs to collision margins could be transported to the adjacent slopes and the deep sea even during high sea-level conditions (Milliman and Syvitski, 1992). Thus tectonically active margins may not follow the traditional sequence stratigraphy model, which predicts high stand shelf trapping immediately following a rapid sea-level rise such as the Holocene transgression. Further analysis of active margin sedimentation patterns is needed in order to refine our understanding of sequence stratigraphy, carbon sequestration, and stratigraphic signals of climate change and landscape evolution.

The Waipaoa River, located along the mountainous and tectonically active northeast region of the North Island, New Zealand, is one of the main focus sites for the MARGINS Source-to-Sink (S2S) program which is sponsored by the National Science Foundation. An important objective of the S2S program is to determine how climate, tectonics, and anthropogenic impacts affect the processes responsible for the production, transport, and accumulation of sediment on margins (Gomez et al., 2001). It was previously thought that the majority of the sediment leaving the Waipaoa River is deposited and preserved on the continental shelf due to the closed nature of the shelf basin (Foster and Carter, 1997). However, recent results by Alexander et al. (2006) indicate that a portion of the sediment is being transported to the slope. This suggests that both the continental shelf and slope presently are important final repositories for terrestrially derived sediment and can be informative records of natural and anthropogenic impacts.

Terrestrial organic carbon is an important component of riverine particulate matter and its distribution on the shelf is closely linked with the dispersal of riverine sediment (Leithold and Hope, 1999). It is estimated that approximately 86% of carbon burial takes place nearshore, or on the continental shelves and slopes (Berner, 1982; Leithold and Hope, 1999). Areas such as the Waipaoa continental shelf are important components in the global carbon cycle because the removal of organic carbon from the biosphere and its resultant storage in margin sediments has contributed to the accumulation of O₂ and depletion of CO₂ in the Earth's atmosphere (Berner, 1982; Blair et al., 2004).

Depositional patterns of both organic material and inorganic sediments can help to elucidate the transport processes across the shelf as well as the signals preserved from natural and anthropogenic perturbations. This study uses radioisotope geochronology to identify modern sedimentation patterns and provide a sediment budget for the shelf. A comparison between modern sediment accumulation and Holocene accumulation leads to a better understanding of the factors controlling sedimentation and provides insight into the impact of both natural and anthropogenic perturbations. This study also uses organic carbon content and carbon isotopic data to elucidate accumulation patterns and sources of carbon on the shelf.

BACKGROUND

Tectonic and Climate Settings of the Waipaoa Catchment

The Waipaoa River is located on the East Coast of the North Island, New Zealand (NZ) (Figure 1). The Waipaoa catchment is a 2205 km² area located on the tectonically active Hikurangi Margin where the Pacific Plate is being obliquely subducted beneath the Australian Plate. The catchment originates in the axial ranges of eastern North Island, New Zealand where tectonic uplift is estimated at 4 mm yr⁻¹ with a maximum uplift of 10 mm yr⁻¹ (Berryman et al., 2000; Hicks et al., 2000). At the Waipaoa mouth, freshwater and suspended sediment are emptied into Poverty Bay via the coastal plains of Gisborne. Geologic, climatic, and anthropogenic factors have resulted in significantly high suspended sediment concentration and sediment yield (Page et al., 2001). The Waipaoa River has the fourth highest suspended sediment concentration of all NZ rivers and has an annual sediment discharge of 15 Mt. (Hicks et al., 2000; Hicks et al., 2004; Griffiths, 1982).

The Waipaoa catchment is underlain by Cretaceous and Paleocene mudstone and argillite, Jurassic to early Cretaceous greywacke, and Miocene-Pliocene sandstone, siltstone, and mudstone (Page et al., 2001; Hicks et al., 2000). These soft, fine-grained rocks are easily erodible and thus contribute much suspended sediment to the Waipaoa River. Approximately 6750 t km⁻² of sediment are eroded per year (Hicks et al., 2004). Contributing to this erosion is the variable climate for the catchment. The Waipaoa catchment displays an annual average rainfall of 1000 mm yr⁻¹ at the coast to greater than

2500 mm yr⁻¹ in the headwaters and is periodically disturbed by intense cyclonic storms (Page et al., 2001; Wilmhurst et al., 1999). The sediment is mainly delivered to the river via gully erosion, earthflows, and shallow landsliding. Gully erosion dominates the erosional regime in the catchment; however, shallow landsliding frequently accompanies high rainfall events (Foster and Carter, 1997).

Modern land use practices are another factor contributing to erosion in the catchment. Podocarp/hardwood forests were the indigenous vegetative cover of the Waipaoa catchment before Maori settlement occurred between 450 and 980 years B.P. (Wilmhurst, 1997; Page et al., 2001). During this settlement, much of the podocarp forests were cleared by fires and replaced with a bracken fern-scrubland (Wilmhurst, 1997; Wilmhurst et al., 1997; Wilmhurst et al., 1999). This change in vegetation decreased the stability of the soil and led to a slight increase in soil erosion. A dramatic increase in erosion and sedimentation rates occurred between 1880 and 1920 due to extensive deforestation by European settlers (Wilmhurst, 1997; Wilmhurst et al., 1997; Wilmhurst et al., 1999; Page et al., 2001). The European settlers cleared the majority of the hardwood forest and fern-scrublands in the catchment and converted these lands to pastures. This greatly destabilized the soil leaving it vulnerable to erosion and landsliding. Today, less than 3% of the indigenous forest cover remains in the Waipaoa catchment.

Continental Shelf

Much of the sediment carried by the Waipaoa River is transported to the adjacent continental shelf by hypopycnal plumes (Foster and Carter, 1997). These plumes carry

sediment in a northeastward or southward direction on the shelf, depending upon prevailing wind driven circulation. However, hyperpycnal plumes may be formed during intense floods that greatly increase the suspended sediment concentration of the Waipaoa River (Foster and Carter, 1997). Hicks et al. (2004) estimated that the suspended sediment concentration in the Waipaoa River discharge would need to be between 37,100 and 40,300 mg L⁻¹ to generate a hyperpycnal plume off the river mouth. Hicks et al. (2004) predict that the recurrence interval for hyperpycnal plumes from the Waipaoa River is greater than 40 years.

The growing Ariel and Lachlan anticlines, located on the outer shelf (Figure 1), are natural barriers that are thought to hinder sediment from dispersing to the slope (Foster and Carter, 1997). The shelf is also bordered by the Monowai Rocks to the north and the Mahia Peninsula located 65 km to the south. The shelf extends 22-26 km seaward to the shelf break at a water depth of 140-170 m (Foster and Carter, 1997). The circulation on the shelf is dominated by the semi-permanent East Cape Current which travels along the shelf break (Foster and Carter, 1997; Carter et al., 1996). The East Cape Current has a net southward flow with periodic reversals resulting from prolonged changes in wind direction (Carter et al., 2002). Circulation on the inner shelf is dominated by periodic incursions of the Wairarapa Coastal Current which flows to the north (Foster and Carter, 1997). The shelf circulation is only weakly affected by the tides.

Sediment facies on the continental shelf follow a pattern of fine sands being deposited on the inner shelf and silts and clays being deposited on the mid-shelf synclinal basins and the outer shelf (Foster and Carter, 1997; Wood, 2006). The transition from

sand to mud occurs at approximately 30-40 m depth. The mud deposit extends from the middle shelf to the Ariel and Lachlan anticlines and through the corridor located between the anticlines to the continental slope. Gravel sized sediments were located around rocky exposures associated with the Ariel and Lachlan anticlines (Foster and Carter, 1997).

Radioisotope Geochronology

Radioisotope geochronology is a frequently used tool in the study of marine sediment deposits. Lead-210 is commonly used to quantify modern (<100 y) sediment accumulation on continental shelves (e.g. Nittrouer et al., 1979; Kuehl et al., 1986; Sommerfield and Nittrouer, 1999). Lead-210 is a naturally occurring radioisotope in the ^{238}U decay series and has a half-life of 22.3 years. Lead-210 atoms are highly particle reactive and decay by low energy beta emissions. This radioisotope is incorporated into the water column via river inflow, atmospheric fallout, and in-situ production from the decay of ^{226}Ra in the water column (Smoak et al., 1996). Due to its particle reactive nature, ^{210}Pb is rapidly removed from the water column and deposited on the sea floor. This results in ^{210}Pb activities in the seabed that are in excess of the levels supported by the secular equilibrium with ^{226}Ra .

Under steady-state conditions, ^{210}Pb profiles of the seabed are affected by sediment accumulation rate and particle mixing. The activity of the ^{210}Pb decreases with time (depth) as ^{210}Pb undergoes beta decay, with the gradient a function of the decay constant and the sediment accumulation rate. Lead-210 profiles are also affected by particle mixing. Sediments can be reworked by biological and physical mixing. The biological reworking is considered a diffusive process in which particles diffuse deeper in

the sediments causing ^{210}Pb activities to be higher than they would if sediment accumulation and radioactive decay were the sole processes. Physical mixing, due to wave and current activity eroding and transporting the sediments, can result in a relatively homogenous layer in the upper portion of the activity profile (Nittrouer et al., 1979).

As biological and physical mixing can affect the ^{210}Pb gradient and hence interpretation of the accumulation rate; a second radioisotope was used in this study to verify ^{210}Pb -derived rates. Commonly, bomb-produced ^{137}Cs is used to verify ^{210}Pb rates, however, the low atmospheric fallout of bomb-produced radionuclides in the southern hemisphere has resulted in ^{137}Cs activities that are too low to detect by traditional methods (Kniskern, 2007). For this study, $^{239,240}\text{Pu}$ measured by Inductively Coupled Mass Spectrometry (ICP-MS), were used as alternatives to ^{137}Cs . Pu-239,240 are bomb-produced radionuclides associated with atmospheric testing of nuclear weapons; thus they have different input functions and hence different activity profiles than the naturally produced ^{210}Pb isotope. Pu-239 and Pu-240 have half-lives of $24,110 \pm 30$ and $6,564 \pm 11$ years respectively. Pu-239,240 isotopes are very particle reactive. Thus they adhere to atmospheric particles and are removed to the water column by washout and dry deposition (Ketterer et al., 2004a). Once in the water column, they adhere to particulate matter and are subsequently deposited in the sediment. Profiles for $^{239,240}\text{Pu}$ activity are similar to those for ^{137}Cs in that they show first appearance at a depth corresponding to 1953/1954 and a peak associated with the 1963/1964 fallout maximum, rather than a logarithmic decay profile as seen with ^{210}Pb . The 1963/1964 timeframe is when the peak

global fallout from atmospheric testing of nuclear weapons occurred (Kenna, 2002; Ketterer et al, 2004a).

MATERIALS AND METHODS

Field Techniques and Sampling

In January 2005, a suite of 86 box cores and 85 kasten cores were collected aboard the R/V Kilo Moana on the continental shelf adjacent to the Waipaoa River for sedimentological and geochemical studies (Figure 2). The majority of the sediment cores were collected between 26 to 75 m water depth on the shelf landward of the Ariel and Lachlan anticlines, with fewer cores collected between the seaward edge of the anticlines and the shelf break.

The box cores recovered short lengths of sediment (up to 60 cm) with well preserved sediment-water interfaces. Due to the short lengths of the box cores, kasten cores were often taken in the same locations in order to provide a longer record of the sediment stratigraphy. Kasten cores are gravity cores that provide up to 3 meters of sediment and have a cross section of (12 x 12 cm). These cores provided adequate length for geochemical analyses such as ^{210}Pb and $^{239,240}\text{Pu}$. However, unlike box cores, kasten cores do not preserve the sediment-water interface well. Onboard, a geometric sampling plan was used to sub-sample all cores for geochemical and textural analysis. Sub-cores were removed for x-radiographic analysis to provide information on sedimentary structure. Many of the x-radiograph samples from the box cores were then frozen for future targeted sampling and carbon analysis.

Laboratory Techniques

Analyses for ^{210}Pb were performed on all 85 Kasten cores to calculate sediment accumulation rates. The ^{210}Po daughter was measured as a proxy for ^{210}Pb (assuming secular equilibrium) using the procedure described in Nittrouer et al. (1979). The only variation in our procedure was the use of a ^{209}Po spike instead of a ^{208}Po spike. The Po activities were determined using an octet alpha spectrometer and MAESTRO processing software. Supported ^{210}Pb activities varied across the study region; therefore, supported levels of ^{210}Pb were determined for each individual core by averaging the activities occurring over depths displaying low and uniform activity, where excess activities had decayed to negligible levels.

Pu-239,240 activity profiles from five spatially diverse kasten cores were determined using the method described by Ketterer et al. (2004b). Samples were spiked with a ^{242}Pu solution and acid leached with HNO_3 . The remaining solvent was then filtered and the oxidation state was adjusted to Pu(IV) with NaNO_2 . TEVA resin was used for column chemistry. The column was rinsed with HNO_3 and HCl to remove Uranium and Thorium from the sample. The Pu fraction was eluted with aqueous ammonium oxalate. These samples were run at Northern Arizona University using an Inductively Coupled-Mass Spectrometer (ICP-MS) which is used for rapid determination of Pu activities. This method is more efficient, accurate, and sensitive than the traditional method of alpha spectrometry (Ketterer et al., 2004a; Kim et al., 2000). The typical detection limit for $^{239,240}\text{Pu}$ is 0.1 Bq kg^{-1} for a sample size of 0.5 g (Ketterer et al., 2004b). The $^{239,240}\text{Pu}$ profiles identified the 1963/1964 $^{239,240}\text{Pu}$ peaks, allowing for a rough estimate of accumulation rates to be made. This was calculated by dividing the

distance from the surface of the cores to the $^{239,240}\text{Pu}$ peak, by the time elapsed since maximum global fallout in 1963/1964. The accumulation rates found from $^{239,240}\text{Pu}$ were used to verify ^{210}Pb rates.

Grain size analysis was performed on samples from two kasten cores exhibiting non steady-state ^{210}Pb activity profiles to identify any grain size influence on ^{210}Pb activities. The sand fraction of each sample was separated from the silt and clay by wet sieving. Pipette analysis (Gee and Bauder, 1986) was used to quantify the silt and clay fractions.

Total organic carbon (TOC) was measured on samples from 10, 20, and 30 cm depths in 20 spatially diverse box cores that had been frozen / refrigerated since collection. The sediment samples were thawed, dried, and homogenized prior to analysis. Inorganic carbon was removed from the samples by acidifying with 10% HCl using the method described by Hedges and Stern (1984). TOC was then analyzed using a Thermo Electron Flash EA1112 elemental analyzer. All samples were run in duplicate and acetanilide was used as the standard. The isotopic composition of organic matter was determined in 5 cm increments in eight box cores using an elemental analyzer interfaced with a continuous flow Isotope Ratio Mass Spectrometer (IRMS) at the University of California's Davis Stable Isotope Facility. The results were used to identify changes in sources of organic matter preserved in the sedimentary record.

RESULTS

Radiochemical Data

Three main patterns of ^{210}Pb activity profiles were identified on the shelf: those showing logarithmic excess ^{210}Pb decrease with depth (steady-state); cores with uniform, low activities; and non-steady state cores exhibiting fluctuating ^{210}Pb activity with depth (Figure 3). Supported activities were estimated on an individual core basis by averaging the activities at depth supported by ^{226}Ra .

The steady-state profiles exhibiting logarithmic decrease were located on the middle (30-70 m water depth) and outer shelf (70-150 m water depth) and ranged in length from 20-175 cm (Figure 4, 5). On the inner and central mid-shelf these cores had very short excess ^{210}Pb activity penetration (usually less than 40 cm) and commonly exhibited accumulation rates less than 0.5 cm y^{-1} (Figure 5). Most cores on the northern and southern mid-shelf landward of the anticlines were characterized by steady-state profiles as well. These cores had much longer ^{210}Pb excess activity profiles and exhibited accumulation rates between 0.5 and 1.5 cm y^{-1} (Figure 5). Eleven of the cores in these two regions showed a 5-10 cm zone of nearly uniform activity at the surface indicating the presence of a surface mixed layer resulting from biological or physical mixing. The cores located on the outer shelf were also characterized by steady-state excess activity with accumulation rates ranging from 0.25 - 1.0 cm y^{-1} (Figure 5). The steady-state profiles often correlated with x-radiographs dominated by mottling and fewer laminations.

The majority of cores on the inner shelf, off Poverty Bay, tended to be short (< 50 cm), with fairly uniform ^{210}Pb activities around 1 dpm g^{-1} (Figure 3, 4). X-radiographs of these cores tended to show laminated facies with little evidence of biological mixing. This area of the shelf is also characterized by a high bulk density indicating it has a higher sand fraction (Rose and Kuehl, submitted).

The non steady-state cores exhibited a general logarithmic decrease interrupted by layers of lower activity, and were found in the two depocenters landward of the anticlines (Figure 4, 5). The majority of these cores exhibited relatively long excess activity profiles (>50 cm) and had apparent accumulation rates (estimated from the slope of the linear regression) similar to the surrounding steady-state cores.

Activity profiles for $^{239,240}\text{Pu}$ were characteristic of bomb-produced radionuclides, with activities increasing to maximum values corresponding with a 1963 depth and then decreasing upward to the surface (Figure 6). The maximum activity peaks for all five kasten cores exhibited activities ranging from 0.015-0.02 dpm g^{-1} . The depths of the maximum $^{239,240}\text{Pu}$ activity peaks were similar to 1963 depths estimated from ^{210}Pb accumulation rates, providing verification for ^{210}Pb accumulation (Figure 6).

Grain Size

Grain size analysis was conducted on two non steady-state cores (KC35 and KC86) to determine whether low activity peaks in the ^{210}Pb data were related to changes in grain-size. In the northern depocenter (KC86), the sediment was composed of 22-35% clay (Figure 7), 45-70% silt, and 3-30% sand, with the largest percent of the sand fraction located at the surface and at a depth of 85-100 cm. In the southern depocenter (KC35),

the clay sized fraction ranges from 25-70%, silt fraction ranges from 35-60%, and the sand fraction ranges from 0-10% (Appendix D).

Carbon Analysis

Total organic carbon (TOC) was measured for 20 box cores on the shelf. Average %TOC values for the cores ranged from 0.31% to 0.84%TOC. Stable carbon isotopes ($\delta^{13}\text{C}$) and carbon to nitrogen ratios were used to establish the provenance of organic carbon on the shelf for eight cores (Appendix E). The average $\delta^{13}\text{C}$ ranged from -23.45‰ to -25.15‰ and the average N/C was between 0.103 and 0.121 (Figure 8).

DISCUSSION

Sediment Geochronology

Steady-state accumulation. Steady-state profiles of ^{210}Pb activity commonly exhibit three characteristic regions (e.g., Koide et al., 1973; Nittrouer et al., 1979). The first region is the surface mixed layer in which sediment is being reworked by biological and physical processes resulting in a zone of nearly uniform excess activity. This zone is present in 11 of the steady-state profiles on the Waipaoa shelf. In cores where a surface mixed layer was present, its thickness was generally <10 cm, which is common for many continental shelves (e.g., Koide et al., 1973; Nittrouer et al., 1979). The second region in a steady-state profile displays a logarithmic decrease of excess activity down-core, as a function of accumulation rate and radioactive decay. The accumulation rate is calculated from the slope of the excess ^{210}Pb profile in the zone of logarithmic decrease. The lower region of a steady-state ^{210}Pb profile represents the supported levels. Here, ^{210}Pb has reached a uniform activity and has achieved secular equilibrium with ^{226}Ra .

However, the logarithmic decrease used to determine the accumulation rate could be a function of both sediment accumulation and diffusive particle mixing. This would lead to an overestimation of accumulation rates. Therefore, ^{210}Pb accumulation rates were verified by the use of $^{239,240}\text{Pu}$ as a second geochronometer. Activity profiles of $^{239,240}\text{Pu}$ were obtained for three cores displaying steady-state ^{210}Pb profiles and compared to accumulation rates calculated by the ^{210}Pb method. Kasten core 14, located in the northern depocenter, showed a ^{210}Pb derived accumulation rate of 1.37 cm y^{-1} .

This rate was used to estimate the 1963 (year of maximum fallout) depth. Depths of the surface mixed layer were added to the original estimated depth to account for mixing. The ^{210}Pb rate indicated that the 1963 peak should occur at approximately 57 cm which corresponds well with the maximum activity peak shown in the $^{239,240}\text{Pu}$ activity profile (Figure 6). Kasten core 45, located in the southern depocenter, had an accumulation rate of 0.85 cm y^{-1} which corresponded to a 1963 depth of 41 cm. Once again, the $^{239,240}\text{Pu}$ results show a maximum activity peak at this depth (Figure 6). On the outer shelf, KC52 seemed to have a change in accumulation around 25 cm as seen by the change in the slope of the linear regression. The calculated accumulation rate for the first 25 cm was 0.37 cm y^{-1} with a 1963 depth of 15.5 cm which corresponded with the $^{239,240}\text{Pu}$ peak (Figure 6). In each of these cases, the estimated and actual depths of the 1963 maximum fallout agree within a few centimeters, indicating that diffusive particle mixing does not appreciably affect the ^{210}Pb profiles.

Low, uniform activities. A second common profile observed on the Waipaoa shelf exhibits low activities which remain fairly uniform down-core (Figure 3). In some cases, uniform low activities are seen in the upper reaches of the core with a slight decrease to supported activities present lower in the core. This characteristic can be associated with intense biological and/or physical mixing homogenizing the sediments (Kuehl et al., 1986; Dellapenna et al., 1998). On the inner shelf of the Waipaoa, biological mixing is unlikely because x-radiographs of these cores show mostly laminated sediments with little evidence of bioturbation, therefore physical mixing may be responsible for these observed ^{210}Pb profiles (Figure 3). These low, uniform activity profiles could also be a

product of coarse-grained sediment. These inner-shelf cores have a higher silt and sand fraction, which could lead to lower ^{210}Pb activities, as a function of decreased particle surface area. Another possible explanation for these low, uniform activity profiles is that they may result from rapid deposition of one or more large pulses of sediment. This type of deposition is often related to flood events and x-radiographs of these flood events often display laminated sediments. The other cores with low, uniform activity that do not exhibit any decrease in activity, indicate that the ^{210}Pb activities are at supported levels. No accumulation seems to be occurring in these locations.

Non steady-state profiles. A few of the cores on the shelf exhibit non steady-state, quasi-logarithmic decrease characterized by intermittent low activity spikes (Figure 3). Such profiles have been observed elsewhere, and three possible explanations for these non steady-state profiles have been suggested. The first assumes that the residence time of particles in the water column is constant, but that particles may have a different affinity for ^{210}Pb based on the grain size, mineralogy, and/or organic carbon content (Nittrouer et al., 1979; Kuehl et al., 1986; Dukat and Kuehl, 1995). The second explanation assumes that all particles have the same affinity for ^{210}Pb , but the residence time of particles in the water column is variable (e.g. Demaster et al., 1986; Kuehl et al., 1986). The third explanation is that abnormally high suspended sediment concentration can quickly deplete available dissolved oceanic ^{210}Pb , resulting in low-activity layers being emplaced in the sediment. For example, during flood events of the Eel River, sediment layers that have high clay content and low excess ^{210}Pb activity have been documented (Sommerfield and Nittrouer, 1999).

In this study, it is unlikely that the non steady-state conditions results from changes in mineralogy because presumably all of the sediment originates from the Waipaoa catchment, making high-frequency variations in mineralogy unlikely. The organic carbon content is also not likely to affect the ^{210}Pb activity profiles because the non steady-state cores are found within the depocenters which show fairly uniform carbon content with a range between 0.592 and 0.835 %C. It is also unlikely that the non steady-state condition results from changes in grain size, because a positive correlation between increasing ^{210}Pb activities and increasing fine-grained sediment was not observed (Figure 7). On the contrary, grain size analysis of KC35 indicates that fluctuations in ^{210}Pb activity could be due to deposition of fine-grained event layers (Figure 7, 9). In this core, low ^{210}Pb activity spikes occur simultaneously with increases in the percentage of clay-sized particles as would be expected for a preserved flood event layer (Wheatcroft et al., 1997; Wheatcroft and Borgeld, 2000). A correlation between % clay and decay corrected ^{210}Pb excess activity shows an R^2 value of 0.61 (Figure 9). However, there is not enough data to indicate that all of the non steady-state profiles result from this process.

Two non steady-state cores were analyzed for $^{239,240}\text{Pu}$ as well as ^{210}Pb . One (KC35 located in the southern depocenter), exhibited a quasi-logarithmically decreasing ^{210}Pb profile interrupted by peaks of low activity and the other (KC69) had a stepped ^{210}Pb profile with low activity. An apparent accumulation rate of 1.55 cm y^{-1} was determined for KC35 by using the slope of the linear regression including the low activity peaks. The 1963 depth calculated from this rate corresponded with the maximum activity in the $^{239,240}\text{Pu}$ profile (Figure 6). It was not possible to determine an accumulation rate

for KC69 from the ^{210}Pb analysis so no correlation between ^{210}Pb and $^{239,240}\text{Pu}$ activities could be made (Figure 6).

Accumulation Rate Trends

The characteristics of the ^{210}Pb activity profiles and their calculated accumulation rates, change both along-shelf and across-shelf (Figures 5, 10). On the inner-to mid-shelf (30-70 m water depth) off Poverty Bay, the majority of the cores display low, uniform ^{210}Pb activities and laminated facies suggesting little net accumulation. In the shallow waters of the inner shelf, fine-grained sediments can often be reworked by intense waves and currents. It is likely that these sediments are resuspended and transported to other locations on the shelf. Therefore, this region may be acting as a bypassing zone in which sediments are continually being removed and dispersed to other portions of the system rather than accumulating over a decadal timescale. This interpretation is also supported by bulk density measurements (Rose and Kuehl, submitted). This “bypassing region” is characterized by higher than average bulk densities indicating that there is a larger percentage of sand-size material located in this area suggesting that the bulk of the fine sediments are dispersed to other locations.

Accumulation rates on the mid-shelf (40-70 m water depth and landward of the anticlines) increase to the north and south. The cores in these regions commonly exhibit steady-state ^{210}Pb profiles with only a few cores exhibiting the non steady-state profiles. Therefore, it is possible to determine accumulation rates for most of the mid-shelf. These two areas exhibit the highest accumulation rates on the shelf, as much as 1.5 cm y^{-1} , and seem to be the primary depocenters. These regions are also characterized by lower than

average bulk densities indicating that these are loci of recent mud deposits (Rose and Kuehl, submitted). A likely explanation for the presence of these two depocenters is that the mid-shelf, landward of the Lachlan and Ariel anticlines, is experiencing subsidence at a rate of approximately 2 mm y^{-1} creating a synclinal basin which provides accommodation space for the deposition of fluvial sediments (Foster and Carter, 1997).

The outer shelf, extending from 70 m water depth to the shelf break, is characterized by steady-state ^{210}Pb profiles with accumulation rates ranging from 0.25 to 1.0 cm y^{-1} . This suggests that sediment is being transported between or across the Ariel and Lachlan anticlines and is being deposited in a depocenter located along the shelf break. High accumulation along the shelf break suggests that a portion of the sediment may be reaching the continental slope. Recent results from Alexander et al. (2006) indicate that modern sediments are in fact accumulating on the Waipaoa slope.

Fine-grained Sediment Budget

A modern (100 year) sediment budget for the Waipaoa shelf was constructed from the distribution of ^{210}Pb accumulation rates. Since accumulation rates determined by ^{210}Pb analysis only account for the fine fraction of sediments, any accumulation of sandy sediments on the shelf is not taken into consideration. The budget includes the continental shelf extending from the coastline to the shelf break located around 140-170 m water depth. The northern boundary was defined as the bathymetric high associated with the Monowai Rocks. The southern boundary was defined as a line extending from the Mahia Peninsula to the shelf break at approximately $39^{\circ}07'S$ (Figure 10).

For budget calculations, the shelf was divided into sub-regions based on 0.25 cm y^{-1} differences in ^{210}Pb accumulation rates. The midpoint value of the apparent ^{210}Pb accumulation rates for each sub-region was then multiplied by an average dry bulk density value of 0.8 g cm^{-3} (Orpin et al., 2006) and integrated over the entire area to obtain the mass of fine-grained sediment accumulating in each of these regions. This resulted in a value of $3.6 \times 10^6 \text{ tons y}^{-1}$. Even though accumulation rates obtained from $^{239,240}\text{Pu}$ corroborate the ^{210}Pb accumulation rates; this rate could be considered a maximum estimate due to possible influence from deep biological mixing as $^{239,240}\text{Pu}$ was not measured in all cores. Most of this sediment is accumulating in two depocenters located on the mid-shelf landward of the anticlines and one depocenter bordering the shelf break. The inner shelf, off Poverty Bay, accounted for much less of the sediment budget as it seems to be a bypassing region.

The possible errors associated with this budget include: (1) errors in the individual accumulation rate measurements, (2) limited spatial resolution of accumulation rates due to the sampling scheme (3) uncertainty of accumulation rates for non steady-state cores, (4) the use of an average bulk density value for the entire shelf, and (5) variable sediment discharge from the river.

The maximum error for the individual accumulation rates was estimated from the standard error of the slopes calculated from the ^{210}Pb profiles. The average error of the slope estimated from all cores resulted in a 25% uncertainty for the accumulation rates. This equates to an uncertainty of approximately $0.9 \times 10^6 \text{ tons y}^{-1}$ in the overall sediment budget.

Error associated with the spatial resolution of ^{210}Pb data and thus the contouring for the sediment budget, is not easily quantified. The sampling scheme for this project provided fairly good spatial resolution for the mid-shelf and outer shelf but poorer resolution near-shore and near the anticlines. The inner-shelf and coastline is composed of mostly sandy sediments (Foster and Carter, 1997) and thus likely would not greatly contribute to the fine-grained sediment budget. Similarly, the anticlines are topographic highs that have negligible sediment cover based on seismic data (Kuehl et al., 2006) and therefore should be negligible in the overall budget.

The above budget estimate included ^{210}Pb rates from 70 out of the 85 profiles measured. Excluded profiles were those for which a general logarithmic decrease was not apparent because of non steady-state conditions. In an effort to extend the spatial coverage of accumulation-rate estimates, a second sediment budget was calculated using the maximum penetration depths of ^{210}Pb (Figure 11). Accumulation rates were calculated by dividing the maximum penetration depth of ^{210}Pb excess activity (excluding the surface mixed layer depth) by the effective span of time represented by excess ^{210}Pb activity. As is the case for most radioactive decay schemes, ^{210}Pb geochronology is effective over a timescale of 4-5 times the isotope half-life. In this case, the depth of penetration was assumed to represent between 88 and 110 years. The sediment budget calculated using this approach estimated that approximately 21.5-26.5% of the sediment was retained on the shelf. This value supports our earlier estimate and indicates that only a small error may be associated with the use of accumulation rates from the non steady-state cores.

The Waipaoa River discharge is currently estimated to be 15 Mt y^{-1} and is measured at a gauging station located at Kanakanaia Bridge, 48 km upstream from the river mouth. Currently, there is little data on the amount of sediment accreting on the flood plain between the gauging station and the river mouth. Therefore, the current discharge value should be considered a maximum estimate. Errors in the discharge estimate could also arise from the episodic nature of the river discharge due to reoccurring flooding from storms. Based on the sediment budget, $3.6 \pm 0.9 \times 10^6$ tons y^{-1} of river derived sediment is remaining on the shelf over the past 100 years. This only amounts to between 18 and 30% of the total river discharge. A portion of the remaining sediment is likely being transported to the north past the Monowai Rocks by the Wairarapa Coastal current which has a net northward flow. Moderate ^{210}Pb accumulation rates ($0.25\text{-}0.5 \text{ cm y}^{-1}$) calculated from cores in this area indicate that this is a possible sediment dispersal pathway. Moderate ^{210}Pb accumulation rates are also seen at the southern boundary of the budget near the Mahia Peninsula. Southward moving winds have been shown to move sediment plumes to the south around the tip of Mahia Peninsula (Foster and Carter, 1997). Therefore, sediment from the Waipaoa may also be transported south of the budget limits.

A large portion of the fluvial sediments are likely bypassing the narrow shelf and being deposited on the adjacent continental slope as indicated by the high accumulation of modern sediment along the shelf break. In fact, the highest accumulation rate (1.8 cm y^{-1}) seen on the entire shelf is located in the canyon head at the shelf break. It is likely that the canyons along the shelf break are important conduits for sediments leaving the shelf. Possible mechanisms for increasing accumulation at the shelf break and dispersing

sediment to the slope include (1) hemipelagic sedimentation from buoyant plumes, (2) direct bypassing of the shelf by hyperpycnal plumes and wave-driven gravity currents, and (3) resuspension and dispersal of shelf sediments by waves and currents (Sommerfield and Nittrouer, 1999). Ongoing studies by Alexander et al. (2006) indicate that approximately 20% of fluvial sediments are being deposited on the slope.

A distinctive characteristic of the Waipaoa shelf is the small portion of total fluvial sediments actually remaining on the shelf. Similar results have been seen in other tectonically active margins with subsiding mid-shelf basins. Sommerfield and Nittrouer (1999) constructed a sediment budget for the Eel River located off Northern California using ^{210}Pb geochronology. The ^{210}Pb data demonstrate that river derived mud accumulates from the 50 m isobath seaward and that the highest accumulation rates are present in areas associated with flood deposition. They determined that a maximum of 20% of the sediment entering the system remains on the continental shelf in a mid-shelf depocenter similar to the depocenters associated with the Waipaoa shelf. The majority of Eel River sediments bypass the narrow continental shelf and are dispersed to the adjacent slope. Similarly, studies of the Waiapu Shelf, also located on the east coast of the North Island, NZ, exhibited highest accumulations on the mid-to-outer-shelf. A sediment budget of this region indicated that between 32-39% of fluvial load was retained on the shelf (Kniskern, 2007). In contrast, passive margin shelves adjacent to rivers such as the Amazon typically exhibit clinoform deposition rather than mid-shelf mud belts and retain more of the fluvially derived sediments on the shelf. For example, sediment budgets for the Amazon, Adriatic, and Canadian Beaufort shelves estimated that 40-70%, 90%, and

85% of sediment, respectively, is retained on these shelves. (Kuehl et al., 1986; Frignani et al., 2005; Macdonald et al., 1998).

Long vs. Short-term Accumulation

Modern sedimentation patterns based on ^{210}Pb geochronology compare favorably with Holocene highstand patterns obtained from seismic mapping in other studies of the Waipaoa shelf (Gerber et al., submitted; Kuehl et al., 2006; Orpin et al., 2006). The Holocene isopach from Gerber et al. (submitted) depicts major depocenters for Holocene sediments located in subsiding synclinal basins landward of the anticlines and along the shelf break, with less sediment accumulation on the inner shelf and between the two anticlines. The largest contrast between the sedimentation patterns of these two timescales is that for modern sedimentation, the northern and southern depocenters are both significant repositories for sediment with the southern depocenter having only a slightly larger load. The modern budget also indicates that the outer shelf depocenter is not as significant a repository as the two mid-shelf depocenters. The Holocene highstand budget (5530 YBP-present) from Gerber et al. (submitted), indicates that the southern mid-shelf basin is the primary depocenter containing 60-65% of the total estimated sediment load.

Gerber et al, (submitted) suggests that the discrepancy between the sediment infilling of the two mid-shelf basins is a result of differential subsidence. Acoustic reflectors in the southern depocenter define an underfilled synclinal basin in which the accommodation space available seems to be greater than the fluvial sediment supply. Reflectors in the northern depocenter show a more progradational pattern which Gerber

et al. (submitted) suggests results from sediment supply being greater than the accommodation space created by subsidence.

One possible explanation for the similarity between the northern and southern depocenters in the modern budget may be that the subsidence rate in the northern depocenter has recently increased as a result of recent cosiesmic subsidence. Earthquake related displacement has occurred at least six times in the Hawke`s Bay region (directly south of the Waipaoa Basin) over the last 7200 years with a net subsidence of 7 m (Hayward et al., 2006). Another possible explanation for the similarity between depocenters in the modern budget may result from the recent increase in fluvial sediment supply. The six-fold increase in sediment yield estimated by Wilmshurst et al., 1999; Page et al., 2001; Gerber et al., submitted, may have changed the southern depocenter from a supply-limited system to a basin limited by accommodation space. In this case, both mid-shelf depocenters would be accommodation limited and sediment would likely accumulate at the same rate as the tectonic subsidence.

Tectonic influence on Holocene and modern sedimentation is also seen on other active margins such as the Eel River margin in northern California. Like the Waipaoa shelf, Holocene sedimentation on the Eel shelf is characterized by high sediment accumulation in a subsiding synclinal basin on the mid- to outer shelf (Sommerfield and Nittrouer, 1999). Sommerfield and Nittrouer (1999) also report findings that modern (100 y) accumulation from ^{210}Pb analysis generally occurs over these same regions of thick Holocene deposits.

Gerber et al. (submitted) estimated that 1.5-2.5 Mt of sediment per year accumulated on the shelf during the last 5530 years. Kettner et al. (2007) estimated a

sediment yield during this time period of 2.3 Mt of sediment per year indicating that the shelf has a high trapping efficiency (Gerber et al., submitted). A comparison of the Late Holocene budget with the modern (100 y) budget indicates an increase between a factor of 1.5 and 2.5 in the sedimentation rate. However, the riverine sediment supply is estimated to have increased by a factor of six since the settlement, and subsequent deforestation, of the Waipaoa catchment (Kettner et al., 2007; Gerber et al., submitted). This suggests that the shelf has evolved from a shelf with a high trapping efficiency (Gerber et al., submitted) to a system in which much of the riverine sediment is bypassing the shelf due to the sediment load exceeding the tectonically produced accommodation space.

There are many uncertainties when comparing sedimentation rates over different timescales. Not only can fluvial loads be significantly different due to climate shifts, tectonics, and land use changes; but the oceanographic conditions on the margin can also change leading to differences in the ability to retain sediment on the shelf (Goodbred and Kuehl, 1999). Another potential problem in the comparison of sedimentation rates over different timescales results from hiatuses in the sedimentary record, which can be attributed to periods of non-deposition or erosion. Hiatuses typically cause accumulation rates to be time-variant; the rates decrease with an increase in the time measured due to greater likelihood of stratigraphic incompleteness (Sadler, 1981). This so-called “Sadler effect” is not evident on the Waipaoa shelf considering that a factor of six increase in sediment input only results in a factor of two increase in the shelf budget. These observations further support the idea that the shelf is presently accommodation limited

and that a large fraction of the modern Waipaoa sediment delivered to the shelf escapes the study area.

Carbon Analysis

Continental shelves are major sinks for removal of organic carbon due to the high sediment accumulation rates on the shelves and hence are an important term in the global carbon budget. Sediments in coastal regions are predominantly comprised of terrigenous material, and it is estimated that particulate terrigenous organic matter accounts for 0.5-1 wt. % of the sediment deposits in these regions (Meybeck, 1982; Hedges, 1992). This range is similar to the organic carbon content values calculated for the sediments off the Waipaoa River as discussed below.

Organic carbon content in sediments is generally dependent upon texture, with fine-grained sediments having greater TOC than coarser sediments (Keil and Hedges, 1993; Jouanneau et al., 2002). TOC content and source of carbon to the shelf are also impacted by any changes in riverine delivery of organic material and/or marine productivity. The source of organic carbon can be determined from its C/N ratio and its carbon isotopic signature ($\delta^{13}\text{C}$). Terrestrial C_3 plants comprise more than 95% of global terrestrial plant biomass and exhibit $\delta^{13}\text{C}$ values between -24‰ and -28‰ and C/N ratios between 25 and 50 (Leithold and Hope, 1999). Marine phytoplankton typically exhibits a C/N ratio of 7 and a $\delta^{13}\text{C}$ value ranging from -18‰ to -21‰.

Depth averaged $\delta^{13}\text{C}$ and N/C values plotted according to Leithold and Hope (1999), indicate that all cores exhibit a mixed marine and terrestrial carbon source with a slight terrestrial leaning (Figure 8). A two source $\delta^{13}\text{C}$ mixing model indicates that seven

out of the eight box cores are comprised of 69-83% terrestrial carbon. One core located within the southern depocenter is composed evenly of marine and terrestrial source carbon. Values for the three regions of the shelf exhibited $\delta^{13}\text{C}$ values ranging from -23.45‰ to -25.15‰ and N/C values between 0.103 and 0.124, indicating similarities in organic carbon sources within the three regions.

In contrast to the depth averaged $\delta^{13}\text{C}$ and N/C values, the organic carbon content of surface sediments varied spatially throughout the Waipaoa shelf. The highest %TOC content is seen on the outer shelf (mean \pm standard deviation = 0.74 ± 0.10 %TOC). High %TOC content is also seen in the northern and southern depocenters. TOC contents averaged 0.68 ± 0.20 and 0.66 ± 0.09 in the northern and southern depocenters, respectively. The inner shelf is characterized by lower %TOC values (0.48 ± 0.20). These results indicate that the three depocenters have a higher %TOC than the inner shelf. A likely explanation for this observation is that the inner shelf is composed of sandier sediments. Since organic carbon is commonly associated with finer sediments, it is to be expected that areas of mud deposition will have higher %TOC than the regions with coarser grained sediment.

Organic carbon burial rates can be determined for modern sedimentary environments by multiplying the average TOC concentrations by the mass accumulation rates (Van Weering et al., 1998; Brunskill et al., 2001). This calculation is shown by the equation $J_z = \rho(1-\phi)\omega[C]$ where J_z is the flux of carbon at sediment depth z , ρ is the dry bulk density, ϕ is the porosity, ω is the sedimentation rate, and $[C]$ is the organic carbon concentration at depth z (Lin et al., 2000). Average carbon burial rates were calculated for the inner shelf, northern depocenter, southern depocenter, and outer shelf. For each

region, the average carbon concentration for the box cores was multiplied by the average mass accumulation rate, obtained from corresponding kasten cores. The average carbon burial rates for the inner shelf, northern depocenter, southern depocenter, and outer shelf are $7.93 \pm 5.37 \times 10^{-4}$, $4.24 \pm 2.31 \times 10^{-3}$, $4.26 \pm 1.63 \times 10^{-3}$, and $3.91 \pm 1.51 \times 10^{-3}$ gC cm⁻² y⁻¹ respectively. Since carbon burial rates are dependent upon mass accumulation rate, it is not surprising that the highest carbon burial rate is seen in the southern depocenter which also exhibits the highest accumulation rate. The lowest carbon burial rates occur on the inner shelf resulting from the low TOC content and low sediment accumulation in this region. It should be noted however, that data were obtained for three to four cores in each region and therefore significant error may arise from the limited spatial resolution.

The carbon burial for the entire shelf was estimated to be $2.62 \pm 1.30 \times 10^4$ tons C y⁻¹. This was calculated by multiplying the average burial rate by the area of the corresponding region and then summing the total burial for the four regions on the shelf and an estimated burial for the mid-shelf region between the anticlines. Since there were no carbon data for this last region, the average organic carbon value of the two mid-shelf depocenters was multiplied by the average accumulation rate found in this region.

Gomez et al. (2003) estimated that 13×10^4 tons POC y⁻¹ is discharged to the basin from the Waipaoa catchment. This is approximately five times the amount of organic carbon that is being buried within the upper 30 cm of the seafloor. Considering that the sediment TOC is comprised of both terrestrial and marine-derived carbon, the amount of organic carbon in the sediments is much less than that discharged from the river. Much of the difference in TOC between the water surface and the sediments can be accounted for by the sediment budget. Only 18-30% of the sediment is accumulating

on the shelf with the rest bypassing the shelf; thus a large fraction of the TOC associated with the sediment is likely also escaping from the system. Another reason for the decrease in TOC between the riverine input and the sediments is that organic carbon can be remineralized in the water column and the sediment-seawater interface, further reducing burial relative to riverine input (Lee et al., 1998).

Marine organic carbon is generally more easily remineralized than the more recalcitrant terrestrial organic materials; a greater fraction of POC is preserved in coastal sediments rather than deep water sediments (Hedges, 1992). In a study of global carbon flux conducted by Hedges (1992), it was estimated that less than 0.2% of marine primary production and less than 20% of the terrigenous input can be preserved in the sediment. On the Waipaoa shelf, there is not a current estimate for primary production, however, the value for the terrigenous POC input and the carbon burial rates indicate that less than 20% of POC is being preserved in the sediment: remaining consistent with the sediment budget and global flux estimates.

CONCLUSIONS

The major conclusions of this paper are summarized below.

(1) Three characteristic ^{210}Pb activity profiles are seen on the Waipaoa shelf. The inner shelf is characterized by low, uniform activity profiles which likely result from physical mixing and resuspension of sediment by energetic waves and currents. Steady-state profiles are observed in the northern and southern depocenters and on the outer shelf.

Non steady-state ^{210}Pb activity profiles also occur in the two mid-shelf depocenters.

These non steady state profiles likely result from event deposition.

(2) Fine-grained sediments from the Waipaoa seem to be bypassing the inner shelf and being primarily deposited in two mid-shelf depocenters located in the subsiding synclinal basins landward of the anticlines. A portion of the sediment is also being deposited on the outer shelf along the shelf break indicating that sediment may be reaching the slope.

(3) A sediment budget indicates that $3.6 \pm 0.9 \times 10^6$ tons y^{-1} of sediment accumulates on the Waipaoa continental shelf. This amounts to only 18-30% of the total sediment discharged from the river. The remainder of the sediment is probably transported to the slope and/or out of the system to the north or south.

(4) Modern sedimentation patterns are similar to Holocene patterns. This suggests that sediment deposition is mainly controlled by regional tectonics and shelf morphology rather than oceanographic forces. A comparison of the modern (100 y) budget and late Holocene budget indicates that a much smaller percent of the sediment input from the river is retained on the shelf in modern times. This suggests that the Waipaoa shelf has

evolved from a system with a high trapping efficiency to a system in which a large portion of the sediment escapes the shelf due to limited accommodation space.

(5) Carbon analysis indicates that the percent of organic carbon and carbon burial rates are higher in the depocenters than on the inner shelf. The organic carbon seems to be from a mixture of marine and terrestrial sources with approximately 70-80% being from terrestrial origin. The carbon burial for the entire shelf was estimated to be $2.62 \pm 1.30 \times 10^4$ tons C y^{-1} .

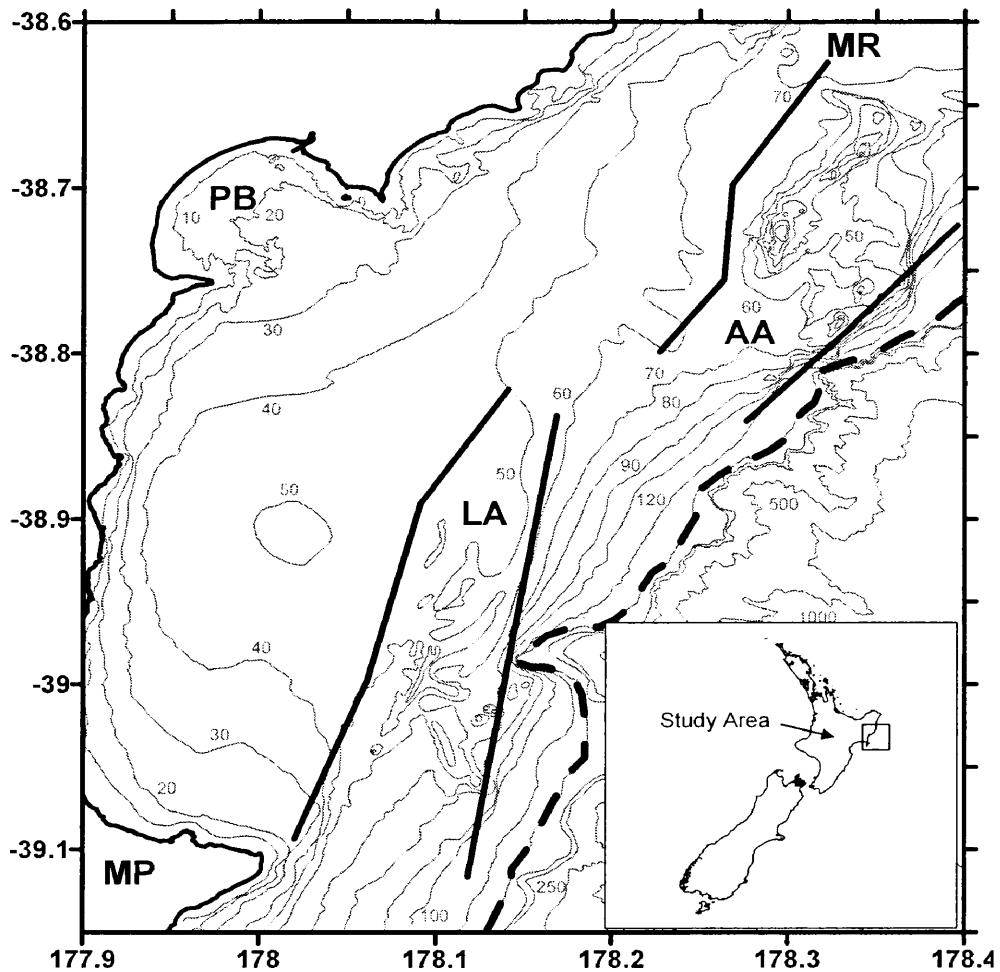


Figure 1: Continental shelf off the Waipaoa River located on the North Island of New Zealand, with bathymetric lines provided by NIWA. LA = Lachlan Anticline, AA = Ariel Anticline, PB = Poverty Bay, MR = Monowai Rocks, MP = Mahia Peninsula. Dashed line indicates shelf break located at 150 m. Solid lines outline the edges of the two mid-shelf anticlines.

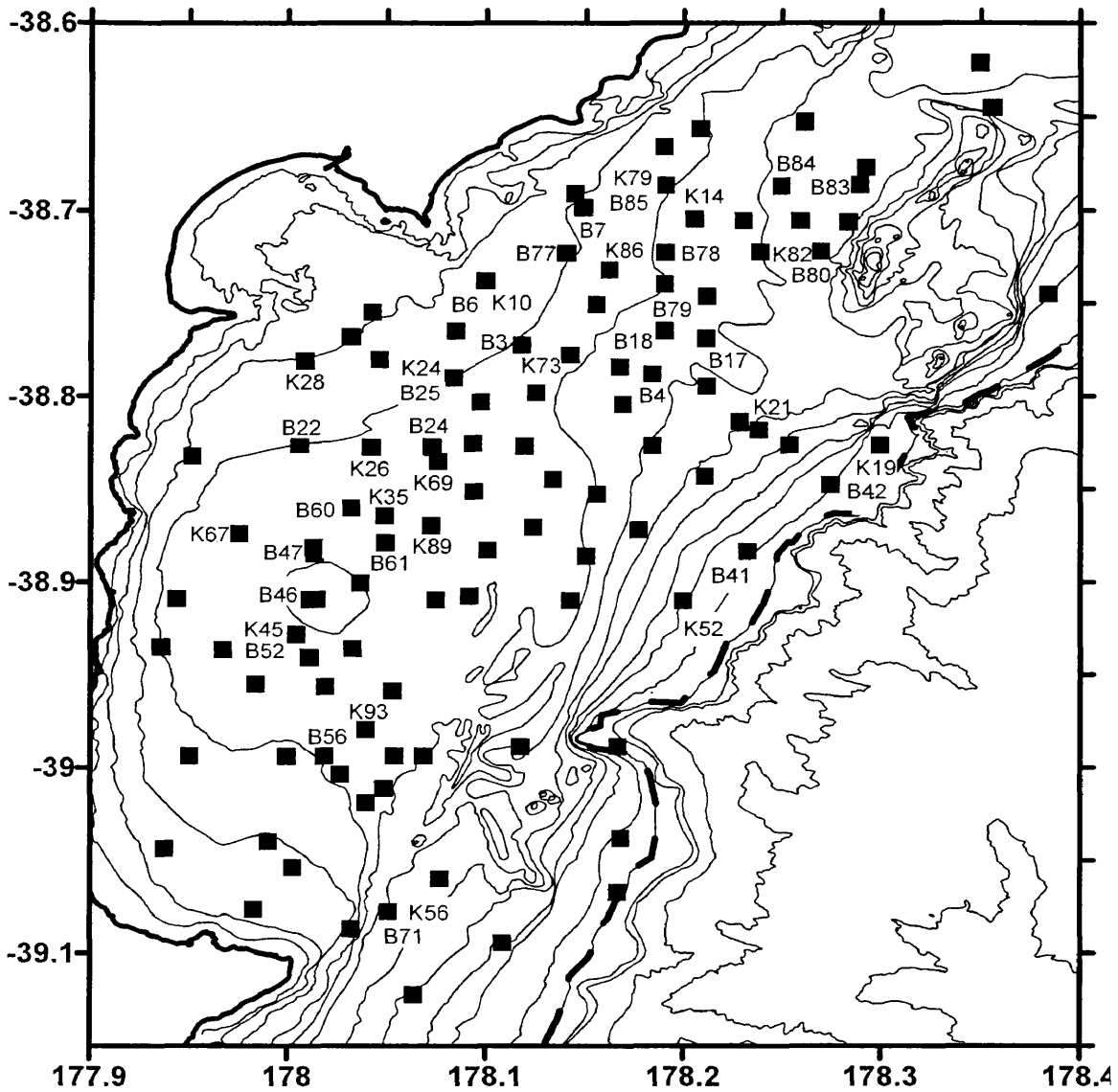


Figure 2: Locations of kasten and box cores (black squares) collected on the Waipaoa shelf in January, 2005 using the R/V Kilo Moana. In total, 85 kasten and 86 box cores were collected. All cores mentioned in text are labeled by core type (K = kasten; B = box) and number. Dashed line indicates shelf break at 150 m.

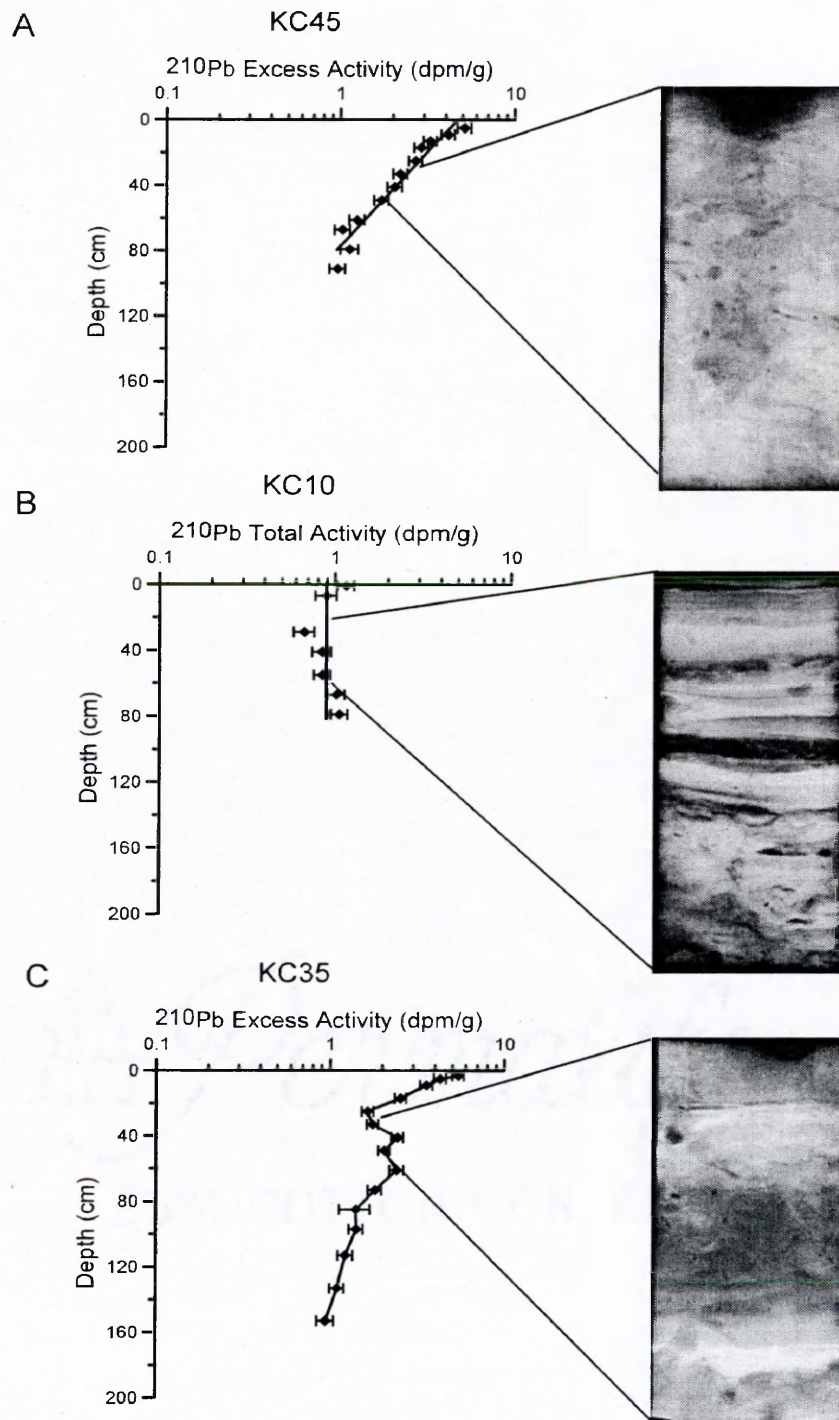


Figure 3: Characteristic ^{210}Pb profiles for steady-state profiles (A), low, uniform activity profiles (B), and non steady-state profiles (C). X-radiographs shown are for the 30-60 cm interval in each core.

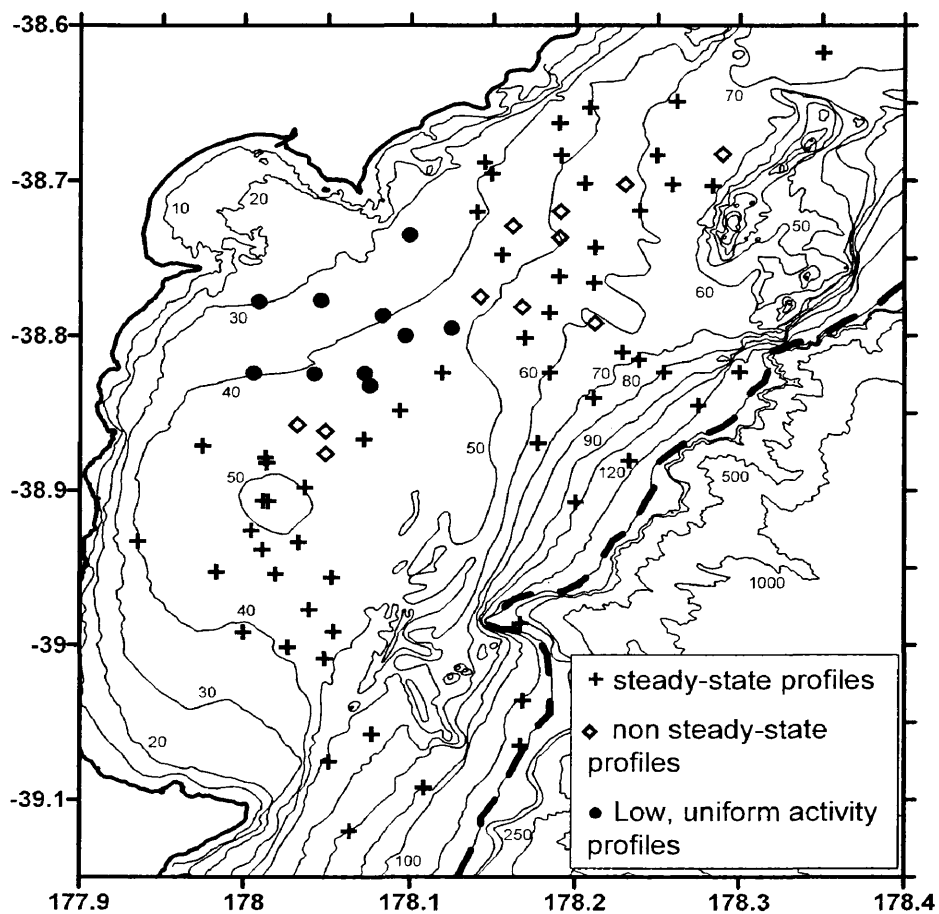


Figure 4: Locations of three characteristic ^{210}Pb activity profiles (see figure 3). Profiles exhibiting low, uniform activities are found exclusively on the inner shelf; steady-state cores are found on the mid-shelf and outer shelf; and non steady-state cores are located primarily in the mid-shelf depocenters. Dashed line indicates shelf break at 150 m.

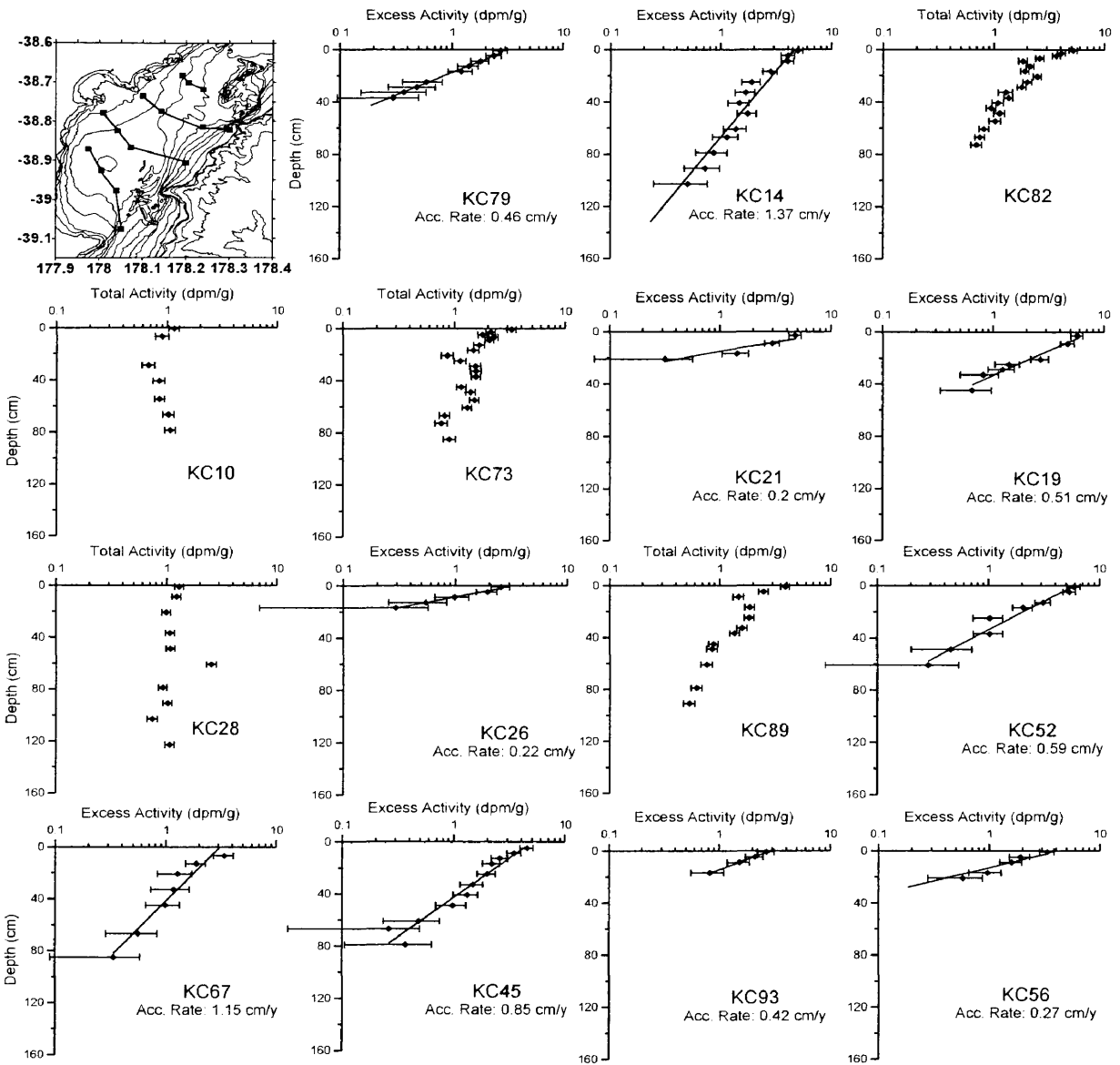


Figure 5: ^{210}Pb profiles for the Waipaoa River shelf. Excess activity profiles and calculated accumulation rates are shown for steady-state cores and total activity profiles are shown for non steady-state cores and cores displaying low, uniform activity. ^{210}Pb profiles are oriented with North at the top of page and East at the left of page along transects as shown in inset.

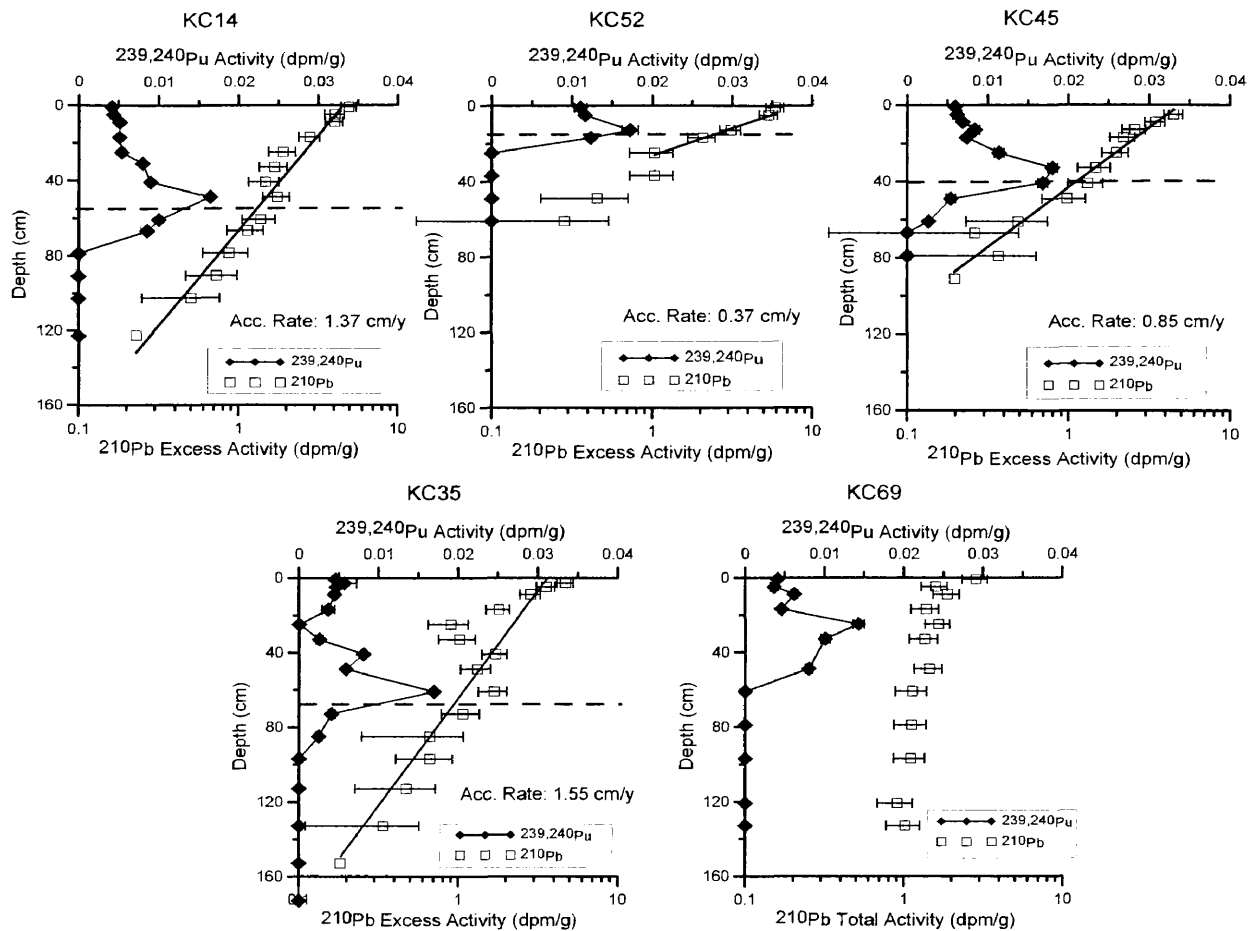


Figure 6: $^{239,240}\text{Pu}$ and ^{210}Pb profiles for selected cores. Dashed line indicates 1963 maximum fallout date calculated from ^{210}Pb accumulation rates. Profiles for kasten cores 14, 52, 45, and 35 show that the depths of the 1963 maximum bomb fallout agree with ^{210}Pb derived accumulation rates. This concordance indicates minimal influence of diffusive mixing (i.e. bioturbation) on ^{210}Pb profiles and confirms accumulation rates calculated from the gradient of excess activity profiles. An accumulation rate could not be estimated in KC69 (see text for details).

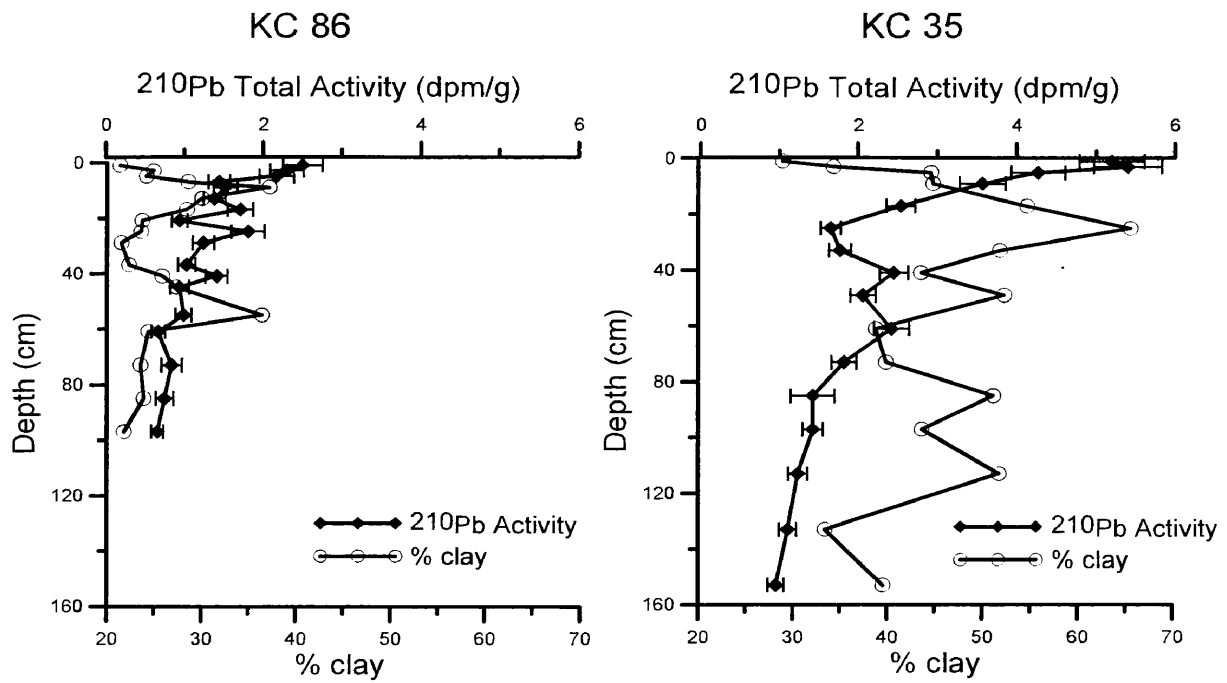


Figure 7: ^{210}Pb activity profiles for cores KC86 and KC35 plotted against clay fraction. K35 shows a potential correlation between low ^{210}Pb activity spikes and higher % clay indicating possible event deposition (see figure 9).

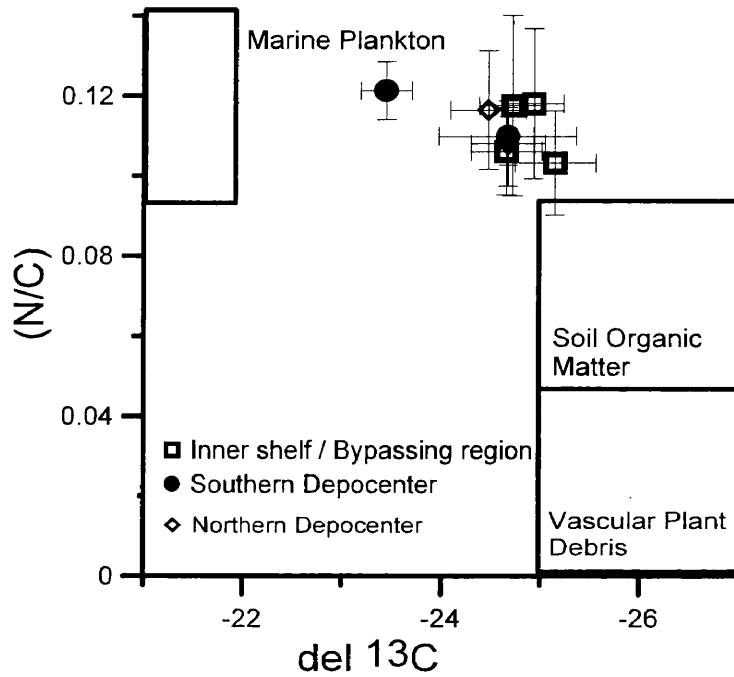


Figure 8: N/C vs. $\delta^{13}\text{C}$ for 8 box cores located in the northern and southern depocenters, and the inner shelf/bypassing region. Carbon data for each core were averaged over total depth. This figure indicates that all three regions of the shelf have a mixture of marine and terrestrial sources of carbon with most cores exhibiting a 70-80% terrestrial source.

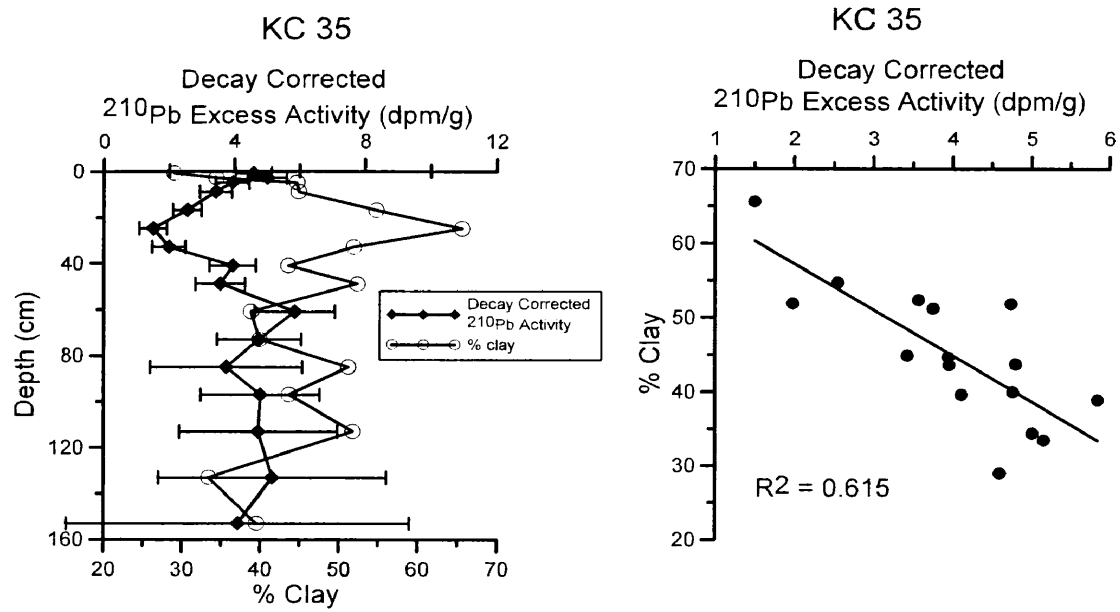


Figure 9: Percent clay and decay corrected ^{210}Pb excess activity for KC35 (left). Correlation between ^{210}Pb activity and % clay (right). Correlation between % clay and corrected ^{210}Pb activity shows an R^2 value of 0.615. This likely indicates flood event deposition when ^{210}Pb -poor sediment is rapidly deposited.

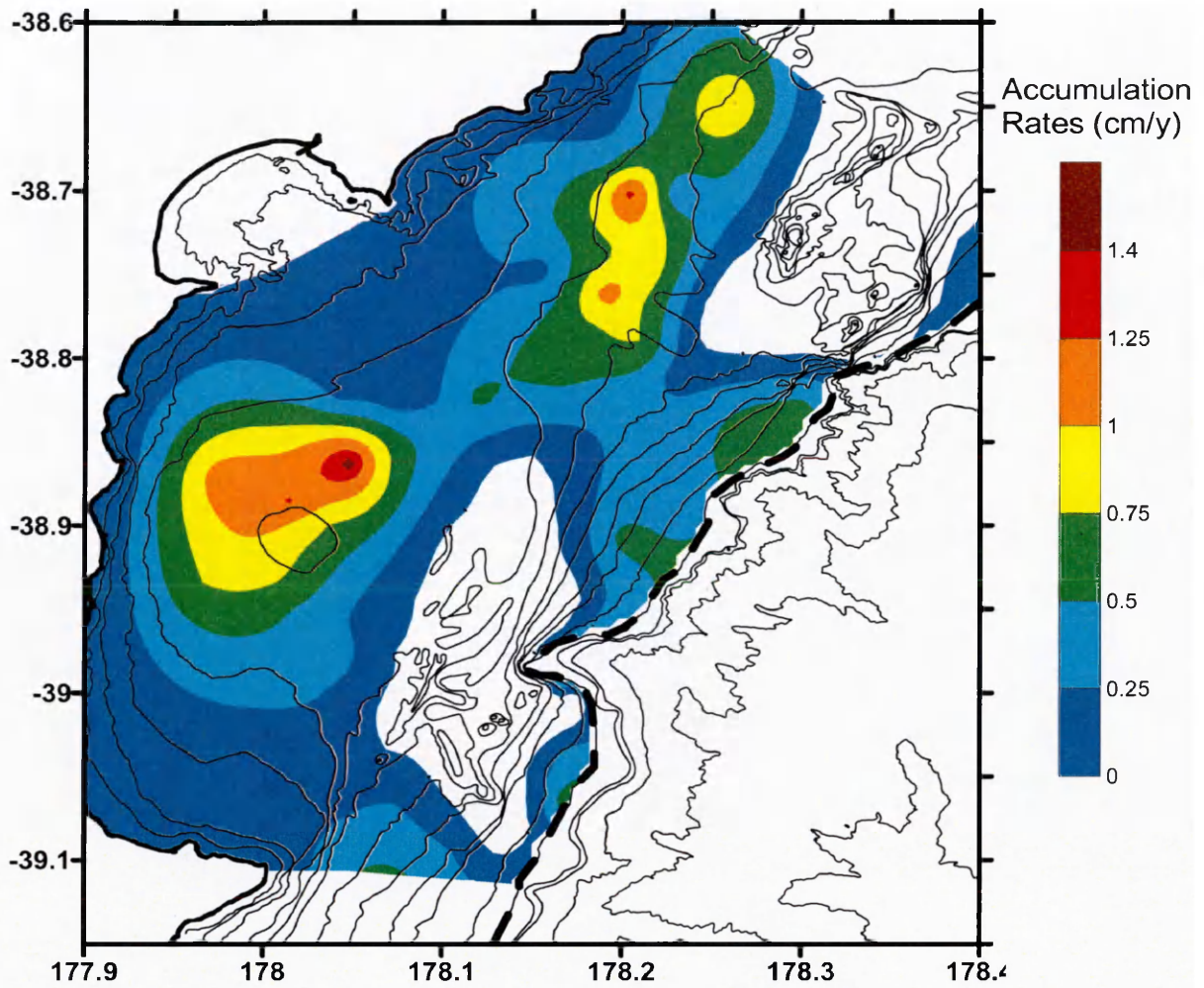


Figure 10: Spatial distribution of ^{210}Pb accumulation rate (cm y^{-1}). Highest accumulation rates are seen in the northern and southern mid-shelf depocenters and along the shelf break. An estimated $3.6 \pm 0.9 \times 10^6$ tons y^{-1} of sediment is accumulating on the shelf which corresponds to 18-30% of the sediment discharged from the Waipaoa River. Regions without color indicate area outside of boundaries for the budget or represent anticlines where sediment cover is negligible.

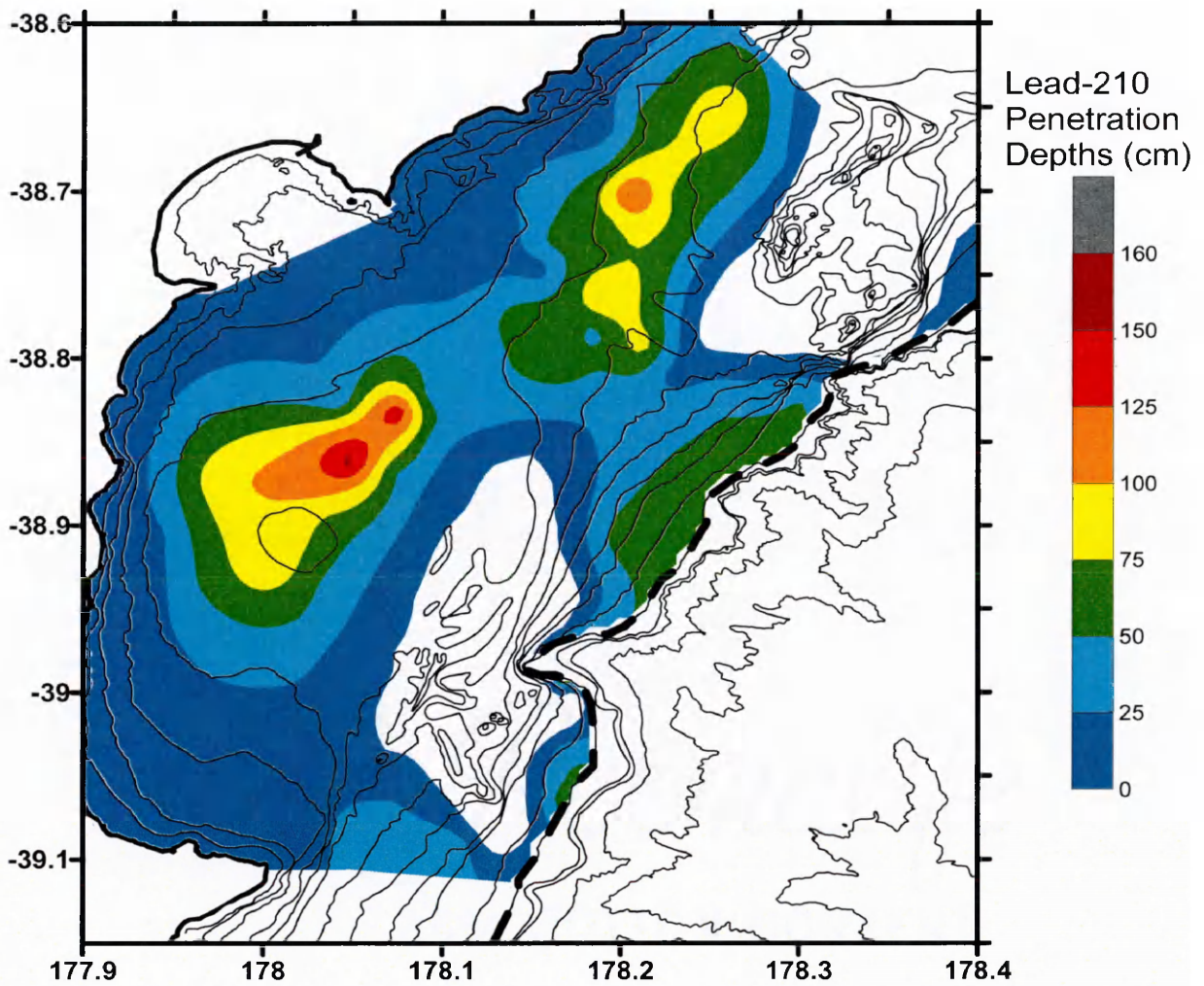


Figure 11: Spatial distribution of ^{210}Pb penetration depths (cm) estimated from excess activity profiles. Depocenters are seen on the northern and southern mid-shelf regions and along the shelf break. ^{210}Pb penetration depth data is used to estimate that 21.5-26.5% of the sediment discharged from the Waipaoa is retained on the shelf.

APPENDIX A

Kasten and Box Core Locations

Kasten Cores Core Name	Latitude (S)	Longitude (E)	Water Depth (m)	Length (cm)	Date of Collection
KC1	-38.7920	178.2118	59	126	1/15/2005
KC2	-38.7854	178.1840	54	82	1/15/2005
KC6	-38.6420	178.3566	68	unsuccessful	1/15/2005
KC7	-38.6491	178.2618	61	222	1/15/2005
KC8	-38.6532	178.2086	48	206	1/15/2005
KC9	-38.6957	178.1490	38	48	1/15/2005
KC10	-38.7353	178.0996	31	8	1/16/2005
KC11	-38.6177	178.3503	76	200	1/16/2005
KC12	-38.7035	178.2838	63	185	1/16/2005
KC13	-38.7026	178.2593	62	204	1/16/2005
KC14	-38.7020	178.2056	52	216	1/16/2005
KC15	-38.7434	178.2120	55	153	1/16/2005
KC16	-38.7660	178.2115	56	181	1/16/2005
KC17	-38.7619	178.1904	52	160	1/16/2005
KC18	-38.7479	178.1554	44	65	1/16/2005
KC19	-38.8236	178.2999	123	219	1/17/2005
KC20	-38.8237	178.2541	79	178	1/17/2005
KC21	-38.8155	178.2384	70	146	1/17/2005
KC22	-38.8240	178.1843	60	117	1/17/2005
KC23	-38.8243	178.1191	48	68	1/18/2005
KC24	-38.7872	178.0832	38	99	1/18/2005
KC25	-38.8245	178.0724	46	220	1/18/2005
KC26	-38.8249	178.0421	44	203	1/18/2005
KC27	-38.8244	178.0055	41	222	1/18/2005
KC28	-38.7784	178.0087	30	130	1/18/2005
KC29	-38.7654	178.0319	28	unsuccessful	1/18/2005
KC30	-38.8109	178.2286	65	82	1/20/2005
KC31	-38.8450	178.2750	112	230	1/20/2005
KC32	-38.8807	178.2327	109	235	1/20/2005
KC33	-38.8693	178.1771	64	30	1/20/2005
KC34	-38.8486	178.0935	48	77	1/20/2005
KC35	-38.8617	178.0487	48	180	1/20/2005
KC36	-38.8790	178.0127	48	240	1/20/2005
KC37	-38.8981	178.0364	49	171	1/20/2005
KC38	-38.9049	178.0914	40	unsuccessful	1/20/2005
KC39	-38.9913	178.0684	50	unsuccessful	1/21/2005
KC40	-38.0162	178.0394	45	108	1/21/2005
KC41	-38.9915	178.0186	43	20	1/21/2005
KC42	-38.9916	177.9995	41	32	1/21/2005
KC43	-38.9915	177.9496	38	unsuccessful	1/21/2005

Kasten Cores Core Name	Latitude (S)	Longitude (E)	Water Depth (m)	Length (cm)	Date of Collection
KC44	-38.9328	177.9354	38	25	1/21/2005
KC45	-38.9259	178.0042	50	202	1/21/2005
KC46	-38.9383	178.0108	49	220	1/21/2005
KC47	-38.9069	178.0143	50	225	1/21/2005
KC48	-38.8820	178.0135	49	247	1/21/2005
KC49	-38.9068	178.0112	50	240	1/21/2005
KC50	-38.8295	177.9507	33	unsuccessful	1/21/2005
KC51	-38.9065	177.9429	42	40	1/21/2005
KC52	-38.9076	178.2000	95	229	1/23/2005
KC53	-38.9861	178.1667	256	270	1/23/2005
KC54	-39.0650	178.1666	130	229	1/23/2005
KC55	-39.0577	178.0768	70	138	1/23/2005
KC56	-39.0754	178.0510	62	150	1/23/2005
KC57	-39.0088	178.0482	50	47.5	1/23/2005
KC58	-39.0014	178.0263	43	60	1/23/2005
KC59	-38.9528	177.9833	46	146	1/23/2005
KC60	-38.9341	177.9666	46	172	1/23/2005
KC61	-39.1204	178.0636	79	145	1/23/2005
KC62	-39.0923	178.1083	91	184	1/23/2005
KC63	-39.0359	178.1681	119	210	1/23/2005
KC64	-38.9562	178.0527	47	35	1/24/2005
KC65	-38.9335	178.0326	49	202	1/24/2005
KC66	-38.8763	178.0489	49	170	1/24/2005
KC67	-38.8712	177.9746	47	215	1/24/2005
KC68	-38.8577	178.0318	48	170	1/24/2005
KC69	-38.8325	178.0756	47	215	1/24/2005
KC70	-38.7776	178.0461	32	128	1/24/2005
KC71	-38.8228	178.0931	47	142	1/24/2005
KC72	-38.8003	178.0969	43	69	1/24/2005
KC73	-38.7753	178.1422	50	107	1/24/2005
KC74	-38.7817	178.1674	50	94	1/24/2005
KC75	-38.8017	178.1690	53	153	1/24/2005
KC76	-38.8403	178.2110	72	172	1/24/2005
KC77	-38.6883	178.1447	37	28	1/26/2005
KC78	-38.6631	178.1902	46	77	1/26/2005
KC79	-38.6838	178.1910	47	116	1/26/2005
KC80	-38.6839	178.2499	61	160	1/26/2005
KC81	-38.6831	178.2897	65	178	1/26/2005
KC82	-38.7196	178.2391	59	76	1/26/2005
KC83	-38.7026	178.2303	57	129	1/27/2005
KC84	-38.7200	178.1909	50	139	1/27/2005
KC85	-38.7369	178.1905	50	180	1/27/2005
KC86	-38.7294	178.1620	43	102	1/27/2005
KC87	-38.7204	178.1401	38	52	1/27/2005
KC88	-38.8802	178.1005	42	unsuccessful	1/28/2005
KC89	-38.8670	178.0719	49	92	1/28/2005

Kasten Cores Core Name	Latitude (S)	Longitude (E)	Water Depth (m)	Length (cm)	Date of Collection
KC90	-38.7954	178.1248	45	87	1/28/2005
KC91	-38.7978	178.9833	33	78	1/28/2005
KC92	-38.9540	178.0188	47	129	1/28/2005
KC93	-38.9771	178.0392	47	61	1/28/2005
KC94	-38.9913	178.0538	49	97	1/28/2005

Box Cores Core Name	Latitude (S)	Longitude (E)	Depth (m)	Length (cm)	Date of Collection
B1	-38.7522	178.0426	27	0.17	1/15/2005
B2	-38.7621	178.0845	32	0.26	1/15/2005
B3	-38.7698	178.1176	38	0.21	1/15/2005
B4	-38.7854	178.1840	54	0.44	1/15/2005
B5	-38.7920	178.2118	59	0.39	1/15/2005
B6	-38.7352	178.0990	33	0.26	1/15/2005
B7	-38.6960	178.1485	40	0.33	1/16/2005
B8	-38.6535	178.2083	49	0.37	1/16/2005
B9	-38.6499	178.2615	61	0.40	1/16/2005
B10	-38.6421	178.3556	67	0.31	1/16/2005
B11	-38.6181	178.3501	75	0.41	1/16/2005
B12	-38.6740	178.2927	64	0.20	1/16/2005
B13	-38.7031	178.2840	62	0.32	1/16/2005
B14	-38.7026	178.2596	62	0.43	1/16/2005
B15	-38.7018	178.2059	52	0.45	1/16/2005
B16	-38.7438	178.2120	55	0.45	1/16/2005
B17	-38.7664	178.2116	57	0.43	1/16/2005
B18	-38.7623	178.1905	53	0.37	1/16/2005
B19	-38.7482	178.1555	45	0.38	1/16/2005
B20	-38.7651	178.0314	29	0.37	1/16/2005
B21	-38.7784	178.0082	31	0.35	1/16/2005
B22	-38.8245	178.0060	42	0.44	1/17/2005
B23	-38.8247	178.0416	43	0.40	1/17/2005
B24	-38.8248	178.0729	46	0.36	1/17/2005
B25	-38.7872	178.0831	38	0.27	1/17/2005
B26	-38.8244	178.1190	48	0.42	1/17/2005
B27	-38.8240	178.1842	59	0.38	1/17/2005
B28	-38.8155	178.2385	70	0.44	1/17/2005
B29	-38.8237	178.2541	79	0.49	1/17/2005
B30	-38.8236	178.2999	123	0.45	1/17/2005
B31	-38.9050	178.0914	41	0.07	1/19/2005
B32	-38.8980	178.0365	52	0.40	1/19/2005
B33	-38.8790	178.0127	49	0.45	1/19/2005
B34	-38.8617	178.0485	49	0.41	1/19/2005
B35	-38.8485	178.0936	49	0.34	1/19/2005

Box Cores Core Name	Latitude (S)	Longitude (E)	Depth (m)	Length (cm)	Date of Collection
B36	-38.8680	178.1234	41	unsuccessful	1/19/2005
B37	-38.8419	178.1334	44	0.16	1/19/2005
B38	-38.8499	178.1558	49	unsuccessful	1/19/2005
B39	-38.8833	178.1502	47	unsuccessful	1/19/2005
B40	-38.8693	178.1770	62	0.32	1/19/2005
B41	-38.8807	178.2327	107	0.50	1/19/2005
B42	-38.8451	178.2752	112	0.46	1/19/2005
B43	-38.8108	178.2286	65	0.36	1/19/2005
B44	-38.9066	177.9432	43	0.38	1/20/2005
B45	-38.8295	177.9508	32	0.30	1/20/2005
B46	-38.9067	178.0109	49	0.39	1/20/2005
B47	-38.8818	178.0131	48	0.48	1/20/2005
B48	-38.9068	178.0141	49	unsuccessful	1/20/2005
B49	-38.9071	178.0745	45	unsuccessful	1/21/2005
B50	-38.9074	178.1424	46	0.13	1/21/2005
B51	-38.9380	178.0105	49	0.41	1/21/2005
B52	-38.9255	178.0040	50	0.39	1/21/2005
B53	-38.9325	177.9350	39	0.16	1/21/2005
B54A	-38.9080	177.9492	46	0.41	1/21/2005
B54B	-38.9914	177.9495	39	0.22	1/21/2005
B55	-38.9914	177.9992	41	0.31	1/21/2005
B56	-38.9914	178.0183	43	0.33	1/21/2005
B57	-39.0168	178.0392	45	0.35	1/21/2005
B58	-38.9913	178.0684	50	0.08	1/21/2005
B59	-38.8712	177.9746	56	0.51	1/22/2005
B60	-38.8577	178.0318	47	0.46	1/22/2005
B61	-38.8763	178.0491	49	0.44	1/22/2005
B62	-38.9340	177.9665	47	0.40	1/22/2005
B63	-38.9526	177.9833	47	0.45	1/22/2005
B64	-39.0413	177.9369	27	unsuccessful	1/22/2005
B65	-39.0377	177.9898	32	unsuccessful	1/22/2005
B66	-39.0013	178.0262	43	0.31	1/22/2005
B67	-39.0089	178.0485	49	0.34	1/22/2005
B68	-39.0515	178.0023	29	unsuccessful	1/22/2005
B69	-39.0741	177.9824	26	0.15	1/22/2005
B70	-39.0848	178.0323	40	unsuccessful	1/22/2005
B71	-39.0754	178.0510	62	0.48	1/22/2005
B72	-39.0577	178.0768	67	0.47	1/22/2005
B73	-39.0650	178.1665	129	0.32	1/23/2005
B74	-38.9864	178.1173	63	0.07	1/23/2005
B75	-38.9862	178.1665	254	0.50	1/23/2005
B76	-38.9076	178.2001	95	0.43	1/23/2005
B77	-38.7206	178.1396	38	0.31	1/26/2005
B78	-38.7201	178.1906	50	0.43	1/26/2005

Box Cores Core Name	Latitude (S)	Longitude (E)	Depth (m)	Length (cm)	Date of Collection
B79	-38.7369	178.1905	51	0.42	1/26/2005
B80	-38.7196	178.2391	59	0.40	1/26/2005
B81	-38.7193	178.2699	62	0.28	1/26/2005
B82	-38.7421	178.3845	111	0.43	1/26/2005
B83	-38.6832	178.2896	64	0.33	1/26/2005
B84	-38.6839	178.2499	61	0.42	1/26/2005
B85	-38.6838	178.1911	46	0.40	1/26/2005
B86	-38.6631	178.1902	45	0.36	1/26/2005
B87	-38.6883	178.1447	37	0.33	1/26/2005

APPENDIX B

B1. Definition of Terms and Equations Used to Determine Excess ^{210}Pb Activity

$^{209}\text{Po}_{\text{GA}}$ = Gross Area of ^{209}Po at time of counting

$^{210}\text{Po}_{\text{GA}}$ = Gross Area of ^{209}Po at time of counting

S_{wt} = sample weight

E_{w} = Weighing error = 0.01

T_{coll} = Date collected

T_{plt} = Date of plating

T_{cnt} = Date sample was counted

T_{spike} = Date spike was calibrated

A_{supp} = Supported ^{210}Pb activity = mean activities for the section of the core where background levels have been reached

E_{supp} = Supported ^{210}Pb Activity Error = 0.12

A_{s} = Spike activity at time of calibration

V_{s} = Spike volume

$E^{209}\text{Po}_{\text{cal}}$ = ^{209}Po calibrated activity error (per ml) = 3

$^{209}\text{Po}_{\text{corr}}$ = ^{209}Po activity corrected for volume used and decay from time of spike calibration to counting

$E^{209}\text{Po}_{\text{corr}}$ = Corrected ^{209}Po Activity Error

A_{total} = Total ^{210}Pb Activity at time of Plating

E_{total} = Absolute error total at time of plating

A_{xs} = Excess ^{210}Pb Activity at time of sample collection

E_{xs} = Absolute error excess at time of sample collection

$$^{209}\text{Po}_{\text{corr}} = A_s * V_s * \exp [-\ln(2) / (102 * 365.25) * (T_{\text{cnt}} - T_{\text{spike}})] \quad (1-B)$$

$$E^{209}\text{Po}_{\text{corr}} = E^{209}\text{Po}_{\text{cal}} * V_s * \exp [-\ln(2) / (102*365.25) * (T_{\text{cnt}} - T_{\text{spike}})] \quad (2-B)$$

$$A_{\text{total}} = (^{210}\text{Po}_{\text{GA}} / ^{209}\text{Po}_{\text{GA}} * ^{209}\text{Po}_{\text{corr}} / S_{\text{wt}}) / \exp [-\ln(2) / 138.4 * (T_{\text{cnt}} - T_{\text{plt}})] \quad (3-B)$$

$$E_{\text{total}} = ((((\text{SQRT} (^{210}\text{Po}_{\text{GA}} / ^{210}\text{Po}_{\text{GA}}^2 + ^{209}\text{Po}_{\text{GA}} / ^{209}\text{Po}_{\text{GA}}^2) * ^{210}\text{Po}_{\text{GA}} / ^{209}\text{Po}_{\text{GA}}) / (^{210}\text{Po}_{\text{GA}} / ^{209}\text{Po}_{\text{GA}} + E^{209}\text{Po}_{\text{corr}} / ^{209}\text{Po}_{\text{corr}}) * (^{210}\text{Po}_{\text{GA}} / ^{209}\text{Po}_{\text{GA}}) * ^{209}\text{Po}_{\text{corr}})) / ((^{210}\text{Po}_{\text{GA}} / ^{209}\text{Po}_{\text{GA}}) * ^{209}\text{Po}_{\text{corr}} + E_w / S_{\text{wt}}) * ^{210}\text{Po}_{\text{GA}} / ^{209}\text{Po}_{\text{GA}} * ^{209}\text{Po}_{\text{corr}} / S_{\text{wt}}) / \exp (-\ln(2) / 138.4 * (T_{\text{cnt}} - T_{\text{plt}})) \quad (4-B)$$

$$A_{\text{xs}} = (A_{\text{total}} - A_{\text{supp}}) / \exp [-\ln(2) / (22.3 * 365.25) * (T_{\text{plt}} - T_{\text{coll}})] \quad (5-B)$$

$$E_{\text{xs}} = (E_{\text{total}} + E_{\text{supp}}) / \exp [-\ln(2) / (22.3*365.25) * (T_{\text{plt}} - T_{\text{coll}})] \quad (6-B)$$

B2. ²¹⁰Pb Depths and Activities

Core Name	Depth (cm)	Total Activity (dpm/g)	Absolute Error Total (dpm/g)	Excess Activity (dpm/g)	Absolute Error Excess (dpm/g)
KC01	1	5.18	0.51	4.69	0.65
KC01	5	4.15	0.47	3.63	0.61
KC01	9	2.87	0.32	2.30	0.46
KC01	17	1.74	0.26	1.13	0.39
KC01	25	2.43	0.28	1.85	0.42
KC01	33	2.52	0.31	1.93	0.44
KC01	41	1.76	0.17	1.15	0.30
KC01	45	1.46	0.15	0.84	0.28
KC01	49	1.28	0.16	0.65	0.29
KC01	61	1.14	0.17	0.51	0.30
KC01	79	0.80	0.09	0.15	0.22
KC01	97	0.72	0.12	0.07	0.25
KC01	123	0.58	0.07	-0.07	0.19
KC02	1	4.54	0.36	4.02	0.50
KC02	5	3.07	0.26	2.51	0.40
KC02	9	2.18	0.18	1.59	0.31
KC02	13	2.23	0.21	1.64	0.34
KC02	21	1.81	0.18	1.21	0.31
KC02	29	1.78	0.17	1.17	0.30
KC02	37	1.36	0.13	0.74	0.26
KC02	41	1.17	0.11	0.55	0.24
KC02	49	1.00	0.12	0.38	0.25
KC02	55	0.96	0.11	0.33	0.24
KC02	61	0.93	0.10	0.30	0.22
KC02	67	0.75	0.09	0.11	0.22
KC02	79	0.64	0.09	0.00	0.21
KC07	1	4.89	0.42	4.17	0.55
KC07	5	5.38	0.45	4.67	0.59
KC07	9	4.56	0.39	3.83	0.52
KC07	17	3.09	0.26	2.31	0.40
KC07	25	2.60	0.22	1.81	0.36
KC07	29	2.55	0.22	1.76	0.35
KC07	33	2.27	0.20	1.47	0.33
KC07	41	2.31	0.21	1.51	0.34
KC07	49	2.34	0.21	1.54	0.34
KC07	61	1.51	0.13	0.69	0.26
KC07	73	1.59	0.17	0.77	0.30
KC07	85	1.18	0.14	0.34	0.27
KC07	97	1.03	0.10	0.19	0.23
KC07	113	1.07	0.11	0.24	0.24
KC07	133	0.87	0.09	0.03	0.21
KC07	153	0.76	0.10	-0.09	0.23
KC07	173	0.63	0.07	-0.22	0.19

Core Name	Depth (cm)	Total Activity (dpm/g)	Absolute Error Total (dpm/g)	Excess Activity (dpm/g)	Absolute Error Excess (dpm/g)
KC08	3	2.43	0.21	1.90	0.34
KC08	9	1.84	0.17	1.28	0.30
KC08	17	1.44	0.16	0.88	0.29
KC08	21	1.13	0.11	0.55	0.24
KC08	33	0.75	0.07	0.15	0.20
KC08	45	0.62	0.06	0.03	0.19
KC08	55	0.54	0.05	-0.06	0.18
KC08	67	0.61	0.06	0.01	0.19
KC08	79	0.65	0.06	0.06	0.19
KC08	97	0.57	0.06	-0.03	0.18
KC08	123	0.61	0.07	0.01	0.19
KC09	1	1.91	0.23	1.30	0.36
KC09	3	1.96	0.19	1.36	0.33
KC09	5	2.02	0.22	1.41	0.35
KC09	7	1.71	0.16	1.10	0.29
KC09	9	1.38	0.17	0.75	0.30
KC09	13	1.34	0.13	0.71	0.26
KC09	17	1.11	0.14	0.47	0.27
KC09	21	0.96	0.10	0.32	0.23
KC09	25	0.76	0.08	0.11	0.21
KC09	29	0.58	0.07	-0.08	0.20
KC09	33	0.68	0.07	0.03	0.19
KC09	41	0.60	0.06	-0.06	0.19
KC10	1	1.15	0.13	0.28	0.26
KC10	7	0.90	0.12	0.01	0.25
KC10	29	0.67	0.09	-0.23	0.22
KC10	41	0.84	0.10	-0.05	0.23
KC10	55	0.85	0.09	-0.04	0.22
KC10	67	1.02	0.12	0.13	0.25
KC10	79	1.06	0.11	0.18	0.24
KC11	7.5	5.59	0.51	5.17	0.65
KC11	9	5.80	0.51	5.35	0.65
KC11	17	3.57	0.33	3.07	0.47
KC11	21	2.88	0.25	2.34	0.38
KC11	25	1.22	0.12	0.63	0.25
KC11	29	1.67	0.17	1.09	0.30
KC11	29	1.53	0.14	0.96	0.27
KC11	33	1.09	0.10	0.49	0.23
KC11	41	0.87	0.11	0.26	0.23
KC11	55	0.63	0.07	0.01	0.20
KC11	61	0.61	0.06	-0.01	0.19
KC11	73	0.59	0.06	-0.03	0.19
KC11	85	0.59	0.07	-0.03	0.19
KC11	103	0.59	0.07	-0.02	0.19

Core Name	Depth (cm)	Total Activity (dpm/g)	Absolute Error Total (dpm/g)	Excess Activity (dpm/g)	Absolute Error Excess (dpm/g)
KC11	133	0.69	0.09	0.08	0.22
KC12	1	4.75	0.42	4.12	0.56
KC12	3	4.27	0.36	3.60	0.50
KC12	7	2.06	0.19	1.32	0.32
KC12	9	1.48	0.14	0.72	0.27
KC12	13	0.89	0.09	0.11	0.22
KC12	21	0.63	0.07	-0.16	0.19
KC12	33	0.66	0.07	-0.13	0.20
KC12	45	0.72	0.09	-0.06	0.21
KC12	55	0.72	0.07	-0.07	0.19
KC12	73	0.78	0.09	0.00	0.22
KC12	85	0.88	0.10	0.10	0.23
KC12	103	1.03	0.09	0.25	0.22
KC12	123	1.12	0.11	0.35	0.24
KC13	3	5.56	0.47	5.05	0.61
KC13	9	3.90	0.33	3.34	0.46
KC13	17	2.52	0.23	1.93	0.36
KC13	21	1.93	0.17	1.31	0.30
KC13	33	1.19	0.11	0.54	0.24
KC13	45	0.89	0.09	0.23	0.22
KC13	55	0.84	0.09	0.18	0.21
KC13	73	0.73	0.07	0.06	0.20
KC13	91	0.55	0.06	-0.12	0.18
KC13	113	0.60	0.06	-0.07	0.19
KC13	143	0.61	0.06	-0.06	0.19
KC14	1	5.65	0.41	4.93	0.54
KC14	5	4.75	0.45	4.02	0.58
KC14	9	4.73	0.39	3.99	0.52
KC14	17	3.55	0.29	2.79	0.41
KC14	25	2.67	0.23	1.90	0.36
KC14	33	2.45	0.21	1.68	0.34
KC14	41	2.25	0.19	1.47	0.32
KC14	49	2.52	0.22	1.75	0.34
KC14	61	2.15	0.20	1.37	0.32
KC14	67	1.92	0.17	1.14	0.29
KC14	79	1.65	0.15	0.87	0.27
KC14	91	1.51	0.13	0.72	0.26
KC14	103	1.30	0.13	0.50	0.26
KC14	123	1.02	0.12	0.23	0.24
KC14	143	0.89	0.09	0.09	0.22
KC14	163	0.73	0.09	-0.07	0.21
KC14	183	0.77	0.08	-0.03	0.21
KC14	211	0.81	0.10	0.01	0.22

Core Name	Depth (cm)	Total Activity (dpm/g)	Absolute Error Total (dpm/g)	Excess Activity (dpm/g)	Absolute Error Excess (dpm/g)
KC15	1	5.26	0.49	4.82	0.63
KC15	7	4.61	0.54	4.15	0.68
KC15	17	2.40	0.21	1.86	0.34
KC15	29	2.00	0.18	1.46	0.31
KC15	41	1.67	0.15	1.12	0.28
KC15	55	1.17	0.11	0.60	0.24
KC15	67	1.34	0.12	0.77	0.25
KC15	79	0.96	0.09	0.38	0.22
KC15	97	0.86	0.08	0.28	0.21
KC15	123	0.65	0.06	0.06	0.19
KC15	133	0.51	0.08	-0.08	0.21
KC15	143	0.61	0.07	0.02	0.20
KC16	1	5.11	0.45	4.67	0.59
KC16	7	4.33	0.38	3.85	0.51
KC16	17	3.48	0.31	2.98	0.45
KC16	29	1.74	0.17	1.18	0.30
KC16	41	2.02	0.19	1.48	0.33
KC16	55	1.15	0.11	0.58	0.24
KC16	67	1.16	0.16	0.59	0.29
KC16	79	0.76	0.08	0.17	0.21
KC16	97	0.59	0.06	0.00	0.19
KC16	113	0.62	0.07	0.03	0.20
KC16	123	0.57	0.06	-0.02	0.18
KC17	3	4.06	0.34	3.45	0.48
KC17	7	3.24	0.28	2.61	0.42
KC17	13	2.06	0.19	1.39	0.32
KC17	17	1.53	0.14	0.85	0.27
KC17	21	2.31	0.20	1.65	0.34
KC17	25	2.33	0.21	1.67	0.34
KC17	33	1.78	0.16	1.10	0.29
KC17	41	1.76	0.16	1.08	0.29
KC17	49	1.74	0.16	1.06	0.29
KC17	55	1.37	0.13	0.68	0.26
KC17	61	1.11	0.13	0.41	0.25
KC17	67	1.16	0.11	0.46	0.24
KC17	79	1.14	0.11	0.44	0.24
KC17	85	1.00	0.10	0.30	0.22
KC17	97	0.96	0.09	0.26	0.22
KC17	113	0.80	0.08	0.09	0.20
KC17	133	0.65	0.06	-0.06	0.18
KC17	153	0.69	0.07	-0.03	0.19
KC18	1	1.90	0.17	1.10	0.30
KC18	3	2.32	0.23	1.50	0.35

Core Name	Depth (cm)	Total Activity (dpm/g)	Absolute Error Total (dpm/g)	Excess Activity (dpm/g)	Absolute Error Excess (dpm/g)
KC18	5	2.02	0.21	1.20	0.33
KC18	7	1.25	0.11	0.43	0.24
KC18	13	1.04	0.11	0.21	0.23
KC18	17	0.92	0.09	0.09	0.21
KC18	29	1.04	0.10	0.22	0.22
KC18	41	0.83	0.08	0.00	0.21
KC18	55	0.76	0.08	-0.07	0.21
KC18	61	0.60	0.06	-0.24	0.19
KC19	3	6.35	0.56	5.70	0.70
KC19	9	5.35	0.52	4.67	0.66
KC19	21	3.40	0.34	2.65	0.48
KC19	25	2.16	0.21	1.38	0.35
KC19	29	2.00	0.19	1.21	0.32
KC19	33	1.61	0.18	0.80	0.31
KC19	45	1.45	0.18	0.64	0.31
KC19	55	0.93	0.10	0.10	0.23
KC19	61	0.62	0.08	-0.22	0.20
KC19	79	0.89	0.09	0.06	0.22
KC19	123	0.92	0.09	0.09	0.21
KC19	173	0.81	0.08	-0.02	0.21
KC20	1	9.06	0.62	7.78	0.75
KC20	5	7.79	0.53	6.48	0.66
KC20	9	6.54	0.47	5.22	0.59
KC20	17	3.78	0.28	2.42	0.40
KC20	25	3.17	0.24	1.81	0.36
KC20	33	1.67	0.13	0.29	0.25
KC20	41	1.80	0.14	0.41	0.26
KC20	49	1.28	0.11	-0.11	0.23
KC20	61	1.32	0.11	-0.07	0.23
KC20	73	1.25	0.13	-0.14	0.26
KC20	85	1.39	0.12	0.00	0.24
KC20	91	1.48	0.12	0.09	0.24
KC20	97	1.45	0.11	0.06	0.24
KC20	103	1.41	0.11	0.02	0.23
KC20	113	1.44	0.11	0.05	0.23
KC20	133	1.39	0.11	0.00	0.23
KC20	153	1.47	0.11	0.08	0.24
KC20	173	1.40	0.11	0.01	0.23
KC21	3	5.57	0.47	4.73	0.61
KC21	9	3.83	0.32	2.93	0.46
KC21	17	2.35	0.25	1.42	0.38
KC21	21	1.29	0.12	0.32	0.24
KC21	25	0.75	0.09	-0.24	0.22

Core Name	Depth (cm)	Total Activity (dpm/g)	Absolute Error Total (dpm/g)	Excess Activity (dpm/g)	Absolute Error Excess (dpm/g)
KC21	33	0.73	0.07	-0.27	0.20
KC21	37	0.89	0.10	-0.10	0.23
KC21	45	1.16	0.11	0.18	0.24
KC21	61	1.02	0.09	0.03	0.22
KC21	79	1.09	0.11	0.11	0.23
KC21	97	1.12	0.10	0.14	0.23
KC21	123	1.08	0.11	0.10	0.23
KC21	143	1.04	0.10	0.05	0.23
KC22	1	3.90	0.33	3.38	0.46
KC22	5	3.22	0.27	2.68	0.40
KC22	7	2.57	0.22	2.01	0.35
KC22	9	2.16	0.19	1.58	0.32
KC22	13	1.44	0.15	0.84	0.28
KC22	17	1.19	0.11	0.58	0.23
KC22	21	1.23	0.11	0.62	0.24
KC22	25	1.08	0.10	0.47	0.23
KC22	29	0.85	0.08	0.24	0.21
KC22	33	0.62	0.07	0.00	0.20
KC22	37	0.65	0.06	0.02	0.19
KC22	41	0.64	0.06	0.02	0.19
KC22	45	0.62	0.06	-0.01	0.19
KC22	49	0.60	0.06	-0.02	0.18
KC22	55	0.70	0.07	0.08	0.19
KC22	67	0.59	0.06	-0.04	0.18
KC22	79	0.54	0.05	-0.08	0.18
KC22	91	0.66	0.06	0.04	0.19
KC23	1	2.24	0.18	1.73	0.31
KC23	3	1.54	0.13	1.01	0.25
KC23	5	1.64	0.13	1.11	0.26
KC23	7	1.45	0.12	0.91	0.25
KC23	9	1.53	0.13	0.99	0.25
KC23	11	1.34	0.11	0.80	0.24
KC23	17	1.05	0.10	0.50	0.22
KC23	21	1.18	0.11	0.63	0.23
KC23	25	1.33	0.12	0.79	0.25
KC23	29	1.09	0.10	0.54	0.23
KC23	33	1.05	0.10	0.50	0.23
KC23	37	0.83	0.08	0.28	0.21
KC23	41	0.68	0.07	0.11	0.19
KC23	45	0.62	0.06	0.06	0.19
KC23	49	0.56	0.06	0.00	0.18
KC23	55	0.57	0.06	0.00	0.18
KC23	61	0.51	0.05	-0.06	0.18

Core Name	Depth (cm)	Total Activity (dpm/g)	Absolute Error Total (dpm/g)	Excess Activity (dpm/g)	Absolute Error Excess (dpm/g)
KC24	1	1.66	0.17	0.89	0.30
KC24	5	1.15	0.12	0.36	0.25
KC24	9	1.12	0.12	0.33	0.25
KC24	13	1.08	0.12	0.29	0.25
KC24	17	1.17	0.13	0.38	0.26
KC24	21	1.18	0.12	0.39	0.25
KC24	25	1.19	0.13	0.40	0.26
KC24	29	0.91	0.10	0.12	0.23
KC24	33	1.15	0.11	0.36	0.23
KC24	37	1.18	0.13	0.40	0.26
KC24	41	0.89	0.09	0.09	0.22
KC24	45	0.79	0.09	-0.01	0.22
KC24	49	0.78	0.08	-0.02	0.20
KC24	55	0.79	0.08	-0.02	0.20
KC24	61	0.98	0.10	0.19	0.22
KC24	67	0.72	0.07	-0.08	0.20
KC24	79	0.65	0.08	-0.16	0.21
KC26	1	3.94	0.35	2.54	0.48
KC26	5	3.33	0.28	1.92	0.41
KC26	9	2.41	0.20	0.98	0.33
KC26	13	1.98	0.17	0.54	0.29
KC26	17	1.73	0.15	0.29	0.28
KC26	25	2.04	0.18	0.61	0.30
KC26	33	1.43	0.15	-0.01	0.27
KC26	41	1.21	0.11	-0.23	0.23
KC26	49	1.72	0.16	0.29	0.28
KC26	61	1.46	0.20	0.02	0.33
KC26	73	1.40	0.13	-0.04	0.25
KC26	85	1.51	0.14	0.07	0.26
KC26	97	1.43	0.13	-0.01	0.26
KC26	113	1.41	0.13	-0.03	0.25
KC26	133	1.39	0.14	-0.05	0.26
KC26	153	1.37	0.15	-0.07	0.27
KC26	173	1.40	0.16	-0.04	0.28
KC26	193	0.95	0.13	-0.50	0.25
KC27	1	4.16	0.33	2.86	0.45
KC27	5	3.76	0.32	2.46	0.45
KC27	9	2.46	0.28	1.13	0.40
KC27	13	1.94	0.17	0.61	0.30
KC27	17	2.12	0.19	0.79	0.31
KC27	25	1.74	0.19	0.40	0.32
KC27	33	1.91	0.17	0.58	0.30
KC27	41	1.61	0.14	0.27	0.27
KC27	49	1.21	0.11	-0.14	0.23
KC27	61	1.71	0.15	0.37	0.27

Core Name	Depth (cm)	Total Activity (dpm/g)	Absolute Error Total (dpm/g)	Excess Activity (dpm/g)	Absolute Error Excess (dpm/g)
KC27	73	1.48	0.12	0.13	0.25
KC27	85	1.54	0.14	0.20	0.26
KC27	97	1.38	0.12	0.03	0.25
KC27	113	1.39	0.11	0.05	0.23
KC27	133	1.54	0.12	0.20	0.24
KC27	153	1.37	0.11	0.03	0.23
KC27	173	0.99	0.10	-0.36	0.22
KC27	211	0.83	0.09	-0.52	0.22
KC28	1	1.30	0.12	0.09	0.25
KC28	9	1.23	0.11	0.02	0.24
KC28	21	0.99	0.09	-0.23	0.22
KC28	37	1.07	0.10	-0.14	0.23
KC28	49	1.09	0.10	-0.13	0.23
KC28	61	2.54	0.25	1.38	0.39
KC28	79	0.92	0.08	-0.30	0.21
KC28	91	1.02	0.10	-0.19	0.22
KC28	103	0.74	0.08	-0.48	0.21
KC28	123	1.07	0.10	-0.14	0.23
KC30	1	5.26	0.52	4.53	0.66
KC30	5	2.95	0.31	2.14	0.44
KC30	9	1.76	0.20	0.90	0.33
KC30	13	1.35	0.20	0.48	0.34
KC30	17	0.78	0.12	-0.12	0.25
KC30	25	0.91	0.10	0.02	0.23
KC30	33	0.77	0.09	-0.13	0.22
KC30	49	0.96	0.11	0.07	0.24
KC30	61	0.92	0.10	0.04	0.23
KC30	79	0.99	0.10	0.11	0.23
KC31	1	10.57	0.72	9.54	0.85
KC31	5	9.06	0.62	8.01	0.75
KC31	9	6.80	0.48	5.72	0.61
KC31	17	6.63	0.45	5.55	0.58
KC31	25	5.86	0.41	4.77	0.54
KC31	33	4.24	0.30	3.12	0.43
KC31	41	5.59	0.39	4.49	0.52
KC31	49	2.38	0.18	1.24	0.30
KC31	61	1.13	0.09	-0.03	0.21
KC31	73	0.88	0.07	-0.28	0.20
KC31	82	0.95	0.08	-0.21	0.20
KC31	88	0.88	0.07	-0.28	0.20
KC31	97	1.13	0.11	-0.03	0.23
KC31	113	1.35	0.11	0.19	0.24
KC31	133	1.44	0.12	0.29	0.24

Core Name	Depth (cm)	Total Activity (dpm/g)	Absolute Error Total (dpm/g)	Excess Activity (dpm/g)	Absolute Error Excess (dpm/g)
KC31	163	1.39	0.11	0.23	0.24
KC31	193	1.36	0.11	0.20	0.24
KC31	229	1.08	0.10	-0.08	0.22
KC32	1	6.94	0.74	6.25	0.89
KC32	5	6.20	0.83	5.48	0.98
KC32	9	6.41	0.69	5.70	0.84
KC32	17	6.31	0.65	5.60	0.80
KC32	25	6.23	0.66	5.52	0.81
KC32	33	4.97	0.91	4.21	1.07
KC32	45	3.06	0.29	2.23	0.42
KC32	55	1.24	0.13	0.34	0.26
KC32	61	1.10	0.13	0.19	0.26
KC32	79	0.96	0.14	0.05	0.27
KC32	97	0.94	0.13	0.03	0.26
KC32	123	0.77	0.09	-0.15	0.21
KC32	143	0.79	0.09	-0.13	0.22
KC33	1	3.25	0.32	2.71	0.45
KC33	5	2.29	0.22	1.72	0.35
KC33	9	1.84	0.18	1.25	0.31
KC33	17	0.83	0.09	0.20	0.22
KC33	25	0.61	0.08	-0.03	0.21
KC33	29	0.66	0.07	0.03	0.20
KC34	1	2.91	0.29	2.44	0.43
KC34	5	1.70	0.24	1.18	0.37
KC34	9	1.80	0.19	1.28	0.32
KC34	17	1.25	0.15	0.72	0.28
KC34	25	0.95	0.10	0.41	0.23
KC34	33	0.97	0.11	0.43	0.24
KC34	37	0.70	0.08	0.14	0.21
KC34	45	0.55	0.06	-0.01	0.19
KC34	49	0.61	0.08	0.05	0.20
KC34	61	0.53	0.07	-0.03	0.20
KC34	73	0.56	0.07	0.00	0.20
KC35	1	5.20	0.41	4.50	0.54
KC35	3	5.40	0.43	4.71	0.56
KC35	5	4.27	0.34	3.56	0.47
KC35	9	3.57	0.29	2.85	0.41
KC35	17	2.54	0.18	1.80	0.31
KC35	25	1.65	0.13	0.90	0.25
KC35	33	1.77	0.14	1.01	0.26
KC35	41	2.45	0.18	1.71	0.31
KC35	49	2.06	0.16	1.31	0.28

Core Name	Depth (cm)	Total Activity (dpm/g)	Absolute Error Total (dpm/g)	Excess Activity (dpm/g)	Absolute Error Excess (dpm/g)
KC35	61	2.42	0.22	1.68	0.35
KC35	73	1.82	0.16	1.07	0.29
KC35	85	1.42	0.28	0.66	0.41
KC35	97	1.42	0.13	0.66	0.25
KC35	113	1.23	0.12	0.47	0.24
KC35	133	1.10	0.11	0.34	0.23
KC35	153	0.95	0.10	0.18	0.23
KC35	173	0.77	0.09	0.00	0.22
KC36	3	4.88	0.45	4.34	0.59
KC36	9	3.89	0.34	3.32	0.47
KC36	21	2.63	0.23	2.01	0.36
KC36	33	2.23	0.20	1.60	0.33
KC36	45	2.06	0.18	1.42	0.31
KC36	61	1.39	0.15	0.73	0.28
KC36	79	1.04	0.16	0.37	0.28
KC36	97	1.02	0.15	0.35	0.28
KC36	123	0.96	0.09	0.28	0.22
KC36	153	0.83	0.08	0.15	0.20
KC36	163	0.45	0.07	-0.23	0.19
KC36	173	0.82	0.09	0.15	0.22
KC36	183	0.56	0.07	-0.13	0.20
KC36	193	0.73	0.07	0.05	0.20
KC36	211	0.37	0.04	-0.32	0.17
KC36	229	0.72	0.08	0.04	0.21
KC37	1	4.62	0.42	4.04	0.56
KC37	9	3.97	0.37	3.36	0.51
KC37	13	3.02	0.28	2.39	0.42
KC37	17	2.62	0.25	1.97	0.38
KC37	25	2.18	0.20	1.52	0.33
KC37	33	1.93	0.18	1.26	0.30
KC37	37	1.70	0.16	1.03	0.29
KC37	41	1.56	0.15	0.88	0.27
KC37	49	1.17	0.12	0.47	0.25
KC37	55	1.09	0.11	0.39	0.23
KC37	61	1.02	0.10	0.32	0.23
KC37	73	0.94	0.09	0.24	0.22
KC37	85	0.84	0.07	0.13	0.20
KC37	97	0.72	0.07	0.02	0.19
KC37	113	0.76	0.08	0.05	0.21
KC37	133	0.65	0.07	-0.06	0.19
KC37	153	0.70	0.07	-0.01	0.19
KC40	1	2.16	0.18	1.73	0.31
KC40	7	2.00	0.17	1.56	0.30
KC40	9	1.80	0.17	1.36	0.30

Core Name	Depth (cm)	Total Activity (dpm/g)	Absolute Error Total (dpm/g)	Excess Activity (dpm/g)	Absolute Error Excess (dpm/g)
KC40	13	1.01	0.09	0.54	0.22
KC40	17	0.00	0.00	-0.51	0.12
KC40	21	0.52	0.05	0.04	0.18
KC40	33	0.45	0.05	-0.04	0.17
KC40	45	0.42	0.04	-0.07	0.17
KC40	55	0.46	0.05	-0.03	0.17
KC40	73	0.57	0.05	0.08	0.18
KC40	85	0.75	0.07	0.27	0.20
KC40	103	0.73	0.07	0.25	0.20
KC41	1	2.97	0.29	1.69	0.42
KC41	5	2.24	0.23	0.93	0.36
KC41	9	7.07	0.86	5.94	1.02
KC41	17	1.32	0.14	-0.03	0.27
KC41	17	1.30	0.13	-0.05	0.26
KC41	33	1.42	0.16	0.07	0.29
KC42	1	3.32	0.29	2.47	0.43
KC42	5	2.87	0.27	2.00	0.40
KC42	9	1.91	0.18	1.01	0.31
KC42	17	1.39	0.15	0.46	0.28
KC42	25	1.23	0.14	0.30	0.27
KC42	29	0.94	0.11	0.00	0.24
KC44	1	1.96	0.23	0.96	0.36
KC44	5	1.91	0.20	0.92	0.33
KC44	9	1.57	0.16	0.56	0.29
KC44	13	1.01	0.11	-0.02	0.24
KC44	17	1.05	0.11	0.02	0.24
KC45	1	4.91	0.42	4.27	0.56
KC45	5	5.13	0.46	4.49	0.60
KC45	9	4.13	0.36	3.46	0.49
KC45	13	3.26	0.29	2.57	0.42
KC45	17	2.89	0.25	2.19	0.39
KC45	25	2.69	0.24	1.98	0.37
KC45	33	2.20	0.21	1.48	0.34
KC45	41	2.05	0.19	1.32	0.32
KC45	49	1.72	0.17	0.98	0.30
KC45	61	1.25	0.13	0.49	0.25
KC45	67	1.03	0.10	0.26	0.23
KC45	79	1.13	0.14	0.37	0.26
KC45	91	0.97	0.10	0.20	0.23
KC45	103	0.78	0.09	0.00	0.22
KC45	123	0.84	0.10	0.07	0.22
KC45	143	0.78	0.09	0.01	0.21
KC45	163	0.75	0.13	-0.02	0.26

Core Name	Depth (cm)	Total Activity (dpm/g)	Absolute Error Total (dpm/g)	Excess Activity (dpm/g)	Absolute Error Excess (dpm/g)
KC45	183	0.72	0.08	-0.06	0.21
KC46	1	5.13	0.43	4.56	0.57
KC46	5	5.00	0.48	4.45	0.62
KC46	9	4.28	0.36	3.69	0.50
KC46	21	7.18	0.71	6.68	0.86
KC46	25	2.34	0.28	1.69	0.42
KC46	29	2.10	0.22	1.44	0.35
KC46	33	1.99	0.17	1.32	0.30
KC46	45	1.53	0.14	0.84	0.27
KC46	61	1.13	0.11	0.42	0.23
KC46	79	0.97	0.09	0.26	0.22
KC46	97	0.82	0.08	0.10	0.21
KC46	123	0.72	0.07	0.00	0.20
KC46	123	0.74	0.08	0.02	0.21
KC46	153	0.68	0.07	-0.04	0.20
KC46	155	0.67	0.08	-0.05	0.20
KC46	183	0.71	0.08	-0.01	0.21
KC46	193	0.69	0.07	-0.03	0.20
KC47	1	6.06	0.42	5.14	0.55
KC47	5	6.48	0.45	5.57	0.58
KC47	9	4.79	0.37	3.85	0.50
KC47	17	3.00	0.22	2.04	0.34
KC47	25	2.85	0.21	1.89	0.34
KC47	33	2.67	0.20	1.71	0.32
KC47	41	2.37	0.19	1.41	0.31
KC47	49	2.07	0.16	1.10	0.28
KC47	67	1.65	0.14	0.68	0.26
KC47	79	1.25	0.10	0.27	0.22
KC47	97	1.06	0.09	0.08	0.22
KC47	113	1.06	0.09	0.08	0.21
KC47	123	1.04	0.09	0.06	0.21
KC47	133	1.05	0.09	0.07	0.21
KC47	163	0.88	0.08	-0.10	0.20
KC47	183	0.95	0.08	-0.04	0.21
KC47	211	0.83	0.07	-0.15	0.20
KC48	3	5.06	0.42	4.52	0.56
KC48	9	3.50	0.30	2.90	0.43
KC48	21	2.56	0.23	1.93	0.36
KC48	29	2.27	0.21	1.64	0.35
KC48	33	2.33	0.31	1.69	0.44
KC48	45	2.09	0.19	1.44	0.32
KC48	55	1.90	0.17	1.25	0.30
KC48	67	1.60	0.14	0.94	0.27
KC48	79	1.27	0.12	0.59	0.24

Core Name	Depth (cm)	Total Activity (dpm/g)	Absolute Error Total (dpm/g)	Excess Activity (dpm/g)	Absolute Error Excess (dpm/g)
KC48	91	1.16	0.11	0.48	0.24
KC48	113	0.97	0.09	0.29	0.22
KC48	143	0.49	0.05	-0.21	0.17
KC48	163	0.73	0.08	0.04	0.21
KC48	183	0.74	0.08	0.05	0.21
KC48	193	0.76	0.07	0.07	0.20
KC48	211	0.74	0.08	0.05	0.21
KC49	1	4.56	0.43	3.88	0.57
KC49	5	5.40	0.49	4.76	0.63
KC49	9	4.39	0.42	3.71	0.56
KC49	17	3.10	0.30	2.37	0.44
KC49	25	2.63	0.25	1.88	0.39
KC49	37	1.91	0.25	1.13	0.38
KC49	49	1.91	0.23	1.14	0.36
KC49	67	1.30	0.22	0.51	0.36
KC49	91	1.02	0.11	0.21	0.23
KC49	123	0.84	0.09	0.02	0.22
KC49	163	0.80	0.10	-0.02	0.22
KC51	1	2.91	0.28	2.39	0.42
KC51	5	1.17	0.10	0.59	0.23
KC51	9	2.36	0.24	1.82	0.37
KC51	13	1.98	0.23	1.43	0.37
KC51	17	1.66	0.17	1.09	0.31
KC51	25	0.66	0.07	0.06	0.20
KC51	37	0.55	0.07	-0.06	0.20
KC52	1	6.43	0.61	5.86	0.76
KC52	5	5.93	0.55	5.34	0.69
KC52	13	3.77	0.34	3.11	0.47
KC52	17	2.77	0.28	2.06	0.41
KC52	25	1.77	0.18	1.03	0.31
KC52	37	1.77	0.17	1.03	0.30
KC52	49	1.22	0.12	0.45	0.25
KC52	61	1.06	0.12	0.28	0.25
KC52	73	0.74	0.08	-0.05	0.21
KC52	91	0.87	0.09	0.09	0.22
KC52	133	0.76	0.08	-0.02	0.21
KC52	173	0.76	0.09	-0.02	0.22
KC53	1	10.30	0.91	9.63	1.07
KC53	5	10.43	0.97	9.77	1.13
KC53	9	11.41	1.11	10.79	1.27
KC53	17	9.12	0.82	8.41	0.98
KC53	25	7.75	0.71	6.99	0.86
KC53	37	5.35	0.57	4.49	0.71

Core Name	Depth (cm)	Total Activity (dpm/g)	Absolute Error Total (dpm/g)	Excess Activity (dpm/g)	Absolute Error Excess (dpm/g)
KC53	49	5.23	0.51	4.37	0.66
KC53	61	5.17	0.50	4.31	0.65
KC53	73	3.21	0.29	2.28	0.43
KC53	91	3.40	0.31	2.48	0.44
KC53	133	1.98	0.19	1.00	0.32
KC53	173	1.62	0.16	0.62	0.29
KC53	211	1.07	0.13	0.05	0.26
KC53	229	1.03	0.11	0.01	0.23
KC53	245	0.98	0.10	-0.04	0.22
KC53	265	0.99	0.17	-0.02	0.30
KC54	1	7.45	0.62	6.83	0.76
KC54	7	8.02	0.68	7.41	0.83
KC54	13	5.84	0.47	5.16	0.61
KC54	21	6.54	0.53	5.89	0.68
KC54	33	4.32	0.36	3.58	0.50
KC54	41	3.61	0.31	2.85	0.44
KC54	49	3.45	0.34	2.70	0.48
KC54	55	1.33	0.13	0.50	0.26
KC54	61	1.63	0.17	0.80	0.30
KC54	67	0.75	0.08	-0.10	0.20
KC54	79	0.81	0.08	-0.04	0.20
KC54	97	0.71	0.07	-0.15	0.19
KC54	113	0.79	0.08	-0.07	0.21
KC54	133	1.04	0.09	0.19	0.22
KC54	183	1.02	0.11	0.17	0.24
KC55	1	4.58	0.41	3.67	0.55
KC55	5	3.99	0.34	3.05	0.48
KC55	7	3.52	0.33	2.57	0.47
KC55	9	2.87	0.26	1.89	0.39
KC55	13	2.50	0.25	1.51	0.38
KC55	17	1.47	0.13	0.44	0.26
KC55	25	0.92	0.09	-0.12	0.21
KC55	33	1.04	0.10	0.01	0.23
KC55	41	1.12	0.11	0.09	0.24
KC55	49	1.22	0.12	0.19	0.25
KC55	61	1.08	0.10	0.05	0.23
KC55	97	0.84	0.08	-0.20	0.20
KC56	1	4.35	0.37	3.34	0.51
KC56	5	2.96	0.26	1.91	0.39
KC56	9	2.65	0.23	1.59	0.36
KC56	17	2.04	0.18	0.96	0.31
KC56	21	1.66	0.17	0.57	0.30
KC56	25	1.29	0.12	0.18	0.25
KC56	33	1.15	0.11	0.04	0.23

Core Name	Depth (cm)	Total Activity (dpm/g)	Absolute Error Total (dpm/g)	Excess Activity (dpm/g)	Absolute Error Excess (dpm/g)
KC56	45	1.05	0.10	-0.06	0.22
KC56	55	1.11	0.10	-0.01	0.23
KC56	73	1.13	0.11	0.02	0.24
KC56	91	1.08	0.11	-0.04	0.23
KC56	123	1.16	0.11	0.05	0.24
KC57	1	2.63	0.25	1.83	0.39
KC57	5	2.26	0.23	1.44	0.37
KC57	9	0.98	0.11	0.11	0.24
KC57	17	0.82	0.10	-0.06	0.23
KC57	25	0.72	0.08	-0.16	0.21
KC57	33	0.91	0.10	0.04	0.23
KC57	45	0.93	0.11	0.06	0.24
KC58	1	2.95	0.34	2.47	0.47
KC58	5	2.38	0.24	1.88	0.37
KC58	9	1.85	0.16	1.33	0.29
KC58	17	1.20	0.13	0.65	0.26
KC58	25	0.75	0.08	0.18	0.20
KC58	33	0.66	0.07	0.09	0.19
KC58	49	0.50	0.06	-0.07	0.18
KC58	55	0.55	0.07	-0.02	0.20
KC59	1	4.91	0.38	4.08	0.50
KC59	5	3.84	0.28	2.99	0.41
KC59	9	3.17	0.23	2.31	0.36
KC59	17	2.66	0.21	1.80	0.34
KC59	21	2.39	0.21	1.53	0.33
KC59	25	2.05	0.15	1.18	0.28
KC59	37	1.50	0.13	0.63	0.25
KC59	45	1.30	0.11	0.42	0.23
KC59	61	0.96	0.09	0.08	0.21
KC59	73	0.93	0.08	0.04	0.20
KC59	85	0.89	0.08	0.01	0.20
KC59	97	0.81	0.07	-0.08	0.19
KC59	103	0.89	0.08	0.00	0.20
KC59	123	0.89	0.07	0.00	0.20
KC59	143	0.85	0.07	-0.04	0.19
KC60	1	4.81	0.47	4.20	0.61
KC60	5	4.15	0.46	3.52	0.61
KC60	9	3.03	0.32	2.35	0.46
KC60	17	2.52	0.28	1.82	0.41
KC60	25	2.31	0.24	1.60	0.37
KC60	37	1.56	0.17	0.82	0.30
KC60	49	1.36	0.15	0.62	0.28
KC60	61	0.94	0.11	0.18	0.24

Core Name	Depth (cm)	Total Activity (dpm/g)	Absolute Error Total (dpm/g)	Excess Activity (dpm/g)	Absolute Error Excess (dpm/g)
KC60	79	0.83	0.09	0.07	0.21
KC60	91	0.75	0.08	-0.01	0.21
KC60	123	0.71	0.08	-0.06	0.21
KC60	143	0.66	0.07	-0.11	0.20
KC60	163	0.71	0.07	-0.06	0.20
KC61	1	5.71	0.48	4.83	0.62
KC61	5	4.84	0.40	3.94	0.54
KC61	9	4.33	0.40	3.40	0.53
KC61	17	3.00	0.26	2.03	0.39
KC61	25	2.38	0.20	1.39	0.34
KC61	33	2.38	0.21	1.39	0.34
KC61	37	1.93	0.18	0.93	0.32
KC61	45	0.90	0.11	-0.13	0.24
KC61	55	0.89	0.10	-0.15	0.22
KC61	67	1.02	0.10	-0.02	0.22
KC61	79	1.19	0.12	0.16	0.24
KC61	103	1.08	0.12	0.05	0.25
KC61	123	1.13	0.11	0.10	0.24
KC62	1	7.32	0.57	6.38	0.70
KC62	5	6.87	0.55	5.93	0.69
KC62	9	5.56	0.46	4.60	0.58
KC62	13	5.00	0.41	4.03	0.53
KC62	17	4.88	0.42	3.91	0.55
KC62	25	5.27	0.42	4.30	0.55
KC62	33	3.30	0.28	2.30	0.40
KC62	41	1.48	0.14	0.44	0.26
KC62	49	1.04	0.08	0.00	0.21
KC62	61	0.84	0.08	-0.20	0.20
KC62	67	0.92	0.09	-0.12	0.22
KC62	79	1.00	0.09	-0.04	0.22
KC62	85	1.18	0.12	0.14	0.24
KC62	97	1.12	0.15	0.08	0.27
KC62	113	1.13	0.10	0.09	0.22
KC62	133	1.24	0.14	0.21	0.26
KC62	153	0.88	0.11	-0.16	0.23
KC63	1	8.11	0.75	7.49	0.90
KC63	5	7.21	0.69	6.55	0.84
KC63	9	6.44	0.62	5.76	0.77
KC63	17	6.45	0.66	5.77	0.81
KC63	25	2.47	0.26	1.64	0.39
KC63	37	1.25	0.14	0.37	0.26
KC63	49	0.86	0.09	-0.03	0.22
KC63	61	0.71	0.09	-0.19	0.21
KC63	79	0.71	0.07	-0.19	0.20

Core Name	Depth (cm)	Total Activity (dpm/g)	Absolute Error Total (dpm/g)	Excess Activity (dpm/g)	Absolute Error Excess (dpm/g)
KC63	97	1.06	0.14	0.18	0.27
KC63	123	1.07	0.11	0.18	0.24
KC63	183	0.94	0.11	0.05	0.23
KC64	1	2.83	0.27	2.36	0.41
KC64	5	2.37	0.22	1.88	0.35
KC64	9	1.82	0.18	1.31	0.31
KC64	17	0.74	0.08	0.19	0.21
KC64	25	0.56	0.06	0.00	0.19
KC64	33	0.55	0.06	0.00	0.19
KC65	1	5.10	0.45	4.53	0.59
KC65	5	4.21	0.36	3.61	0.49
KC65	9	3.32	0.30	2.69	0.43
KC65	17	2.47	0.22	1.81	0.35
KC65	25	1.79	0.19	1.10	0.32
KC65	33	1.46	0.14	0.77	0.27
KC65	41	1.09	0.11	0.38	0.24
KC65	55	0.94	0.09	0.23	0.22
KC65	73	0.74	0.08	0.02	0.20
KC65	91	0.65	0.07	-0.08	0.19
KC65	123	0.65	0.08	-0.07	0.21
KC65	153	0.62	0.07	-0.10	0.19
KC66	1	2.36	0.20	1.63	0.33
KC66	5	3.41	0.29	2.71	0.43
KC66	9	1.61	0.15	0.85	0.27
KC66	21	1.62	0.15	0.86	0.28
KC66	25	1.32	0.12	0.55	0.25
KC66	33	1.27	0.12	0.49	0.24
KC66	37	1.26	0.15	0.48	0.28
KC66	45	1.18	0.15	0.41	0.28
KC66	49	1.86	0.20	1.11	0.33
KC66	55	1.85	0.17	1.10	0.30
KC66	61	1.91	0.21	1.16	0.35
KC66	67	15.26	2.65	15.02	2.87
KC66	73	1.27	0.12	0.50	0.25
KC66	91	1.00	0.10	0.22	0.22
KC66	97	0.85	0.09	0.06	0.22
KC66	113	0.67	0.08	-0.12	0.21
KC66	133	0.75	0.09	-0.04	0.22
KC66	143	0.68	0.07	-0.12	0.20
KC67	1	3.69	0.35	2.94	0.49
KC67	7	4.12	0.53	3.39	0.68
KC67	13	2.67	0.25	1.89	0.39
KC67	21	2.08	0.31	1.28	0.44

Core Name	Depth (cm)	Total Activity (dpm/g)	Absolute Error Total (dpm/g)	Excess Activity (dpm/g)	Absolute Error Excess (dpm/g)
KC67	33	1.99	0.32	1.18	0.45
KC67	45	1.81	0.21	0.99	0.34
KC67	67	1.39	0.14	0.56	0.27
KC67	85	1.18	0.12	0.34	0.25
KC67	103	0.99	0.11	0.14	0.24
KC67	123	0.87	0.09	0.02	0.21
KC67	153	0.75	0.08	-0.11	0.21
KC67	163	0.84	0.09	-0.01	0.22
KC67	193	0.82	0.09	-0.04	0.21
KC68	1	4.59	0.45	4.03	0.59
KC68	5	3.96	0.41	3.38	0.55
KC68	9	3.14	0.32	2.53	0.46
KC68	13	2.60	0.26	1.97	0.39
KC68	17	2.75	0.39	2.12	0.53
KC68	21	1.48	0.16	0.81	0.29
KC68	25	1.29	0.19	0.61	0.32
KC68	29	1.16	0.13	0.48	0.26
KC68	33	2.20	0.26	1.55	0.39
KC68	37	2.18	0.23	1.54	0.36
KC68	41	2.02	0.19	1.38	0.32
KC68	49	1.25	0.17	0.57	0.3
KC68	55	1.52	0.14	0.85	0.27
KC68	67	1.82	0.22	1.16	0.36
KC68	79	1.35	0.12	0.68	0.25
KC68	97	1.20	0.15	0.52	0.28
KC68	113	1.11	0.12	0.42	0.25
KC68	133	0.70	0.10	0	0.23
KC69	1	2.85	0.38	2.03	0.52
KC69	5	1.58	0.17	0.71	0.3
KC69	9	1.88	0.22	1.02	0.36
KC69	17	1.38	0.14	0.5	0.27
KC69	25	1.65	0.16	0.78	0.29
KC69	33	1.35	0.14	0.47	0.27
KC69	49	1.44	0.16	0.57	0.29
KC69	61	1.13	0.12	0.24	0.25
KC69	79	1.12	0.13	0.23	0.26
KC69	97	1.10	0.11	0.21	0.24
KC69	121	0.90	0.10	0.01	0.23
KC69	133	1.01	0.11	0.12	0.24
KC69	159	0.69	0.08	-0.21	0.21
KC69	173	0.71	0.09	-0.19	0.22
KC69	193	0.77	0.10	-0.13	0.23
KC69	213	0.64	0.08	-0.27	0.21
KC70	1	1.56	0.16	0.72	0.30

Core Name	Depth (cm)	Total Activity (dpm/g)	Absolute Error Total (dpm/g)	Excess Activity (dpm/g)	Absolute Error Excess (dpm/g)
KC70	5	1.57	0.18	0.74	0.31
KC70	9	1.17	0.13	0.32	0.26
KC70	17	1.05	0.12	0.19	0.24
KC70	25	1.06	0.11	0.21	0.24
KC70	33	1.03	0.12	0.17	0.24
KC70	45	0.77	0.10	-0.09	0.23
KC70	61	0.78	0.10	-0.09	0.23
KC70	79	0.72	0.09	-0.15	0.22
KC70	97	0.94	0.11	0.08	0.23
KC70	121	0.74	0.07	-0.13	0.20
KC71	1	2.02	0.19	0.99	0.32
KC71	5	2.04	0.19	1.01	0.32
KC71	9	1.67	0.15	0.63	0.28
KC71	17	1.20	0.12	0.14	0.25
KC71	25	1.26	0.18	0.20	0.30
KC71	33	1.18	0.11	0.12	0.24
KC71	45	0.94	0.12	-0.12	0.24
KC71	55	1.09	0.15	0.02	0.27
KC71	67	1.00	0.14	-0.06	0.26
KC71	85	1.00	0.12	-0.06	0.25
KC71	103	0.97	0.12	-0.09	0.24
KC72	1	1.41	0.17	0.55	0.30
KC72	5	1.05	0.11	0.17	0.23
KC72	9	0.77	0.08	-0.12	0.21
KC72	17	1.24	0.11	0.38	0.24
KC72	25	1.05	0.10	0.18	0.23
KC72	33	1.07	0.11	0.19	0.23
KC72	41	0.94	0.09	0.06	0.22
KC72	67	0.82	0.08	-0.06	0.21
KC73	1	3.26	0.31	2.47	0.44
KC73	3	2.12	0.20	1.32	0.33
KC73	5	1.78	0.17	0.97	0.29
KC73	7	2.22	0.22	1.42	0.35
KC73	9	2.05	0.19	1.24	0.32
KC73	13	1.65	0.19	0.84	0.31
KC73	17	1.47	0.17	0.66	0.30
KC73	21	0.87	0.11	0.04	0.23
KC73	25	1.12	0.13	0.30	0.26
KC73	29	1.54	0.17	0.72	0.30
KC73	33	1.55	0.17	0.74	0.30
KC73	37	1.55	0.15	0.73	0.27
KC73	45	1.15	0.11	0.33	0.24
KC73	49	1.39	0.14	0.58	0.27
KC73	55	1.50	0.14	0.69	0.27

Core Name	Depth (cm)	Total Activity (dpm/g)	Absolute Error Total (dpm/g)	Excess Activity (dpm/g)	Absolute Error Excess (dpm/g)
KC73	61	1.29	0.12	0.47	0.25
KC73	67	0.82	0.09	-0.01	0.22
KC73	73	0.76	0.10	-0.07	0.22
KC73	85	0.90	0.11	0.08	0.23
KC74	1	3.78	0.39	3.07	0.53
KC74	5	2.96	0.29	2.22	0.42
KC74	9	1.81	0.19	1.03	0.32
KC74	13	0.88	0.10	0.07	0.23
KC74	17	1.27	0.14	0.47	0.27
KC74	21	1.93	0.18	1.16	0.31
KC74	29	0.79	0.09	-0.02	0.22
KC74	37	1.32	0.14	0.53	0.27
KC74	37	1.35	0.13	0.55	0.26
KC74	55	1.09	0.13	0.29	0.26
KC74	79	0.83	0.14	0.01	0.27
KC74	91	0.80	0.08	-0.01	0.20
KC75	1	4.68	0.49	4.30	0.63
KC75	5	4.70	0.48	4.33	0.63
KC75	9	5.06	0.52	4.70	0.66
KC75	13	2.37	0.25	1.91	0.39
KC75	17	1.55	0.16	1.05	0.29
KC75	25	1.50	0.16	1.01	0.29
KC75	33	1.82	0.20	1.34	0.33
KC75	41	1.26	0.13	0.75	0.26
KC75	49	1.27	0.13	0.77	0.26
KC75	61	0.91	0.11	0.40	0.24
KC75	79	0.69	0.08	0.16	0.21
KC75	97	0.53	0.08	0.00	0.21
KC75	123	0.53	0.07	0.00	0.19
KC75	153	0.53	0.07	0.00	0.19
KC76	1	6.82	0.60	6.23	0.74
KC76	5	5.89	0.55	5.27	0.69
KC76	9	4.24	0.38	3.56	0.52
KC76	17	2.90	0.28	2.17	0.41
KC76	25	1.45	0.13	0.67	0.26
KC76	37	1.01	0.09	0.22	0.22
KC76	49	0.80	0.08	0.00	0.20
KC76	67	0.55	0.06	-0.26	0.18
KC76	85	0.78	0.07	-0.03	0.20
KC76	113	0.95	0.09	0.15	0.22
KC76	153	0.94	0.09	0.14	0.22
KC77	1	1.58	0.17	1.00	0.31
KC77	5	1.47	0.15	0.88	0.28

Core Name	Depth (cm)	Total Activity (dpm/g)	Absolute Error Total (dpm/g)	Excess Activity (dpm/g)	Absolute Error Excess (dpm/g)
KC77	9	1.16	0.12	0.55	0.25
KC77	17	0.95	0.12	0.34	0.25
KC77	25	0.62	0.08	0.00	0.21
KC78	1	2.25	0.23	1.44	0.37
KC78	5	2.03	0.22	1.21	0.36
KC78	7	1.72	0.18	0.89	0.31
KC78	9	1.29	0.22	0.44	0.35
KC78	17	0.75	0.10	-0.12	0.23
KC78	21	0.73	0.08	-0.14	0.21
KC78	21	0.67	0.09	-0.21	0.22
KC78	25	1.25	0.14	0.39	0.27
KC78	37	0.87	0.10	0.00	0.22
KC78	49	0.84	0.10	-0.02	0.22
KC78	61	0.92	0.11	0.06	0.24
KC78	73	0.90	0.11	0.03	0.23
KC79	1	3.25	0.27	2.71	0.40
KC79	5	2.91	0.25	2.37	0.37
KC79	9	2.35	0.21	1.80	0.33
KC79	13	1.97	0.17	1.41	0.30
KC79	17	1.77	0.17	1.21	0.29
KC79	25	1.16	0.11	0.59	0.23
KC79	29	1.06	0.10	0.49	0.22
KC79	33	0.94	0.09	0.37	0.22
KC79	37	0.87	0.08	0.30	0.20
KC79	41	0.76	0.07	0.19	0.20
KC79	49	0.63	0.06	0.05	0.18
KC79	61	0.54	0.05	-0.04	0.18
KC79	67	0.61	0.07	0.04	0.20
KC79	73	0.57	0.06	-0.01	0.18
KC79	85	0.60	0.06	0.03	0.18
KC79	97	0.59	0.06	0.01	0.19
KC79	103	0.53	0.05	-0.04	0.18
KC79	113	0.53	0.05	-0.04	0.18
KC80	1	5.40	0.52	4.69	0.66
KC80	5	5.91	0.53	5.22	0.67
KC80	9	4.86	0.44	4.13	0.58
KC80	17	2.90	0.28	2.10	0.42
KC80	25	2.91	0.28	2.11	0.41
KC80	33	1.91	0.20	1.07	0.33
KC80	45	1.58	0.19	0.73	0.33
KC80	61	1.05	0.11	0.19	0.24
KC80	79	1.04	0.11	0.18	0.24
KC80	97	0.89	0.10	0.02	0.23
KC80	123	0.71	0.08	-0.17	0.21

Core Name	Depth (cm)	Total Activity (dpm/g)	Absolute Error Total (dpm/g)	Excess Activity (dpm/g)	Absolute Error Excess (dpm/g)
KC80	153	0.68	0.08	-0.21	0.21
KC81	1	5.08	0.52	4.20	0.67
KC81	3	3.25	0.29	2.30	0.43
KC81	5	2.73	0.25	1.77	0.38
KC81	7	1.80	0.19	0.80	0.32
KC81	13	0.98	0.11	-0.05	0.24
KC81	21	1.28	0.15	0.26	0.28
KC81	29	1.36	0.15	0.34	0.28
KC81	37	0.72	0.08	-0.32	0.21
KC81	41	0.78	0.11	-0.25	0.24
KC81	55	1.02	0.11	-0.01	0.24
KC81	67	0.95	0.10	-0.08	0.23
KC81	85	0.93	0.10	-0.10	0.23
KC81	103	1.14	0.12	0.11	0.25
KC81	133	1.22	0.12	0.20	0.25
KC81	163	1.15	0.12	0.13	0.25
KC82	1	5.21	0.44	4.58	0.56
KC82	3	4.09	0.35	3.45	0.48
KC82	5	3.67	0.31	3.02	0.44
KC82	7	2.60	0.23	1.93	0.35
KC82	9	1.84	0.16	1.16	0.28
KC82	13	2.13	0.18	1.46	0.31
KC82	17	1.91	0.17	1.23	0.29
KC82	21	2.46	0.21	1.79	0.33
KC82	25	2.00	0.17	1.33	0.30
KC82	29	1.78	0.16	1.10	0.28
KC82	33	1.29	0.19	0.60	0.32
KC82	37	1.36	0.13	0.67	0.26
KC82	41	1.09	0.13	0.40	0.25
KC82	45	0.94	0.09	0.25	0.21
KC82	49	1.12	0.13	0.44	0.25
KC82	55	1.03	0.12	0.34	0.25
KC82	61	0.81	0.08	0.12	0.21
KC82	67	0.74	0.07	0.05	0.20
KC82	73	0.69	0.08	0.00	0.20
KC83	1	5.09	0.50	4.12	0.65
KC83	9	3.30	0.31	2.27	0.45
KC83	17	1.81	0.19	0.72	0.32
KC83	25	0.81	0.09	-0.32	0.22
KC83	49	3.85	0.37	2.84	0.51
KC83	85	1.08	0.11	-0.04	0.24
KC83	103	1.11	0.12	0.00	0.25
KC83	123	1.16	0.12	0.04	0.25

Core Name	Depth (cm)	Total Activity (dpm/g)	Absolute Error Total (dpm/g)	Excess Activity (dpm/g)	Absolute Error Excess (dpm/g)
KC84	1	3.21	0.40	2.36	0.54
KC84	5	3.14	0.40	2.28	0.54
KC84	9	2.52	0.25	1.64	0.38
KC84	13	1.85	0.21	0.95	0.34
KC84	17	1.93	0.21	1.03	0.34
KC84	25	2.21	0.24	1.32	0.37
KC84	33	2.07	0.21	1.17	0.34
KC84	41	3.35	0.32	2.51	0.46
KC84	49	1.47	0.16	0.55	0.29
KC84	55	1.43	0.15	0.51	0.29
KC84	73	0.98	0.12	0.04	0.24
KC84	113	0.90	0.11	-0.04	0.23
KC85	1	4.21	0.42	3.40	0.56
KC85	7	2.51	0.23	1.64	0.36
KC85	13	2.51	0.25	1.64	0.38
KC85	21	2.40	0.23	1.52	0.37
KC85	29	1.39	0.17	0.47	0.30
KC85	41	1.36	0.14	0.45	0.27
KC85	55	1.62	0.16	0.72	0.29
KC85	67	0.93	0.10	0.00	0.22
KC85	85	1.04	0.11	0.11	0.24
KC85	103	1.10	0.14	0.17	0.26
KC85	133	0.88	0.10	-0.05	0.23
KC85	163	0.70	0.08	-0.24	0.21
KC86	1	2.50	0.25	1.72	0.38
KC86	3	2.30	0.21	1.52	0.34
KC86	5	2.17	0.22	1.39	0.34
KC86	7	1.44	0.14	0.64	0.27
KC86	9	1.52	0.15	0.72	0.27
KC86	13	1.38	0.14	0.58	0.26
KC86	17	1.71	0.16	0.92	0.29
KC86	21	0.94	0.10	0.13	0.22
KC86	25	1.81	0.21	1.02	0.34
KC86	29	1.24	0.14	0.44	0.26
KC86	37	1.03	0.11	0.22	0.23
KC86	41	1.41	0.14	0.61	0.27
KC86	45	0.94	0.12	0.13	0.24
KC86	55	0.99	0.10	0.18	0.23
KC86	61	0.67	0.09	-0.14	0.21
KC86	73	0.84	0.13	0.03	0.25
KC86	85	0.75	0.11	-0.06	0.24
KC86	97	0.66	0.08	-0.15	0.20
KC87	1	1.85	0.18	0.99	0.31
KC87	5	1.50	0.15	0.62	0.28

Core Name	Depth (cm)	Total Activity (dpm/g)	Absolute Error Total (dpm/g)	Excess Activity (dpm/g)	Absolute Error Excess (dpm/g)
KC87	9	1.48	0.15	0.60	0.28
KC87	17	1.23	0.13	0.34	0.26
KC87	25	0.87	0.09	-0.03	0.22
KC87	33	1.00	0.11	0.11	0.24
KC87	49	0.82	0.09	-0.08	0.22
KC89	1	3.88	0.37	3.47	0.50
KC89	5	2.47	0.24	2.01	0.38
KC89	9	1.48	0.16	0.98	0.29
KC89	17	1.87	0.19	1.38	0.32
KC89	25	1.84	0.18	1.36	0.31
KC89	33	1.59	0.16	1.10	0.30
KC89	37	1.36	0.13	0.86	0.26
KC89	45	0.88	0.09	0.37	0.22
KC89	49	0.86	0.10	0.34	0.22
KC89	61	0.76	0.09	0.24	0.22
KC89	79	0.62	0.07	0.09	0.20
KC89	91	0.53	0.06	0.00	0.19

KC90	1	1.53	0.16	0.59	0.29
KC90	5	1.38	0.17	0.43	0.30
KC90	9	1.74	0.18	0.81	0.31
KC90	17	1.43	0.14	0.48	0.27
KC90	25	1.09	0.11	0.13	0.24
KC90	33	1.20	0.13	0.25	0.26
KC90	45	1.04	0.11	0.08	0.24
KC90	61	0.96	0.10	0.00	0.23
KC90	79	0.91	0.12	-0.06	0.24
KC90	85	0.94	0.10	-0.02	0.23
KC91	1	2.13	0.21	1.01	0.34
KC91	5	1.91	0.19	0.78	0.32
KC91	9	1.68	0.28	0.54	0.42
KC91	13	1.86	0.18	0.74	0.31
KC91	17	1.35	0.16	0.20	0.29
KC91	25	1.23	0.14	0.08	0.27
KC91	33	1.15	0.13	0.00	0.26
KC91	49	1.25	0.14	0.10	0.27
KC91	61	1.00	0.12	-0.16	0.25
KC91	67	1.13	0.13	-0.02	0.26
KC92	1	4.86	0.42	4.18	0.55
KC92	5	3.82	0.32	3.13	0.45
KC92	9	3.03	0.26	2.32	0.38
KC92	13	2.38	0.20	1.66	0.33
KC92	17	2.27	0.20	1.55	0.32
KC92	21	1.98	0.18	1.26	0.30

Core Name	Depth (cm)	Total Activity (dpm/g)	Absolute Error Total (dpm/g)	Excess Activity (dpm/g)	Absolute Error Excess (dpm/g)
KC92	25	1.72	0.15	0.99	0.28
KC92	29	1.68	0.15	0.95	0.28
KC92	33	1.32	0.15	0.59	0.27
KC92	41	1.12	0.12	0.39	0.25
KC92	49	0.85	0.08	0.11	0.20
KC92	55	0.83	0.08	0.10	0.21
KC92	61	0.87	0.10	0.13	0.22
KC92	73	0.70	0.10	-0.04	0.22
KC92	85	0.73	0.07	-0.01	0.19
KC92	97	0.67	0.07	-0.07	0.19
KC92	113	0.66	0.07	-0.08	0.19
KC92	123	0.71	0.08	-0.03	0.20
KC93	1	3.12	0.31	2.66	0.45
KC93	5	2.58	0.25	2.10	0.38
KC93	9	2.03	0.22	1.53	0.35
KC93	17	1.35	0.14	0.83	0.27
KC93	25	0.61	0.08	0.06	0.20
KC93	33	0.53	0.06	-0.02	0.19
KC93	49	0.56	0.07	0.01	0.19
KC93	55	0.52	0.06	-0.04	0.19

KC94	1	3.85	0.36	2.96	0.49
KC94	5	2.25	0.22	1.31	0.36
KC94	9	1.55	0.15	0.58	0.28
KC94	17	1.05	0.10	0.07	0.23
KC94	25	0.91	0.09	-0.08	0.22
KC94	33	0.93	0.09	-0.06	0.22
KC94	49	0.95	0.09	-0.04	0.22
KC94	61	0.97	0.09	-0.02	0.22
KC94	79	1.06	0.10	0.08	0.23
KC94	91	1.05	0.10	0.06	0.23

B3. Accumulation Rate Calculations

Core Name	Trendline Equation	Error of Slope	Accumulation Rate (cm/y)	Accumulation Rate Error (cm/y)
KC1	$y = -24.025 \ln(x) + 37.656$	2.7511	0.75	0.23
KC2	$y = -21.575 \ln(x) + 27.335$	1.5439	0.67	0.14
KC7	$y = -33.292 \ln(x) + 52.164$	2.7392	1.03	0.16
KC8	$y = -9.7109 \ln(x) + 12.827$	0.886	0.30	0.18
KC9	$y = -11.127 \ln(x) + 8.1483$	1.1307	0.35	0.20
KC11	$y = -9.8963 \ln(x) + 26.574$	1.0692	0.31	0.22
KC12	$y = -3.1568 \ln(x) + 6.8826$	0.4365	0.10	0.28
KC13	$y = -13.474 \ln(x) + 25.082$	0.2037	0.42	0.03
KC14	$y = -44.201 \ln(x) + 67.116$	2.7024	1.37	0.12
KC15	$y = -32.775 \ln(x) + 47.634$	2.9437	1.02	0.18
KC16	$y = -24.452 \ln(x) + 42.195$	2.5608	0.76	0.21
KC17	$y = -35.872 \ln(x) + 39.077$	3.7822	1.12	0.21
KC18	$y = -4.4761 \ln(x) + 4.9468$	1.2727	0.14	0.51
KC19	$y = -16.329 \ln(x) + 33.121$	1.6889	0.51	0.21
KC20	$y = -10.849 \ln(x) + 26.33$	1.4471	0.34	0.27
KC21	$y = -6.3832 \ln(x) + 15.415$	1.6968	0.20	0.53
KC22	$y = -10.493 \ln(x) + 14.086$	0.8365	0.33	0.16
KC23	$y = -17.903 \ln(x) + 10.729$	2.8397	0.56	0.32
KC26	$y = -7.0808 \ln(x) + 8.6235$	0.4815	0.22	0.14
KC27	$y = -15.057 \ln(x) + 15.299$	3.087	0.47	0.41
KC30	$y = -5.2563 \ln(x) + 8.8917$	0.2228	0.16	0.08
KC31	$y = -24.538 \ln(x) + 59.953$	5.2433	0.76	0.43
KC32	$y = -9.7829 \ln(x) + 46.505$	2.6773	0.30	0.55
KC33	$y = -5.7873 \ln(x) + 8.1946$	0.9203	0.18	0.32
KC34	$y = -14.267 \ln(x) + 12.636$	2.0463	0.44	0.29
KC35	$y = -49.974 \ln(x) + 64.369$	5.1733	1.55	0.21
KC36	$y = -35.142 \ln(x) + 51.508$	2.354	1.09	0.13
KC37	$y = -23.974 \ln(x) + 35.525$	0.7279	0.75	0.06
KC40	$y = -4.7226 \ln(x) + 9.4933$	1.0596	0.15	0.45
KC42	$y = -10.396 \ln(x) + 10.627$	1.0156	0.32	0.20
KC45	$y = -27.199 \ln(x) + 43.385$	1.5657	0.85	0.11
KC46	$y = -20.931 \ln(x) + 42.218$	2.7907	0.65	0.26
KC47	$y = -27.647 \ln(x) + 47.491$	2.5378	0.86	0.18
KC48	$y = -43.125 \ln(x) + 58.482$	2.4476	1.34	0.11
KC49	$y = -28.731 \ln(x) + 46.063$	1.5694	0.89	0.11
KC52	$y = -18.946 \ln(x) + 33.84$	1.4801	0.59	0.16
KC53	$y = -57.62 \ln(x) + 136.31$	2.8822	1.79	0.10
KC54	$y = -20.354 \ln(x) + 53.233$	3.9678	0.63	0.39
KC55	$y = -7.0097 \ln(x) + 12.873$	1.3205	0.22	0.38
KC56	$y = -8.7887 \ln(x) + 13.034$	1.3543	0.27	0.31
KC57	$y = -2.3355 \ln(x) + 4.0563$	1.1178	0.07	0.96
KC58	$y = -9.1527 \ln(x) + 10.867$	0.8711	0.28	0.19
KC59	$y = -19.976 \ln(x) + 27.937$	0.6522	0.62	0.07
KC60	$y = -24.601 \ln(x) + 34.273$	1.7985	0.76	0.15

Core Name	Trendline Equation	Error of Slope	Accumulation Rate (cm/y)	Accumulation Rate Error (cm/y)
KC61	$y = -22.142\text{Ln}(x) + 35.432$	1.8797	0.69	0.17
KC62	$y = -6.6036\text{Ln}(x) + 36.263$	1.7139	0.21	0.52
KC63	$y = -10.742\text{Ln}(x) + 28.008$	1.942	0.33	0.36
KC64	$y = -5.7115\text{Ln}(x) + 8.1613$	1.203	0.18	0.42
KC65	$y = -16.653\text{Ln}(x) + 26.418$	0.5998	0.52	0.07
KC67	$y = -36.783\text{Ln}(x) + 41.77$	3.4675	1.14	0.19
KC71	$y = -5.9292\text{Ln}(x) + 5.5843$	0.6137	0.18	0.21
KC75	$y = -22.975\text{Ln}(x) + 34.425$	3.5364	0.71	0.31
KC76	$y = -10.217\text{Ln}(x) + 21.814$	0.6609	0.32	0.13
KC77	$y = -13.737\text{Ln}(x) + 1.805$	1.6146	0.43	0.24
KC78	$y = -5.7849\text{Ln}(x) + 4.9253$	2.0757	0.18	0.72
KC79	$y = -14.938\text{Ln}(x) + 17.805$	0.4598	0.46	0.06
KC80	$y = -19.565\text{Ln}(x) + 36.365$	1.9827	0.61	0.20
KC81	$y = -3.6926\text{Ln}(x) + 6.4185$	0.4829	0.11	0.26
KC82	$y = -16.78\text{Ln}(x) + 25.017$	1.3794	0.52	0.16
KC83	$y = -8.8685\text{Ln}(x) + 14.638$	1.6209	0.28	0.37
KC85	$y = -20.84*\text{Ln}(x) + 26.06$	6.6394	0.65	0.64
KC87	$y = -15.288\text{Ln}(x) + 0.0929$	2.5791	0.48	0.34
KC89	$y = -22.167\text{Ln}(x) + 25.944$	2.324	0.69	0.21
KC92	$y = -14.301\text{Ln}(x) + 23.177$	1.0594	0.44	0.15
KC93	$y = -13.476\text{Ln}(x) + 14.562$	0.4834	0.42	0.07
KC94	$y = -4.8816\text{Ln}(x) + 6.3048$	0.0038	0.15	0.00

Average Error = 0.25

B4. Penetration Depths of Excess ^{210}Pb Activity

Core Name	Penetration Depth of Excess ^{210}Pb Activity (cm)
KC1	88
KC2	39
KC7	86
KC8	50
KC9	26
KC11	48
KC12	17
KC13	50
KC14	133
KC15	73
KC16	73
KC17	105
KC18	12
KC19	50
KC20	45
KC21	23
KC22	31
KC23	47
KC26	29
KC30	15
KC31	55
KC32	33
KC33	13
KC34	41
KC35	160
KC36	110
KC37	67
KC40	15
KC45	92
KC46	65
KC47	83
KC48	102
KC49	75
KC52	67
KC53	192
KC54	64
KC55	21
KC56	29
KC57	7
KC58	21
KC59	53
KC60	55
KC61	41

Core Name	Penetration Depth of Excess ²¹⁰Pb Activity (cm)
KC62	45
KC63	43
KC64	21
KC65	48
KC67	87
KC70	21
KC71	34
KC75	61
KC76	43
KC78	13
KC79	45
KC80	65
KC81	10
KC84	64
KC85	61
KC87	21
KC90	39
KC91	21
KC92	52
KC93	21
KC94	13

Appendix C

^{239,240}Pu Activities

Core Name	Midpoint Depth (cm)	Activity (dpm/g)	Standard Deviation (dpm/g)
KC14	1	0.0041	0.0004
KC14	5	0.0044	0.0005
KC14	9	0.0052	0.0001
KC14	17	0.0051	0.0002
KC14	25	0.0054	0.0004
KC14	31	0.0080	0.0000
KC14	41	0.0090	0.0004
KC14	49	0.0164	0.0003
KC14	61	0.0100	0.0002
KC14	67	0.0086	0.0009
KC14	79	0.0000	0.0000
KC14	91	0.0000	0.0000
KC14	103	0.0000	0.0000
KC14	123	0.0000	0.0000
KC35	1	0.0046	0.0004
KC35	3	0.0057	0.0015
KC35	5	0.0047	0.0004
KC35	9	0.0044	0.0002
KC35	17	0.0037	0.0008
KC35	25	0.0000	0.0001
KC35	33	0.0025	0.0004
KC35	41	0.0081	0.0003
KC35	49	0.0059	0.0000
KC35	61	0.0169	0.0001
KC35	73	0.0041	0.0004
KC35	85	0.0025	0.0004
KC35	97	0.0000	0.0000
KC35	113	0.0000	0.0000
KC35	133	0.0000	0.0000
KC35	153	0.0000	0.0000
KC35	173	0.0000	0.0000

Core Name	Midpoint Depth (cm)	Activity (dpm/g)	Standard Deviation (dpm/g)
KC45	1	0.0059	0.0003
KC45	5	0.0062	0.0006
KC45	9	0.0069	0.0003
KC45	13	0.0084	0.0006
KC45	17	0.0074	0.0002
KC45	25	0.0114	0.0006
KC45	33	0.0180	0.0006
KC45	41	0.0168	0.0006
KC45	49	0.0054	0.0006
KC45	61	0.0026	0.0002
KC45	67	0.0000	0.0000
KC45	79	0.0000	0.0000
KC45	91	0.0000	0.0000
KC45	165	0.0000	0.0000
KC45	183	0.0000	0.0000
KC52	1	0.0110	0.0008
KC52	5	0.0116	0.0002
KC52	13	0.0172	0.0010
KC52	17	0.0124	0.0001
KC52	25	0.0000	0.0000
KC52	37	0.0000	0.0000
KC52	49	0.0000	0.0000
KC52	61	0.0000	0.0000
KC69	1	0.0041	0.0000
KC69	5	0.0037	0.0005
KC69	9	0.0062	0.0004
KC69	17	0.0046	0.0003
KC69	25	0.0142	0.0007
KC69	33	0.0101	0.0006
KC69	49	0.0080	0.0005
KC69	61	0.0000	0.0000
KC69	79	0.0000	0.0000
KC69	97	0.0000	0.0000
KC69	121	0.0000	0.0000
KC69	133	0.0000	0.0000
KC69	159	0.0000	0.0000

APPENDIX D

Kasten Core Grain Size Computations

Core Name	Midpoint Depth (cm)	% Sand	% Silt	% Clay
KC35	1	10.47	60.60	28.92
KC35	3	5.05	60.62	34.32
KC35	5	2.01	53.38	44.60
KC35	9	1.54	53.64	44.81
KC35	17	0.77	44.51	54.72
KC35	25	0.14	34.29	65.57
KC35	33	0.90	47.24	51.86
KC35	41	2.79	53.66	43.55
KC35	49	2.25	45.42	52.33
KC35	61	4.72	56.47	38.81
KC35	73	3.82	56.28	39.90
KC35	85	1.01	47.81	51.18
KC35	97	3.55	52.80	43.65
KC35	113	1.73	46.50	51.77
KC35	133	9.09	57.50	33.41
KC35	153	1.26	59.19	39.55
KC86	1	20.92	57.72	21.36
KC86	3	16.50	58.55	24.95
KC86	5	9.11	66.71	24.18
KC86	7	6.24	65.16	28.61
KC86	9	3.94	58.86	37.19
KC86	13	4.09	65.85	30.06
KC86	17	11.92	59.64	28.45
KC86	21	12.80	63.46	23.74
KC86	25	11.35	65.04	23.62
KC86	29	12.34	66.14	21.52
KC86	37	5.68	71.98	22.34
KC86	41	12.47	61.66	25.87
KC86	45	5.96	66.70	27.34
KC86	55	3.82	59.78	36.40
KC86	61	12.35	63.28	24.37
KC86	73	25.47	50.97	23.56
KC86	85	30.96	45.12	23.92
KC86	97	30.67	47.53	21.81

APPENDIX E

E1. Box Core Total Organic Carbon and Nitrogen Data

Core Name	Interval	%TOC	Mean %TOC	STDEV TOC	%TN	Mean %TN	STDEV TN
B4	10-11A	0.654	0.650	0.006	0.079	0.078	0.0007
B4	10-11B	0.646			0.078		
B4	20-21A	0.571	0.533	0.053	0.062	0.059	0.0046
B4	20-21B	0.495			0.055		
B4	30-31A	0.672	0.666	0.009	0.074	0.074	0.0001
B4	30-31B	0.659			0.074		
B7	10-11A	0.412	0.420	0.011	0.052	0.052	0.0000
B7	10-11B	0.428			0.052		
B7	20-21A	0.475	0.466	0.012	0.051	0.051	0.0003
B7	20-21B	0.458			0.050		
B7	30-31A	0.252	0.248	0.005	0.037	0.037	0.0002
B7	30-31B	0.245			0.036		
B17	10-11A	0.877	0.874	0.004	0.103	0.102	0.0018
B17	10-11B	0.871			0.101		
B17	20-21A	0.798	0.796	0.002	0.089	0.090	0.0017
B17	20-21B	0.795			0.092		
B22	10-11A	0.809	0.800	0.012	0.090	0.088	0.0024
B22	10-11B	0.791			0.086		
B22	20-21A	0.613	0.614	0.002	0.077	0.076	0.0013
B22	20-21B	0.615			0.075		
B22	30-31A	0.828	0.828		0.101	0.101	
B24	10-11A	0.550	0.554	0.006	0.065	0.066	0.0009
B24	10-11B	0.558			0.066		
B24	20-21A	0.260	0.255	0.007	0.035	0.035	0.0002
B24	20-21B	0.249			0.035		
B24	30-31A	0.590	0.576	0.020	0.066	0.064	0.0035
B24	30-31B	0.562			0.061		
B25	10-11A	0.248	0.249	0.001	0.035	0.035	0.0011
B25	10-11B	0.250			0.036		
B25	20-21A	0.299	0.309	0.014	0.038	0.040	0.0020
B25	20-21B	0.319			0.041		
B25	30-31A	0.388	0.383	0.006	0.047	0.046	0.0012
B25	30-31B	0.379			0.045		
B41	10-11A	0.722	0.722	0.000	0.088	0.088	0.0005
B41	10-11B	0.722			0.088		
B41	20-21A	0.682	0.683	0.000	0.085	0.085	0.0001
B41	20-21B	0.683			0.085		
B41	30-31A	0.634	0.635	0.002	0.076	0.076	0.0006
B41	30-31B	0.636			0.077		
B42	10-11A	0.673	0.680	0.009	0.087	0.088	0.0018
B42	10-11B	0.686			0.089		
B42	20-21A	0.829	0.833	0.006	0.108	0.106	0.0034

Core Name	Interval	%TOC	Mean %TOC	STDEV TOC	%TN	Mean %TN	STDEV TN
B42	20-21B	0.838			0.103		
B42	30-31A	0.895	0.895	0.000	0.115	0.115	0.0000
B42	30-31B	0.895			0.115		
B46	10-11A	0.730	0.729	0.001	0.094	0.094	0.0001
B46	10-11B	0.728			0.093		
B46	20-21A	0.749	0.753	0.005	0.090	0.091	0.0011
B46	20-21B	0.756			0.092		
B46	30-31A	0.647	0.643	0.006	0.083	0.083	0.0010
B46	30-31B	0.639			0.082		
B47	10-11A	0.739	0.740	0.002	0.091	0.092	0.0008
B47	10-11B	0.741			0.092		
B47	20-21A	0.741	0.723	0.026	0.091	0.089	0.0033
B47	20-21B	0.705			0.086		
B47	30-31B	0.592	0.592		0.072	0.072	
B52	10-11A	0.685	0.670	0.021	0.088	0.086	0.0025
B52	10-11B	0.656			0.085		
B52	20-21A	0.579	0.579		0.075	0.075	
B52	30-31A	0.534	0.527	0.010	0.067	0.068	0.0014
B52	30-31B	0.519			0.069		
B56	10-11A	0.423	0.433	0.014	0.055	0.055	0.0001
B56	10-11B	0.443			0.055		
B56	20-21A	0.305	0.326	0.028	0.042	0.044	0.0028
B56	20-21B	0.346			0.046		
B56	30-31A	0.272	0.271	0.001	0.038	0.039	0.0016
B56	30-31B	0.270			0.040		
B60	10-11A	0.705	0.708	0.005	0.082	0.083	0.0011
B60	10-11B	0.712			0.084		
B60	20-21A	0.885	0.872	0.019	0.102	0.099	0.0039
B60	20-21B	0.858			0.097		
B60	30-31A	0.886	0.889	0.005	0.104	0.103	0.0005
B60	30-31B	0.892			0.103		
B71	10-11B	0.712	0.712	0.089	0.091	0.091	
B71	20-21B	0.587	0.587		0.075	0.075	
B71	30-31A	0.589	0.585	0.005	0.072	0.072	0.0002
B71	30-31B	0.581			0.071		
B77	10-11A	0.470	0.477	0.011	0.057	0.057	0.0007
B77	10-11B	0.485			0.058		
B77	20-21A	0.316	0.334	0.025	0.041	0.044	0.0043
B77	20-21B	0.352			0.047		
B77	30-31A	0.344	0.353	0.012	0.042	0.044	0.0025
B77	30-31B	0.361			0.046		
B78	10-11A	0.629	0.612	0.024	0.075	0.075	0.0007
B78	10-11B	0.595			0.076		
B78	20-21A	0.677	0.665	0.017	0.081	0.078	0.0042
B78	20-21B	0.652			0.075		
B78	30-31A	0.754	0.710	0.063	0.070	0.069	0.0006

Core Name	Interval	%TOC	Mean %TOC	STDEV TOC	%TN	Mean %TN	STDEV TN
B78	30-31B	0.665			0.069		
B79	10-11A	0.790	0.781	0.012	0.085	0.084	0.0010
B79	10-11B	0.772			0.084		
B79	20-21A	0.506	0.506		0.065	0.065	
B79	30-31A	0.536	0.509	0.038	0.063	0.061	0.0021
B79	30-31B	0.482			0.060		
B80	10-11A	0.663	0.665	0.003	0.077	0.075	0.0026
B80	10-11B	0.667			0.073		
B80	20-21A	0.666	0.656	0.015	0.074	0.072	0.0025
B80	20-21B	0.645			0.070		
B80	30-31A	0.622	0.654	0.046	0.073	0.074	0.0017
B80	30-31B	0.687			0.076		
B83	10-11A	0.517	0.520	0.004	0.062	0.063	0.0014
B83	10-11B	0.522			0.064		
B83	20-21A	0.430	0.436	0.009	0.051	0.051	0.0002
B83	20-21B	0.442			0.050		
B83	30-31A	0.460	0.451	0.012	0.051	0.049	0.0024
B83	30-31B	0.443			0.048		
B84	10-11A	0.752	0.738	0.019	0.093	0.092	0.0008
B84	10-11B	0.725			0.092		
B84	20-21A	0.665	0.668	0.004	0.080	0.080	0.0002
B84	20-21B	0.671			0.080		
B84	30-31A	0.653	0.654	0.001	0.079	0.079	0.0002
B84	30-31B	0.654			0.079		

E2. Carbon Burial Rate Calculations

Region	Area (m ²)	Avg. %TOC	Avg. Mass Accumulation Rate (g cm ⁻² y ⁻¹)	Carbon Burial Rate (gC cm ⁻² y ⁻¹)	Carbon Burial * Rate Error
Inner Shelf	5.60E+08	0.475	0.167	7.93E-04	5.37E-04
Outer Shelf	2.34E+08	0.741	0.528	3.91E-03	1.51E-03
Northern Depocenter	1.32E+08	0.679	0.625	4.24E-03	2.31E-03
Southern Depocenter	1.27E+08	0.662	0.645	4.26E-03	1.63E-03

* Error = Stdev(C) + Average ²¹⁰Pb Accumulation Rate Error

E3. Box Core Carbon Data: $\delta^{13}\text{C}$, Carbon, Nitrogen

Core Name	Midpoint Depth (cm)	Sample Weight (mg)	C (mg)	N (mg)	$\delta^{13}\text{C}$
B3	0.50	34.58	0.075	0.011	-24.60
B3	5.5	32.072	0.091	0.011	-24.94
B3	10.5	39.849	0.215	0.025	-25.29
B3	15.50	38.66	0.130	0.018	-24.66
B3	20.50	36.58	0.058	0.010	-25.18
B6	0.50	36.24	0.069	0.011	-24.55
B6	5.5	38.645	0.063	0.010	-24.25
B6	10.50	32.92	0.146	0.015	-24.74
B6	15.50	35.45	0.077	0.013	-24.72
B6	20.50	29.93	0.106	0.013	-25.28
B6	25.50	36.97	0.140	0.017	-24.78
B18	0.50	39.14	0.195	0.028	-23.99
B18	5.5	31.003	0.158	0.021	-24.24
B18	10.50	33.87	0.175	0.024	-24.83
B18	15.50	38.73	0.148	0.016	-25.02
B18	20.50	38.99	0.162	0.019	-24.24
B18	25.50	34.45	0.186	0.026	-24.43
B18	30.50	28.64	0.092	0.013	-24.18
B18	32.50	33.25	0.069	0.011	-24.87
B24	0.50	31.23	0.167	0.020	-25.11
B24	5.5	33.896	0.158	0.020	-24.98
B24	10.50	36.89	0.170	0.019	-24.49
B24	15.50	35.27	0.189	0.021	-24.97
B24	20.50	36.35	0.081	0.012	-24.11
B24	25.50	25.85	0.128	0.015	-24.29
B24	30.50	34.28	0.172	0.021	-24.56
B24	33.50	37.82	0.110	0.014	-24.73
B25	0.50	37.45	0.125	0.016	-24.66
B25	5.5	37.787	0.202	0.024	-24.88
B25	10.50	37.85	0.101	0.013	-24.65
B25	15.50	30.46	0.147	0.016	-25.58
B25	20.50	37.04	0.151	0.014	-25.49
B25	25.50	36.53	0.082	0.011	-25.25
B25	30.50	33.61	0.165	0.019	-25.54

Core Name	Midpoint Depth (cm)	Sample Weight (mg)	C (mg)	N (mg)	$\delta^{13}\text{C}$
B52	0.50	31.68	0.178	0.026	-23.38
B52	5.5	35.994	0.202	0.026	-22.97
B52	10.50	37.43	0.186	0.027	-23.39
B52	15.50	32.66	0.132	0.020	-23.65
B52	20.50	35.72	0.167	0.025	-23.74
B52	25.50	34.81	0.168	0.023	-23.46
B52	30.50	33.67	0.139	0.020	-23.27
B52	34.50	35.84	0.156	0.020	-23.72
B61	0.50	37.55	0.196	0.024	-23.62
B61	5.5	38.595	0.200	0.028	-24.71
B61	10.50	37.41	0.212	0.029	-25.28
B61	15.50	36.42	0.162	0.022	-25.10
B61	20.50	37.26	0.294	0.035	-25.31
B61	25.50	33.26	0.292	0.034	-25.75
B61	30.50	32.06	0.247	0.032	-25.61
B61	34.50	35.21	0.144	0.019	-24.47
B85	0.50	35.26	0.137	0.020	-24.09
B85	5.5	36.823	0.160	0.017	-24.73
B85	10.50	34.70	0.139	0.019	-24.98
B85	15.50	30.44	0.097	0.012	-24.30
B85	20.50	37.01	0.135	0.018	-25.14
B85	25.50	31.50	0.124	0.014	-24.89
B85	30.50	32.76	0.121	0.014	-24.85
B85	34.50	38.13	0.132	0.017	-24.34

REFERENCES

- Alexander, C., Walsh, J., Sumner, B., Orpin, A., Kuehl, S., 2006. Continental slope sediment delivery and storage on an active margin: the Waipaoa Margin example. *Eos Trans. AGU*, 87(52), Fall Meeting Supplement, Abstract OS12A-03.
- Berner, R.A., 1982. Burial of organic carbon and pyrite sulfur in the modern ocean: its geochemical and environmental significance. *American Journal of Science*, 282: 451-473.
- Berryman, K., Marden, M., Eden, D., Mazengarb, C., Ota, Y., Moriya, I., 2000. Tectonic and paleoclimatic significance of Quaternary river terraces of the Waipaoa River, East Coast, New Zealand. *New Zealand Journal of Geology and Geophysics*, 43: 229-245.
- Blair, N.E., Leithold, E.L., Aller, R.C., 2004. From bedrock to burial: the evolution of particulate organic carbon across coupled watershed-continental margin systems. *Marine Chemistry*, 92: 141-156.
- Brunskill, G.J., Zagorskis, I., Pfitzner, J., 2001. Carbon burial rates in sediments and a carbon mass balance for the Herbert River region of the Great Barrier Reef Continental shelf, North Queensland, Australia. *Estuarine, Coastal and Shelf Science*, 54: 677-700.
- Carter, L., Carter, R.M., McCave, I.N., Gamble, J., 1996. Regional sediment recycling in the abyssal Southwest Pacific Ocean. *Geology*, 24 (8): 735-738.
- Carter, L., Manighetti, B., Elliot, M., Trustrum, N., Gomez, B., 2002. Source, sea level and circulation effects on the sediment flux to the deep ocean over the past 15 ka off eastern New Zealand. *Global and Planetary Change*, 33: 339-355.
- Dellapenna, T.M.; Kuehl, S.A., Schaffner, L.C., 1998. Sea-bed mixing and particle residence times in biologically and physically dominated estuarine systems: a comparison of Lower Chesapeake Bay and the York River subestuary. *Estuarine, Coastal and Shelf Science*, 46 (6): 777-795.
- DeMaster, D.J., Kuehl, S.A., Nittrouer, C.A., 1986. Effects of suspended sediments on geochemical processes near the mouth of the Amazon River: examination of biological silica uptake and the fate of particle-reactive elements. *Continental Shelf Research*, 6 (1-2): 107-125.
- Dukat, D.A., Kuehl, S.A., 1995. Non-steady-state ^{210}Pb flux and the use of $^{228}\text{Ra}/^{226}\text{Ra}$ as a geochronometer on the Amazon continental shelf. *Marine Geology*, 125 (3-4): 329-350.

Foster, G., Carter, L., 1997. Mud sedimentation on the continental shelf at an accretionary margin – Poverty Bay, New Zealand. *New Zealand Journal of Geology and Geophysics*, 40: 157-173.

Frignani, M., Langone, L., Ravaioli, M., Sorgente, D., Alvisi, F., Albertazzi, S., 2005. Fine-sediment mass balance in the western Adriatic continental shelf over a century time scale. *Marine Geology*, 222-223: 113-133.

Gee, G.W., Bauder, J.W., 1986. Particle-size analysis. In: Klute, A. (Ed.), *Methods of Soil Analysis: Part 1. Physical and Mineralogical Methods*, 2nd edn., Agronomy, 9. Soil Science Society of America, Madison, USA, 383-411.

Gerber, T.P., Pratson, L.F., Kuehl, S.A., Walsh, J.P., Alexander, C., Palmer, A., 2008. The influence of sea level and tectonics on Late Pleistocene through Holocene sediment storage along the high-sediment supply Waipaoa continental shelf. *Marine Geology*, submitted.

Gomez, B., Fulthorpe, C., Carter, L., Berryman, K., Browne, G., Green, M., Hicks, M., Trustum, N., 2001. Continental Margin Sedimentation to be studied in New Zealand. *Eos, Transactions, American Geophysical Union*, 82 (14): 161, 166-167.

Gomez, B., Trustum, N.A., Hicks, D.M., Rogers, K.M., Page, M.J., Tate, K.R., 2003. Production, storage, and output of particulate organic carbon: Waipaoa River Basin, New Zealand. *Water Resources Research*, 39 (6): 1161, doi.10.1029/2002WR001619.

Goodbred, S.L., Kuehl, S.A., 1999. Holocene and modern sediment budgets for the Ganges-Brahmaputra river system: Evidence for highstand dispersal to flood-plain, shelf, and deep-sea depocenters. *Geology*, 27 (6): 559-562.

Griffiths, G.A., 1982. Spatial and temporal variability in suspended sediment yields of North Island basins, New Zealand. *Water Resources Bulletin*, 8 (4): 575-583.

Hayward, B.W., Grenfell, H.R., Sabaa, A.T., Carter, R., Cochran, U., Lipps, J.H., Shane, P.R., Morely, M.S., 2006. Micropaleontological evidence of large earthquakes in the past 7200 years in southern Hawke's Bay, New Zealand. *Quaternary Science Reviews*, 25 (11-12): 1186-1207.

Hedges, J.I., 1992. Global biogeochemical cycles: progress and problems. *Marine Chemistry*, 39: 67-93.

Hedges, J.I., Stern, J.H., 1984. Carbon and nitrogen determinations of carbonate-containing solids. *Limnology and Oceanography*, 29: (3), 657-663.

Hicks, D.M., Gomez, B., Trustum, N.A., 2000. Erosion thresholds and suspended sediment yields, Waipaoa River Basin, New Zealand. *Water Resources Research*, 36 (4): 1129-1142.

- Hicks, D.M., Gomez, B., Trustrum, N.A., 2004. Event suspended sediment characteristics and the generation of hyperpycnal plumes at river mouths: East Coast Continental Margin, North Island, New Zealand. *The Journal of Geology*, 112: 471-485.
- Jouanneau, J.M., Weber, O., Drago, T., Rodrigues, A., Oliveira, A., Dias, J.M.A., Garcia, C., Schmidt, S., Reyss, J.L., 2002. Recent sedimentation and sedimentary budgets on the western Iberian shelf. *Progress in Oceanography*, 52: 261-275.
- Keil, R.G., Hedges, J.I., 1993. Sorption of organic matter to mineral surfaces and the preservation of organic matter in coastal marine sediments. *Chemical Geology*, 107 (3-4): 385-388.
- Kenna, T.C., 2002. Determination of plutonium isotopes and neptunium-237 in environmental samples by inductively coupled plasma mass spectrometry with total sample dissolution. *Journal of Analytical Atomic Spectrometry*, 17: 1471-1479.
- Ketterer, M.E., Hafer, K.M., Jones, V.J., Appleby, P.G., 2004(a). Rapid dating of recent sediments in Loch Ness: inductively coupled plasma mass spectrometric measurements of global fallout plutonium. *Science of the Total Environment*, 322: 221-229.
- Ketterer, M.E., Hafer, K.M., Link, C.L., Kolwaite, D., Wilson, J., Mietelski, J.W., 2004(b). Resolving global versus local/regional Pu sources in the environment using sector ICP-MS. *Journal of Analytical Atomic Spectrometry*, 19: 241-245.
- Kettner, A.J., Gomez, B., Syvitski, J.P.M., 2007. Modeling suspended sediment discharge from the Waipaoa River system, New Zealand: The last 3000 years. *Water Resources Research*, v. 43, W07411, doi: 10.1029/2006WR005570.
- Kim, C.S., Kim, C.K., Lee, J.I., Lee, K.J., 2000. Rapid determination of Pu isotopes and atom ratios in small amounts of environmental samples by an on-line sample pre-treatment system and isotope dilution high resolution inductively coupled plasma mass spectrometry. *Journal of Analytical Atomic Spectrometry*, 15: 247-255.
- Kniskern, T.A., 2007. Shelf sediment dispersal mechanisms and deposition on the Waiapu river shelf, New Zealand. Dissertation, School of Marine Science: the College of William and Mary.
- Koide, M., Bruland, K.W., Goldberg, E.D., 1973. Th-228/Th-232 and Pb-210 geochronologies in marine and lake sediments. *Geochimica et Cosmochimica Acta*, 37: 1171-1187.

- Kuehl, S.A., Alexander, C.A., Carter, L., Gerald, L., Gerber, T., Harris, C., McNinch, J., Orpin, A., Pratson, L., Syvitski, J., and Walsh, J.P., 2006. Understanding Sediment Transfer from Land to Ocean. EOS, Transactions of the American Geophysical Union, V.87 (29).
- Kuehl, S.A., DeMaster, D.J., Nittrouer, C.A., 1986. Nature of sediment accumulation on the Amazon continental shelf. *Continental Shelf Research*, 6: 209-225.
- Lee, C., Murray, D.W., Barber, R.T., Buesseler, K.O., Dymond, J., Hedges, J.I., Honjo, S., Manganini, S.J., Marra, J., Moser, C., Peterson, M.L., Prell, W.L., Wakeham, S.G., 1998. Particulate organic carbon fluxes: compilation of results from the 1995 US JGOFS Arabian Sea Process Study. *Deep Sea Research II*, 45: 2489-2501.
- Leithold, E.L, Hope, R.S., 1999. Deposition and modification of a flood layer on the northern California shelf: lessons from and about the fate of terrestrial particulate organic carbon. *Marine Geology*, 154: 183-195.
- Lewis, K.B., Lallemand, S.E., Carter, L., 2004. Collapse in a Quaternary shelf basin off East Cape, New Zealand: evidence for passage of a subducted seamount inboard of the Ruatoria giant avalanche. *New Zealand Journal of Geology and Geophysics*, 47: 415-429.
- Lin, S., Huang, K.M, Chen, S.K., 2000. Organic carbon deposition and its control on iron sulfide formation of the southern East China Sea continental shelf sediments. *Continental Shelf Research*, 20: 619-635.
- Macdonald, R.W., Solomon, S.M., Cranston, R.E., Welch, H.E., Yunker, M.B., Gobeil, C., 1998. A sediment and organic carbon budget for the Canadian Beaufort shelf. *Marine Geology*, 144: 255-273.
- Meybeck, M., 1982. Carbon, nitrogen, and phosphorus transport by world rivers. *American Journal of Science*, 282: 401-450.
- Milliman, J. and Syvitski, J.P.M., 1992. Geomorphic/tectonic control of sediment discharge to the ocean: the importance of small mountainous rivers. *The Journal of Geology*, 100: 525-544.
- Nittrouer, C.A., Sternberg, R.W., Carpenter, R., Bennett, J.T., 1979. The use of Pb-210 geochronology as a sedimentological tool: application to the Washington continental shelf. *Marine Geology*, 31: 297-316.
- Orpin, A.R., Alexander, C., Carter, L., Kuehl, S., and Walsh, J.P., 2006. Temporal and spatial complexity in post-glacial sedimentation on the tectonically active, Poverty Bay continental margin of New Zealand. *Continental Shelf Research* 26: 2205-2224.

- Page, M., Trustrum, N., Brackley, H., Gomez, B., Kasai, M., Marutani, T., 2001. pg. 86-100, in: Marutani, Tomomi, Gary J. Brierley, Noel A. Trustrum, and Mike Page (eds). Source-to-Sink Sedimentary Cascades in the Pacific Rim Geo-Systems. Matsumoto Sabo Work Office, Ministry of Land, Infrastructure and Transport, Nagano, Japan. 184 p.
- Rose, L.E., Kuehl, S.A., 2008. Insight into recent sedimentation on the Waipaoa River continental shelf. *Marine Geology*, submitted.
- Sadler, P.M., 1981. Sediment accumulation rates and the completeness of stratigraphic sections. *Journal of Geology*, 89 (5): 569-584.
- Smoak, J.M., DeMaster, D.J., Kuehl, S.A., Pope, R.H., McKee, B.A., 1996. The behavior of particle-reactive tracers in a high turbidity environment: ^{234}Th and ^{210}Pb on the Amazon continental shelf. *Geochimica et Cosmochimica Acta*, 60 (12): 2123-2137.
- Sommerfield, C.K., Nittrouer, C.A., 1999. Modern accumulation rates and a sediment budget for the Eel shelf: a flood-dominated depositional environment. *Marine Geology*, 154: 227-241.
- Van Weering, Tj.C.E., Hall, I.R., de Stigter, H.C., McCave, I.N., Thomsen, L., 1998. Recent sediments, sediment accumulation and carbon burial at Goban Spur, N.W. European Continental Margin (47-50°N). *Progress in Oceanography*, 42: 5-35.
- Wheatcroft, R.A., Borgeld, J.C., 2000. Oceanic flood deposits on the northern California shelf: large-scale distribution and small-scale physical properties. *Continental Shelf Research*, 20: 2163-2190.
- Wheatcroft, R.A., Sommerfield, C.K., Drake, D.E., Borgeld, J.C., Nittrouer, C.A., 1997. Rapid and widespread dispersal of flood sediment on the Northern California Margin. *Geology*, 25 (2): 163-166.
- Wilmshurst, J.M., 1997. The impact of human settlement on vegetation and soil stability in Hawke's Bay New Zealand. *New Zealand Journal of Botany*, 35: 97-111.
- Wilmshurst, J.M., Eden, D.N., Froggatt, P.C., 1999. Late Holocene forest disturbance in Gisborne, New Zealand: a comparison of terrestrial and marine pollen records. *New Zealand Journal of Botany*, 37: 523-540.
- Wilmshurst, J.M., McGlone, M.S., Partridge, T.R., 1997. A late Holocene history of natural disturbance in lowland podocarp/hardwood forest, Hawke's Bay, New Zealand. *New Zealand Journal of Botany*, 35: 79-96.
- Wood, M.P., 2006. Sedimentation on a high input continental shelf at the active Hikurangi Margin: Poverty Bay, New Zealand. Master's thesis: School of Geography, Environment and Earth Sciences, Victoria University of Wellington.